Cape Peninsula
University of Technology

The development of an empirical mass transfer relationship for the extraction of Copper ions in a carrier facilitated tubular supported liquid membrane system.

by

Makaka Siphokazi

Thesis submitted in fulfilment of the requirements for the degree

Master of Technology: Chemical Engineering

in the Faculty of Engineering

at the Cape Peninsula University of Technology

Supervisor: Mr.M.Aziz

Co-supervisor: Mr.A.B. Nesbitt

Cape Town

Date submitted: June 2011

DECLARATION

I, Siphokazi Makaka, declare that the contents of this thesis represent my own unaided work, and that the thesis has not previously been submitted for academic examination towards any qualification. Furthermore, it represents my own opinions and not necessarily those of the Cape Peninsula University of Technology.

Signed **Date**

ABSTRACT

Treatment of waste material from mining and mineral processing is gaining increasing importance as a result of the increasing demand for high purity products and environmental concerns. Supported liquid membranes (SLMs) have been proposed as a new technology for the selective removal of metal ions from a solution. This technology can be described as the simultaneous extraction and stripping operation, combined in a continuous single process unit.

Theoretically, the rate of mass transfer through SLM systems could be controlled by three resistances, namely:

- Resistance through the feed-side
- Resistance through the strip-side laminar layers; and
- Diffusion through the membrane.

It has been reported that transport resistance in the feed-side laminar layer is controlling. (Srisurichan *et al*, 2005:186).

The objective of this research was to extract copper ions in a TSLM system, evaluate the effect of the feed characteristics on the feed-side laminar layer and determine a relationship between the applicable dimensionless numbers, i.e. Sherwood, Schmidt and Reynolds numbers.

A Counter-current, double pipe Perspex bench-scale reactor, consisting of a single hydrophobic PVDF tubular membrane mounted vertically within, was used for the test work. The membrane was impregnated with LIX 984N-C and became the support for this organic transport medium. Dilute Copper solution passed through the centre pipe and sulphuric acid, as a strippant, passed through the shell side.

In this test work, Copper was successfully transported from the feed-side to the strip-side and through repetitive results; a relationship between dimensionless numbers was achieved.

.

ACKNOWLEDGEMENTS

I wish to thank:

Almighty God, without whom this work would not have been a success.

- A special thanks to Mr. M. Aziz for his outstanding supervision, for continuous support and encouragement.
- My co-supervisor, Mr.A.B. Nesbitt, for financial assistance, technical expertise in the field of study.
- My parents, Mlamli and Sindiswa Makaka ,the late Mr. Phumzile Winston Makaka , my siblings Sakhi and Simthembile , for love and support
- The chemistry lab staff at CPUT, Mrs Lorna Marshall, Mr Courie and Xolile, etc.
- Mr Alwyn, for his technical assistance and all TSLM members for their support.
- My friends and colleagues, for their support
- CPUT research department for their financial support.
- Lastly, Alison Fletcher, for assisting in editing this work.

TABLE OF CONTENTS

List of Figures

List of Tables

GLOSSARY

1. **Extraction**; transfer of the metal ions into the organic phase by chemical reaction with the extractant
2. **Scrubbing**; removal of co extracted material/metals or excess acid etc. (optional)
3. **Stripping**; transfer of the metal ions back into a second pure aqueous phase for further processing
4. **Solvent make-up**; treatment of the organic phase by a third aqueous phase for purification of solvent or extractant; removal of crude or degradation products; topping with fresh organic (optional)
5. **A distribution coefficient**; is defined as the ratio D = (all species of solute in organic phase)/ (all species of solute in aqueous phase). D is dependent on the initial concentration of the solute and the concentration of other reaction components in question.
6. **pH**; a measure of degree of the acidity or alkalinity of a solution as measured on a scale of 0 to 14.
7. **Membrane**; a selective barrier, between two phases, the term 'selective' being inherent to a membrane or membrane process (Mulder, 1996:12). A membrane can be homogenous or heterogeneous, symmetric or asymmetric in structure, solid or liquid can carry a positive or negative charge or be neutral or bipolar.
8. **Ion**; an electrical charged chemical particle (atom,molecule,or molecule fragment)
9. **Hydrogen**; a colorless, highly flammable gaseous element, the most abundant element on earth.
10. **Flux**; a rate of flow of copper ions through the membrane material per unit time per unit area.
11. **Feed**; the stream that enters the membrane module
12. **Aqueous phase**; is the liquid immiscible made out of water and $CuSO_4$
13. **Permeability coefficient**; a coefficient associated with simple diffusion through a membrane that is proportional to the partition coefficient and the diffusion coefficient and inversely proportional to membrane thickness.
14. **Pores**; the complex network of channels in the interior of a particle of a sorbent
15. **Porosity**; the ratio of the volume of all the pores in a material to the volume of the whole.
16. **Micron**; a linear measure equal to one million of a meter. The symbol for the micron is the Greek letter "μ".
17. **Ultra filtration**; membrane type that removes particles in size range between 0.002 to 0.1 micron range.

18. **Carrier facilitated transport**; is a transport of a substance across the plasma membrane by carrier molecules but without energy

Nomenclature

M	Metal species
R	Organic extractant
D_{MRn}	Mean diffusion coefficient of the complex (cm^2s^{-1})
$D_{cu\ (f)}$	Distribution coefficient of copper ions on the feed side ($cm^2.s^{-1}$)
$D_{cu(s)}$	Distribution coefficient of copper ions on the strip side ($cm^2.s^{-1}$)
N_{cu}	Mass flux of copper (mol. $cm^{-2}.s^{-1}$)
k_f	Aqueous mass transfer coefficient ($cm.s^{-1}$)
k_m	Membrane mass transfer coefficient ($cm.s^{-1}$)
$K_{ex,f}$	Extraction equilibrium constant for Cu
d_i	Effective module inner diameter (cm)
d_o	Effective module outer diameter (cm)
L	Fiber length (cm)
P	Permeability coefficient ($cm.s^{-1}$)
r_i and r_o	Inner and outer radius of the membrane (cm)
t_m	Thickness of the fiber membrane (cm)
v	Velocity of the feed solution ($cm.s^{-1}$)
S	Strip
F	Feed
R_2H	Hydrogen complex
T	Time (s)

Greek symbols

P	Density ($g.cm^{-3}$)
μ	Viscosity (Pa.s)
ε	Porosity of the membrane
τ	Tortousity of the membrane
δ	Thickness of the membrane

Subscripts

i	Inner
o	Outer
f	Feed side
s	Strip side
aq	Aqueous
org	Organic

Abbreviations

PVDF	Polyvinyldene fluoride
SLM	Supported liquid membrane
TSLM	Tubular Supported Liquid membrane
HFSLM	Hollow Fibre Supported Liquid Membrane
DWAF	Department of Water Affairs and Forestry
EMU	Electron Microscopic Unit
WWTP	Waste Water Treatment Plants
Zn	Zinc
Ni	Nickel
Cu	Copper
Sh	Sherwood number
Sc	Schmidt’s number
Re	Reynold’s number
Mr.	Molar mass of the metal ion

CHAPTER ONE

1 Introduction

1.1 Statement of research problem

Research efforts are being made to recover metal ions from industrial waste waters as a result of the increasing demand for high purity products, as well as the increased environmental concerns. Processing these industrial waste waters can be profitable when recovering metal ions and as a result, fines can be avoided.

1.2 Background to the research problem

There is a need to recover metals from industrial effluents, the disposal of which may cause environmental problems. Expensive metals are being lost in waste waters (Gill *et al*, 2000:113). In the past few years, there has been an increase in environmental awareness. This has forced industries to become more careful with waste generated. The cleaning and upgrading of metal containing waste has become not only a demanding research, but also a lucrative business (Smit *et al*, 1996:249).

1.3 South African Background

The minimum requirement for waste disposal to landfill sites, according to the Department of Water affairs and Forestry (DWAF), is that all hazardous waste sites should have a leachate management system. The minimum requirements for the classification, handling and disposal of hazardous waste, according to DWAF, states that all leachates are hazardous; and DWAF is beginning to encourage waste disposal companies to manage leachate treatment effectively. As a result, suitable technologies will be required for the successful treatment of these hazardous leachates (Schoeman *et al*, 2003: ii).

Waste water from metallurgical plants usually contains a large amount of ions of various metals (Zn, Cd, Cu and Pb) (Kaminski *et al*, 2000:41).

Table 1.1: Typical compositions of copper-containing ammoniacal solutions (Yang *et al*, 2007:122)

Ammoniacal wastewater	
pH	7.25
Cu(II)	5.6×10^{-3} M
Total NH_3	0.4 M
Cl^-	0.5 M
Zn(II)	5.5×10^{-3} M
Ni(II)	3.7×10^{-4} M
Cd(II)	1.8×10^{-6} M

The most common form of effluent treatment involves the precipitation of metals such as hydroxide, basic salt or sulphides.

These products are rarely processed for metal recovery, since this method is expensive. Solvent extraction and ion exchange allow the recovery of metals, but are rarely used due to high capital and operating costs, in comparison with the value of materials recovered; and losses of solvents, due to solubility and entrainment in the raffinates (Gill *et al*, 2000:114)

1.4 Conventional Wastewater Treatment Processes

1.4.1 Adsorption

Adsorption is described as the concentration of a substance at the interface or surface (Barrow, 1996:344). The Adsorption at the interface or surface is largely due to binding forces between ions, atom and molecules of the adsorbate on the sorbent surface (Levine, 1995). An ideal adsorbent should have a very strong affinity for the target contaminants, and simultaneously have the ability to release the adsorbate from the adsorbent under a different condition so that the adsorbent can be regenerated.

Since cost is an important consideration for selection adsorbent materials, natural materials, such as biopolymeric sorbent vermiculite and clays which are readily available in large quantities, cheap and environmentally-friendly have recently been paid increasing attention (Dho *et al*, 2003:177; Ersoz *et al*, 2006:272).

The commercial adsorbents used for the removal of contaminants from wastewater include a variety of gels, activated carbon, silica, activated alumina, zeolites, ion exchange resin and other resinous materials (Saleem *et al*, 1992:239). For example,

activated alumina and ion exchange resin have been demonstrated to be effective in removing arsenic from water. Several different sorbents such as natural clays and biopolymeric sorbent vermiculite have been investigated in terms of decontamination of the discharged effluents and concentration of heavy metal ions (Dho *et al*, 2003:177; Ersoz *et al*, 2006:272). The adsorption methods are confronted with some problems, such as poor selectivity and slow regeneration.

1.4.2 Electrocoagulation

In electrocoagulation process, the coagulant is produced by electrolytic oxidation of a certain anode material (Mollah *et al*, 2001:29) and colloid matters are coagulated and separated with the direct current. During the electrocoagulation process, hydrogen gas evolution at cathode is accompanied with metal anode's dissolution.

The main advantages of electrocoagulation are simple and can be easily operated. Wastewater treated by electrocoagulation produced clear, colorless, and odorless water. Furthermore, flocs generated by electrocoagulation can be treated easily and they are de-waterable. Main disadvantage of electrocoagulation is that anode electrodes need to be regularly replaced due to the dissolution of electrodes with oxidation. Another disadvantage is high conductivity of the water suspension is required and high usage of electricity is needed during the process (Mollah *et al*, 2001:29) .The electrocoagulation process can be used in municipal or industrial wastewater treatment plants (WWTP) as well as in water treatment.

1.4.3 Ion Exchange

During the ion exchange process, exchange between counter ion on bead surface and ion in the solution with the different electrostatic force is reversibly occurred. In the process, cation, such as copper, nickel, cadmium, is exchanged with H+. Also, anion, as chlorides, sulfates and chromates is exchanged with OH-. This technology has been mainly used for water softening, pharmaceutical purification, production of ultra-pure water for semiconductor processes, purification in the food industry, etc. Ion exchange processes have also been demonstrated to remove heavy metal ions including copper and cadmium from the wastewater effectively (Wang *et al*, 2005:80). For ion exchange

processes, it is difficult to develop novel ion exchange resins with highly selective functional groups for greater selectivity for the removal of contaminants alone.

1.4.4 Solvent Extraction

Solvent extraction is a well known wastewater treatment for its ability to selectively separate and concentrate metals (Deorkar *et al*, 1997:399). However, the solvent extraction process suffers from drawbacks, such as a large amount of solvent consumption, solvent degradation and inadequate decontamination efficiency (Liu *et al*, 2006:137).

Currently, this process is widely used in the mining industry. However, and specifically from an operational perspective, this technique is not yet satisfactorily resolved and many difficulties are normally observed when convectional mixer-settler extractors are utilised (Valenzuela *et al*, 2002:385)

1.4.5 Precipitation

Precipitation is a conventional process for wastewater treatment. This process offers a non-contaminating approach for wastewater treatment since the purposely added chemicals into the wastewater is generally precipitated out together with the contaminant.

In comparison with aforementioned conventional wastewater treatment processes, membrane processes provide a number of advantages including higher standards, the potential for mobile treatment units and decreased environmental impact of effluents.

Membrane processes are competitively efficient in removing particulate and dissolved contaminants, including micro-organisms and toxic species.

Supported liquid membranes (SLMs) offer a potentially attractive alternative to these processes in that they combine the process of extraction and stripping in a single unit operation (Gill *et al*, 2000:114).

1.5 Research Topic

The development of an empirical mass transfer relationship for the extraction of base metals in a carrier facilitated tubular supported liquid membrane system.

Geankoplis (2003:4) has described mass transfer as a mass that being transferred from one phase to another distinct phase. The basic mechanism is the same, whether the phases are gas, liquid or liquid-liquid. This includes distillation, absorption, liquid-liquid extraction; and leaching, filtration and membrane processes.

Mass transfer occurs when a component mixture migrates in the same phase or phase-to-phase of a difference in concentration between two points (Geankoplis, 1983:2).

The mass transfer rate through a liquid membrane can be characterised by permeability P, times the driving force for the extraction, which depends on the concentrations on both sides of the membrane (Breembroek *et al*, 1998:186).

The rate of mass transfer in the case of HFSLM is controlled by three individual resistances, which are the resistance in a solution inside the fibre, across the membrane and outside the fibre. Often one of the resistances will dominate the overall resistance. Normally, the flow through the tube side of hollow fibres is laminar and the mass transfer coefficient (k_f) could be estimated based on the Sherwood-Graetz number correlation (Kocherginsky *et al*, 2007:173)

Transport resistance of the feed boundary layer was obtained and found to be higher than other resistances; and fouling resistance increased significantly with time (Scrisurichan *et al*, 2005:186).

1.6 Scope of this study

The reactor system that will be used in this study is a Perspex bench-scale reactor with two in and outlets; and was designed and built with a single tubular supported liquid membrane, mounted vertically inside it - used as the transport medium. Counter-current flow will be utilised, so as to increase the transfer of ions. The membrane used is made of polyvinyldene flouride material.

The parameters that will be monitored are as follows:

- Temperature: room temperature; i.e. 21 ºC, 30, 40 and 50 ºC.
- Flowrate: 30-120 $ml.min^{-1}$

- pH level: will be kept at pH5 for all the metal ion extracting experiments with LIX 984N-C.
- LIX 984 N-C: will be used as a solvent dissolved in a diluent (kerosene) for the extraction of copper ions.

The constraints on this study will be as follows:

- Low concentrations will be used, 100ppm for feed solutions.
- Only Copper solution will be used for solvent extraction and the partition coefficient can be obtained.
- The partition coefficients will assists in determining the diffusivity of the metal.

.

1.7 Research Questions

- What effect do the characteristics of the feed solution have on the resistance in the laminar layer of the TSLM?
- What is the relationship between the Sherwood, the Schmidt and the Reynolds number for mass transport of metal ions aqueous feed through TSLM?
- How much metal is extracted at varying feed characteristics (Viscosity, density, pH and velocity)?

1.8 Objectives

- Extract metal ions from a low concentration metal solution, using TSLM and LIX 984N-C dissolved in Kerosene, using a bench-scale apparatus system.
- Determine the partition coefficients across the membrane.
- Evaluate the effect of the feed characteristics (Viscosity, density, constant pH and velocity) on resistance of the laminar layer of the aqueous feed side of TSLM.
- Utilise the permeation on the TSLM to determine a mass transport relationship using the dimensionless numbers.

1.9 Research Design and Methodology

The following measures were applied in order to achieve the research objectives;
A literature review was conducted, based on the related topics of mass transfer and extraction of the metal ions, using the supported liquid membrane.

Test work was conducted on a TSLM reactor, a 200ml volume of 100ppm concentration of one of the metal ion solutions, Copper, was transported on the tube side and a strippant, sulphuric acid was transported on the shell side of the reactor.

The following parameters were monitored for the experiments:

- Flow rates,
- pH; and
- Temperature.

The partition coefficients were obtained from the solvent extraction process. The equipment was available at the Chemical Engineering lab 1.11 at the Cape Peninsula University of Technology.
LIX 984N-C dissolved in kerosene was used as the carrier for the copper ion extraction. The pH of the feed solution was controlled by sodium hydroxide and Hydrochloric acid. An online pH controller was used to measure the desired pH level. The samples were analysed at Analytical Chemistry lab, Bemlab and University of Cape Town.

CHAPTER TWO

2 Literature Review

2.1 Introduction

Membrane science and technology is an expanding field and has become a prominent part of many activities within the process industries (Scott *et al*, 1996: v). The key property exploited is the ability of a membrane to control the permeation rate of a chemical species through the membrane (Baker, 2004:1).

There is a need for the new developments in applications, and theories of membrane separation could be transmitted to both scientists and engineers, in order to continue the thrust in membrane separation technology (Scott *et al*, 1996: v).

This chapter highlights the developments made in Tubular supported liquid membrane, which includes some of the factors that affect the laminar layer of the tubular supported liquid membrane for the extraction of metal ions. The literature and principles that are required to understand this work are discussed in this chapter.

2.2 Membrane Definition

The membrane can be defined as a selective barrier, between two phases - the term 'selective' being inherent to a membrane or membrane process (Mulder, 1996:12). A membrane can be homogenous or heterogeneous, symmetric or asymmetric in structure, solid or liquid; and can carry a positive or negative charge, or be neutral or bipolar.

The functioning of the membrane will depend on its structure, as this essentially determines the mechanism of separation and thus, the application.

Two types of structures are generally found in membranes: (i) symmetric and (ii) asymmetric. Symmetric membranes are uniform in structure and are produced by stretching, casting, phase inversion, etching and extrusion (Scott *et al*, 1996:5). Asymmetric membranes are produced by either phase inversion from single polymers, or as composite structures. According to Scott *et al* (1996:5), the membranes are made up of a relatively thick porous support layer (0.2-0.5mm), with a dense active skin layer (<1μm).

An asymmetric membrane is comprised of a very thin (0.1-1.0 μm) skin layer on a highly porous (100-200 μm) thick substructure. The thin skin acts as the selective membrane. The separation characteristics are determined by the nature of the membrane material or pore size. The mass transport rate is determined mainly by the skin thickness. The porous sub-layer acts as a support for the thin, fragile skin and has little effect on the separation characteristics (Biocompare, 2008).

2.3 Membrane Processes

Transport through the membrane takes place when a driving force is applied to the components in the feed. In most of the membrane processes, the driving force is a pressure difference or a concentration (or activity) difference across the membrane.

Another driving force in membrane separations is the electrical potential difference. This driving force only influences the transport of charged particles or molecules. The membrane processes, according to their driving forces, are classified in Table 2.1 (Mulder, 1996); the status of developed, developing and yet-to-be developed industrial membrane technologies is summarized in Table 2.2 (Baker, 2004).

Table 2.1: The membrane processes, according to their driving forces

Pressure difference	Concentration (activity) difference	Temperature difference	Electrical potential difference
Microfiltration	Gas separation	Membrane distillation	Electrodialysis
Ultrafiltration	Pervaporation		
Nanofiltration	Carrier mediated transport		
Reverse osmosis	Dialysis		
Piezodialysis	Diffusion dialysis		

Table 2.2: Status of membrane processes

Category	Process	Status
Developed industrial membrane separation technologies	Microfiltration, ultrafiltration, reverse osmosis, electrodialysis	Well-established unit operations. No major breakthroughs seem imminent.
Developing industrial membrane separation technologies	Gas separation, pervaporation	A number of plants have been installed. Market size and number of applications served are expanding.
To-be-developed industrial membrane separation technologies	Carrier facilitated transport membranes, piezodialysis	Major problems remain to be solved before industrial systems will be installed on a large scale

2.4 Carrier-Facilitated Transport

Carrier facilitated transport is described as transport of a substance across the plasma membrane by carrier molecules but without energy. Facilitated diffusion (also known as facilitated transport or passive-mediated transport) is a process of passive transport, facilitated by integral proteins. Facilitated diffusion is the spontaneous passage of molecules or ions across a membrane passing through specific transmembrane integral proteins.

Facilitated diffusion uses a carrier to facilitate (assist) the transfer of a particular substance across the membrane “down hill” from high to low concentration. The movement in this process occurs naturally down a concentration gradient (Sherwood, 2006).

The characteristic of a facilitated or carrier mediated transport in liquid membrane systems is the occurrence of a reversible chemical reaction or complexation process in combination with a diffusion process. This implies that two cases can be distinguished:

• Diffusion is rate-limiting (fast reaction)

• Reaction is rate-limiting (slow reaction and relatively fast diffusion)

The latter case does not occur frequently and only the former case will be considered (Mulder, 1996; Kargari et al, 2004).Carrier mediated transport has very large and various applications, Cations such as copper (Cu2+), mercury (Hg2+), nickel (Ni2+), cadmium (Cd2+), zinc (Zn2+) and lead (Pb2+), and anions such as nitrate (NO3-) and chromate (Cr2O7-) can be easily removed via facilitated transport. Gases can also be removed by facilitated transport.

Because the carrier facilitated transport process employs a reactive carrier species, very high membrane selectivities can be achieved. These selectivities are often far larger than the selectivities achieved by other membrane processes. This one fact has maintained interest in facilitated transport for the past 30 years, but no commercial applications have developed. The principal problem is the physical instability of the liquid membrane and the chemical instability of the carrier agent.

In recent years a number of potential solutions to this problem have been developed, which may yet make carrier facilitated transport a viable process (Baker, 2004; Kargari et al, 2004).

There are three basic types of liquid membranes (Ravanchi et al, 2009),

• Bulk liquid membrane (BLM)
• Emulsion liquid membrane (ELM)
• Supported liquid membrane (SLM)

Bulk liquid membranes usually consist of an aqueous feed and stripping phase, separated by a water-immiscible liquid membrane phase in a U-tube. These membranes are often used to study the transport properties of novel carriers and a small membrane surface area of BLMs makes them technologically not very attractive (Kocherginsky et al, 2007).

Emulsion liquid membranes have a very high surface area per unit volume and a low thickness and it means the separation process and accumulation inside the emulsion vehicle is fast. The problem is that the vehicles have to be produced before the process; they have to be stable enough so that leakage is reduced to minimum, but still not very stable so that they could be destroyed after the separation, thus allowing the removal of

the transported species. As a result the process has to use several unit operations and becomes technologically not very attractive. (Kocherginsky et al, 2007)
SLM process is somewhat similar to the solvent extraction process but with extraction and back-extraction performed in just one technological step. And supported liquid membrane extraction targets and removes the solute from bulk solutions based on chemical potential rather than by size difference, unlike the aforementioned pressure-driven membrane processes.

Usually facilitated ion transport through SLM is described based on the idea that the targeted ions in aqueous solutions are reacting at the interface with the chelating agent (carrier) located in the organic membrane phase (Sherwood, 2006).

The supported liquid membranes can be cast as flat sheets, tubes, fine hollow fibres etc. The different types of membrane modules are available for accommodating these shapes and structures. The last decade of membrane and module development has lessened the effects of physical compaction and has brought forth spiral membrane modules capable of operating at pressures in excess of 800 psig (55.2 bar). The techno-economic factors for the selection, design and operation of membrane modules include cost of supporting materials and enclosure (pressure vessels), power consumption in pumping and ease of replaceability (Richardson *et al* ,2002:437)

In this study, tubular supported liquid membrane was used.

2.5 Supported Liquid Membranes Process

Supported liquid membrane (SLM) extraction appears to show a potential to be used to remove traces of metal ions from waste water process streams. An SLM is a thin layer of an organic liquid, absorbed in the pores of a support. It separates the aqueous feed phase and aqueous strip phase. An extractant is dissolved in the organic membrane phase. It acts as a shuttle, extracting the metal ion from the feed phase and releasing it at the stripping side of the membrane (Breembroek *et al*, 1998:185). The permeation of metal species through SLMs can be described as the simultaneous extraction and stripping operation, combined in a single stage (Aziz *et al*, 2005).

In an SLM extraction membrane, automation can be either the extraction process alone, or in combination with the final analytical instrument. Alternatively, the extraction process can be coupled to the analytical instrument, but not in a fully automated way. Important parts of the automation system are peristaltic pumps for pumping the solutions, switch valves for directing solutions, a fraction collector for collecting the extracts; and a computer for programming timed control of events. Such a set-up also allows a fast way to optimise the extraction parameters, since the only demand is changing the parameter; and the extract is collected automatically. If the final analysis is also independently automated, then only work involved is transferring of extracts for analysis.

Although the phenomenon of supported liquid membranes is common in nature, according to Koekemoer, (2004:7), to date, no industrial application for SLMs has been reported in literature. The shortcomings of SLMs have been identified as follows:

- The low stability of the supported liquid membrane.
- Low metal fluxes.
- Osmosis through the membrane.
- The relative high cost of the membrane support.

The SLM technology is said to be one of the most efficient membrane-based methods of separation. The separation in this process is based on difference of chemical energy as a driving factor of the process. Coupled co- or counter-ion transport allows an active transport of the targeted species from the diluted solutions into a more concentrated solution; facilitating the collection of toxic or precious species in a small volume of the acceptor solution. Sometimes, it is even possible to reach saturation of the strip solutions and ultimately, the precipitation of the product (Korcherginsky *et al*, 2007:175).

2.5.1 Mechanism

The technique of SLM involves the transport ions across the membrane under a concentration gradient, by using a suitable carrier dissolved in a water immiscible organic diluent, which is absorbed on a thin microporous polymeric film. The transport process takes place whenever the conditions of the aqueous feed and strip solutions are such that the distribution ratio of the permeating species at the aqueous feed solution membrane interface is much higher than at the aqueous strip solution-membrane interface.

During extraction, a metal extractant complex is formed at the interface of the outer aqueous (feed) phase and the membrane phase. The complex permeates across the membrane and decomplexes at the interface, yielding the metal species to the inner aqueous (strip) phase (Smit, 1997:8).

Two transport schemes (in the main) dominate the membrane processes; namely, co-current and counter-current transport. These two modes are shown in Fig. 2.1 below.

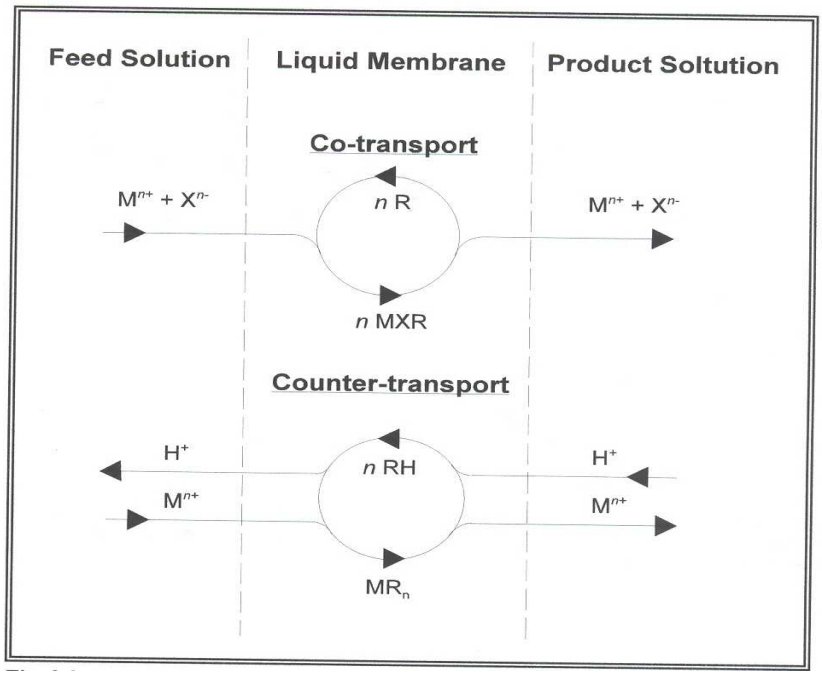

Figure 2.1: Mechanism of transport across a membrane

The mechanism of coupled transport shows that coupled transport is a reversible reaction of the permeating ion species, with the metal carrier confined to the membrane phase (Smit, 1997:8). The permeant is an ionic species or chemical which cannot enter the membrane, due to its low solubility in the hydrophobic organic solvent on the membrane. On the interface between the aqueous (feed) solution and organic solution, the metal carrier, R, reacts with the metal ion to form a neutral complex, MRn. This metal complex can diffuse freely within the organic phase and transports across the membrane to the second aqueous (strip) solution. At the interface, the metal is released, the carrier reacts with the hydrogen cation to obtain a neutral charge; and diffuses back to the feed/membrane interface.

2.5.2 Theoretical Modelling of SLM

The development of theoretical models that explain the experimental data is necessary for comprehending transport mechanisms of species through supported liquid membrane. A number of studies with related mathematical models of transport of species from aqueous solution through liquid membrane containing different carrier have been proposed in order to explain the mechanism of transport (Danesi *et al*., 1981, Sastre *et al*, 1998; Alhuisseini & Ajbar, 2000; Alguacil *et al*, 2000; Valenzuela *et al*, 2001; Benzal *et al*, 2004; Ata, 2005; Ata *et al*, 2005)

In some of the above mentioned studies, the transport rate equation have been derived taking into account aqueous film diffusion, interfacial chemical reaction or fast interfacial chemical reaction and membrane diffusion as simultaneous controlling steps and, the possible rate controlling steps were estimated by comparing the relative values of the successive resistances. These models were developed under the following assumptions;

- Ideal steady- state conditions
- Linear concentration gradient throughout the membrane.

The transport of the metal ion through the supported liquid membrane system is considered to be composed of many elementary steps. These steps are expressed as follows (Alhusseini and Ajbar, 2000; Danesi *et al*, 1981; Marchese *et al*, 1993; Ruey-Shin *et al*, 2000). Diffusion of metal ions from the bulk of the feed phase to the aqueous stagnant layer in the feed-membrane side; interfacial desolvation and solvation reaction at feed-membrane and membrane-stripping interfaces; chelating reaction between metal ion and carrier at the feed-membrane interface; diffusion of hydrogen ions from the feed-membrane interface to the bulk of the feed phase; diffusion of carrier and carrier–metal complex from the feed-membrane interface to the stripping-membrane interface; diffusion of hydrogen ions from the bulk of the stripping to the aqueous stagnant layer in the stripping-membrane side; decomplexation reaction of carrier–metal complex with hydrogen ion at the stripping-membrane interface; diffusion of the regenerated carrier back to the feed-membrane interface and, finally, diffusion of metal ions from the stripping-membrane interface to the bulk of the stripping phase. In the description of the transport model, the following assumptions were made: the chemical reactions were fast and not rate limiting, diffusion of hydrogen ions in both aqueous film layers was rapid, and the resistance of diffusion of the carrier from the feed-membrane interface to the

stripping-membrane interface and diffusion of the regenerated carrier back to the feed-membrane interface were also neglected, and the diffusion processes could be described by Fick's diffusion equations.

Since the concentration of species in the batch SLM process depend both on position and time, the transport of metal ions through supported liquid membrane has been investigated at the unsteady state .The presence of the accumulation term in the inventory rate equation complicates the mathematical problem since the resulting equation is a partial differential equation even if the transport takes place in one direction. The solution of partial differential equations depends not only on the structure of itself but also on boundary conditions.

The boundary layer can be considered as a concentrated solution through which solvent molecules permeate, with the permeability of this stagnant layer depending very much on the concentration and the molecular weight of the solute.
Concentration polarisation phenomena lead to an increase of the solute concentration at the membrane surface. If the solute molecules are completely retained by the membrane, at steady state conditions, the convective flow of the solute molecules towards the membrane surface will be equal to the diffusive flow back to the bulk of the feed. Hence, at 100% rejection, the average velocity of the solute molecules in the boundary layer will be zero. Because of the increased concentration, the boundary layer exerts a hydrodynamic resistance on the permeating solvent molecules (Mulder, 1996:436).

2.6 Previous work done on the SLM modelling

Koekermoer, 2004, evaluated the mechanisms involved in the extraction of nickel from the low concentration effluents by means of supported liquid membrane.

The modelling of the SLM-process was done by solving a system of equations that describe all six steps involved in the extraction process and a special computer program was written to solve the system of equations. The process model showed that the nickel flux through the SLM is determined by the diffusion of the nickel through the feed boundary layer as well as the diffusion of the organo-metallic species through the

membrane and although temperature does not have an effect on the extraction equilibrium, it does have a beneficial effect on both of these transfer steps.
The process model showed that there exists an extractant concentration at which the nickel flux is an optimum and that this optimum is dependent on temperature. The effects of all the variables involved in the extraction process are interdependent and the model is capable of predicting the effect of this interdependence.

In the research done by Alguacil *et al*, 2000, a physico-chemical model is derived describing the transport mechanism which consists of: diffusion process through the feed aqueous diffusion layer, fast interfacial chemical reaction and diffusion through the membrane.
The permeability of the metal seems to be governed by the diffusion of copper species at the feed-membrane interface. The mass transfer coefficient was calculated from the described model as 2.8×10^{-3} $cm.s^{-1}$, the thickness of the aqueous boundary layer of 2.6×10^{-3} cm^{-1} and the membrane diffusion coefficient of copper containing $1.2 \times 10^{-8} cm^2.s^{-1}$.

Ata, 2005 have studied the transport of copper from aqueous solution containing zinc, cadmium, nickel, and cobalt through a flat sheet supported liquid membrane using LIX984 dissolved in different diluents as a mobile carrier.

A transport rate model has been developed as expressed below

- Diffusion of metal ions from the bulk of the feed phase to the aqueous stagnant layer in the feed-membrane side,

$$N_{Cu} = (\frac{D_{Cu}}{\delta})_f ([Cu^{2+}] - [Cu^{2+}]_{i.1}) = k_f ([Cu^{2+}]_f - [Cu^{2+}]_{i,1})$$

Equation 2.1

- Diffusion of carrier-metal complex from the feed-membrane interface to the strip membrane interface,

$$N_{Cu} = (\frac{D_{R2Cu,b^{\varepsilon}}}{l\tau^2})_f ([R_2Cu]_{i,1} - [R_2Cu]_{i,2}) = k_m([R_2Cu]_{i,1} - [R_2Cu]_{i,2})$$

Equation 2.2

- Diffusion of copper ion from the strip-membrane interface to the bulk strip phase.

$$N_{Cu} = (\frac{D_{Cu}}{\delta})_s ([Cu^{2+}]_{i,2} - [Cu^{2+}]_s = k_s([Cu^{2+}]_{i,2} - [Cu^{2+}]_s$$

Equation 2.3

The mass transfer coefficient of aqueous boundary layer, the thickness of the aqueous boundary layer, and the membrane diffusion coefficient of the copper carrier complex were calculated and the results are shown in table 2.3.

Table 2.3: The mass transfer Coefficients

Diluent	Support	K_{ext}	k_f(m/s)	k_m(m/s)	k_s(m/s)	$D_{R2Cu,m}$(m^2/s)	l_f(m)
Kerosene	Teflon	324.3	2.4E-05	6.0E-06	2.3E-05	2.6E-10	3.0E-05
n-Heptane	Teflon	1018.8	2.5E-05	1.3E-05	3.2E-05	5.7E-10	2.9E-05
n-Octane	Teflon	1062.3	2.5E-05	2.5E-05	2.4E-05	1.1E-09	2.9E-05
Kerosene	Durapore	324.3	2.4E-05	4.0E-06	2.3E-05	4.0E-10	3.0E-05

A study done by Yang *et al*, introduces a more detailed and physically reasonable mechanism of copper removal from typical ammoniacal waste aqueous solutions which was developed to fit all experimental results.
The “Big Carrousel” mechanism describes copper facilitated transfer from ammoniacal solution through HFSLM where the possibilities of a carrier distribution between membrane and aqueous phases and simultaneous reactions of the carrier and copper in aqueous reaction layer have been taken into account. The reaction layer plays an important role in the actual mass transfer process, especially when feed copper concentration is low (Korcherginsky *et al*, 2007:104).

The mechanism is based on the idea that the carrier is able to diffuse from organic into the thin aqueous reaction layers where ion exchange reactions are taking place. The following assumptions are made:

- The diffusion of H+ ions is much faster compared to that of Cu(II) ions.
- The chemical reactions (formation of copper-carrier complexes and their decomposition) take place in thin aqueous reaction zones, which are located in the aqueous unstirred diffusion film (Nernst layer) near the organic membrane phase as shown in Fig. 2.2.

The layers of the hollow fibre membrane shown in Fig. 2.2 demonstrate the steps that the feed solution passes through before it reaches the strip solution.

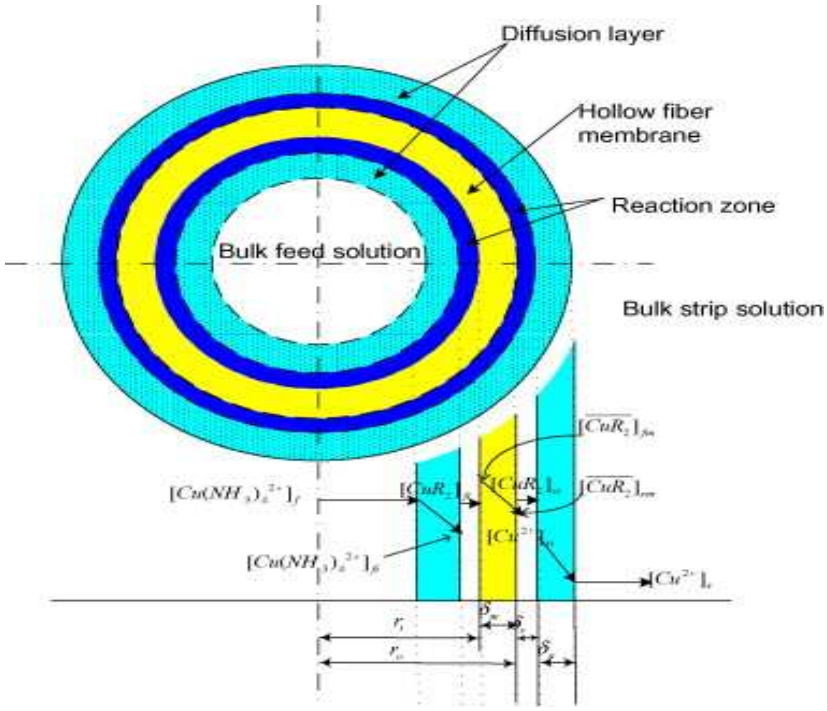

Figure 2.2: Schematic description of Cu (II) transport through HFSLM system (Yang *et al*, 2007)

The process therefore can be described as the following:

Step 1: The predominant form of Cu (II) ions in the feed ammoniacal solution is $[Cu(NH_3)_4]^{2+}$. Due to the concentration gradient, this complex diffuses through an aqueous unstirred diffusion film formed along the hollow fiber wall:

$$J_1 = k_t([Cu(NH_3)_4{}^{2+}]_f - [Cu(NH_3)_4{}^{2+}]_{fi}$$

Equation 2.4

Here subscripts f and fi correspond to the bulk feed phase and the imaginary plane inside the unstirred diffusion layer, which is the outer boundary of reaction zone as shown in Fig. 2.2.

Step 2: When the aqueous reaction zone is reached $Cu(NH_3)_4^{2+}$ ions react with the carrier dissolved from the membrane to form copper-carrier complexes in a homogeneous exchange reaction:

$$Cu(NH_3)_4{}^{2+} + 2HR \xleftrightarrow{K_f} CuR_2 + 2NH_4{}^{+} + 2NH_3$$

Equation 2.5

The process for simplicity is characterized by Eq. (2.5) (equilibrium state) or Eq. (2.6) (rate of copper-carrier complex formation):

$$K_{ex,f} = \frac{k_f}{k_r} = \frac{[CuR_2]_{fi}[NH_3]^2[NH_4{}^{+}]^2}{[Cu(NH_3)_4{}^{2+}]_{fi}[HR]^2{}_{fi}}$$

Equation 2.6

Where k_f and k_r represent the forward and reverse reaction constants, respectively; $K_{ex,f}$ is the equilibrium constant for $Cu(NH_3)_4^{2+}$/LIX54 system.

The distribution of the copper-carrier complexes and the carrier between the organic membrane phase and internal reaction zone can be described by distribution coefficients mCuR_2 and mHR:

$$mCuR_2 = \frac{[CuR_2]_{fm}}{[CuR_2]_{fi}}$$

Equation 2.7

$$mHR = \frac{[HR]_{fm}}{[HR]_{fi}}$$

Equation 2.8

Step 3: The complexes formed in the reaction zone and extracted into the membrane, permeate through the membrane toward the outer side of the hollow fibers:

$$J_3 = k_m([\overline{CuR_2}]_{fm} - [\overline{Cu}R_2]_{sm}$$

Equation 2.9

Here subscript sm indicates species at the external reaction zone/membrane interfaces.

Step 4: After transmembrane transport and back-extraction into the external reaction zone the copper ions are stripped off from the copper-carrier complexes by strong acid present in the shell side of hollow fiber membrane module:

$$CuR_2 + 2H^+ \xleftrightarrow{k'_f} Cu^{2+} + 2HR$$

Equation 2.10

The copper ions formed in the ion exchange diffuse through the unstirred external aqueous film and enter the bulk stripping solution:

$$J_5 = k_s([Cu^{2+}]_{si} - [Cu^{2+}]_s)$$

Equation 2.11

In this case the overall mass transfer coefficient (*K*) or overall mass transfer resistance (*R*) can be described as

$$\frac{1}{K} = \frac{1}{k_t} + \frac{1}{k_m m(\ln r_o / r_i)} + \frac{r_i}{m k_s r_o} + \frac{1}{k_R}$$

Equation 2.12

$$R = R_t + R_m + R_S + R_r$$

Equation 2.12

where k_R is the additional mass transfer coefficient for chemical reaction happening in the aqueous reaction layer; R_t, R_s, R_m and R_r represent the mass transfer resistances due to diffusion inside the fiber tube, in the shell side, across the membrane and the chemical reaction kinetics, respectively.

The “Big Carrousel” mechanism is first time developed to describe the experiment results in the HFSLM systems. The modeling of Cu(II) removal from the ammoniacal wastewater through the HFSLM system based on “Big Carrousel” mechanism and also the experimental results show that the overall Cu(II) mass transfer coefficient is determined based on the resistance-in-series model, which accounts for the mass transfer resistances in the tube, shell side of the membrane contactor, in the organic membrane phase and also macrokinetic resistance of chemical reaction.

The previous work done on the supported liquid membrane by the mentioned researchers indicates that there are many steps involved in the extraction of the metal ions, these steps need to be considered when using all different types of slm’s,e.g flatsheet, hollow fiber, tubular,etc.

Particularly for this study, one investigates the effect of the feed characteristics on the diffusion of metal ions from the bulk of the feed phase to the aqueous stagnant layer in the feed-membrane side and other steps involved as explained above are not part of this research.

It has been indicated that some of the factors that affect resistance in the feed-side laminar layer include; flowrate, density, viscosity and feed concentration. To determine relationships between these parameters, dimensionless-groups are used to allow results to be generalised and are hence used to predict performance for different systems (fuelcellknowledge, 2003).

2.7 Mass transfer description

Mass transfer is described as the movement of mass in response to a departure from equilibrium.

2.7.1 Mechanisms of Mass Transport

- Diffusion: molecular level transport of a species through another species as a result of a concentration gradient (microscopic scale)
- Convection: bulk flow which occurs under a pressure gradient or other imposed external force (macroscopic scale)
- Turbulent mixing: macroscopic packets of fluid, or eddies, move under inertial forces (macroscopic scale)

Mass transfer is quantified by Flux

Flux of species A (in a mixture of A+B) = moles or mass of A crossing a stationary plane/ x-sectional area per time

Flux of A via Diffusion = $J_A = -D_{AB}\left[\frac{dC_A}{db}\right]$

Equation 2.14

J_A = flux of A due to diffusion (moles or mass/area/time) relative to the volume average velocity of the bulk fluid. J_A is similar to heat transfer via conduction and momentum transfer via shear stress.

D_{AB} = diffusivity of A in B (area/time)

C_A = concentration of A (moles or mass/vol)

db is the differential length in the direction of diffusion (length), perpendicular to the x-sectional area across which diffusion is occurring.

The diffusive flux is a vector that depends on concentration gradients.

Flux of A via Convection = $C_A * u_o$ relative to a fixed plane

u_o = volume average velocity of the fluid (length/time)

Often this term is lumped with diffusive and turbulent terms and described using a “mass transfer coefficient” just like convective heat transfer

i.e. $N_A = k_c(C_{A1} - C_{A2})$

Equation 2.15

N_A = total flux of A due to combined mechanisms, k_c= mass transfer coefficient (length/time), C_{A1} and C_{A2} = concentration of A at points 1 and 2 respectively. **k_c** is analogous to **h**, the convective heat transfer coefficient and is function of the system geometry, fluid properties and flow velocity.

Flux of A via Turbulence $= -\varepsilon_M [\frac{dC_A}{db}]$

Equation 2.16

ε_M= mass eddy diffusivity (area/time). In turbulent systems – diffusive, convective & turbulent mechanisms are all at work and transfer is usually described using mass transfer coefficients as stated above.

Total flux of A = N_A= sum of diffusion, convection, turbulence flux of A

$$N_A = -(D_{AB} + \varepsilon_M)[\frac{dC_A}{db}] + C_A * u_o$$

Equation 2.17

2.7.2 Mass Transfer Theories

2.7.2.1 Film Theory

$$k\alpha[D_{AB}]^1$$

Equation 2.18

This theory assumes that the bulk fluid is thoroughly mixed (flow weighted average concentration is used in flux calculations). It is often used in complex problems involving multicomponent diffusion or diffusion plus chemical reaction in a single phase.

2.7.2.2 One-way or Stagnant Film Diffusion

$$N_A = \frac{(D_{AB} + \varepsilon)(C_{A1} - C_{A2)}}{B_T (1 - y_A)_L} = k_c (C_{A1} - C_{A2})$$

Equation 2.19

This is a good approximation for unsteady-state diffusion or a combination of molecular and eddy diffusion in a single phase.

2.7.2.3 Boundary Layer Theory

$$k\alpha[D_{AB}]^{\frac{2}{3}}$$

Equation 2.20

This theory is based on solving differential mass and flow balances in the boundary layer (thin laminar layer next to surface). This theory serves mainly as a guide in developing empirical correlations for k in a single phase.

2.7.2.4 Two-Film Theory

$$N_A = K_A(y^*_A - y_{A)}$$

Equation 2.21

The two-film theory is used to describe diffusion between two phases. This approach is used in equipment design for absorption, extraction and distillation, membrane separation

2.7.3 Mass transfer Coefficient

The mass transfer coefficient k_f depends strongly on the hydrodynamics of the system and can therefore be varied and optimised.
It is related to the Sherwood number as shown in equation 2.22

$$Sh = \frac{k_f L}{D_{fm}}$$

Equation 2.22

The Sherwood number, Sh (also called the mass transfer Nusselt number) is a dimensionless number used in mass-transfer operation. It represents the ratio of convective to diffusive mass transport.

According to Richardson *et al* (2002:651), the Sherwood number can be expressed as a function of Re and Sc indicated by dimensional analysis as shown in equation 2.23 The actual relationship is determined from experimental data. It represents the ratio of length scale to the diffusive boundary layer thickness. Note that the Sherwood number can be defined locally or as an average overall value for a given surface.

$$Sh = C\,\mathrm{Re}^{n}\,Sc^{m}$$

Equation 2.23

The values of C, m & n can be calculated by employing linear regression algorithm (Ata *et al*, 2005:157).

The Reynolds number of a flow strongly influences the velocity boundary layer characteristics and hence, is of great importance in determining transfer coefficients (fuelcellknowledge, 2003). An increase in the feed flow rate will increase the Reynolds number (Equation 2.24) and this will affect the mass transport across the membrane (Ata *et al*, 2005:157).

$$\mathrm{Re} = \frac{\rho L v}{\mu}$$

Equation 2.24

An increase in temperature of the feed will increase the mass transfer rate in the aqueous film at the feed and stripping phases and results in a decrease in viscosity of the liquid phases and the liquid membrane inside the support. (Ata *et al*, 2005:160). This will have a direct effect on the Schmidt's number, Equation 2.25.

$$Sc = \frac{\mu}{\rho D_{AB}}$$

Equation 2.25

According to Treybal (1986:40), an important interpretation of the Schmidt number is the relative thickness of the velocity and concentration boundary layers. Sc provides a

measure of the relative effectiveness of momentum and mass transport, by diffusion in the velocity and concentration boundary layers, respectively.

The parameters that influence the Reynold's number and the Schmidt's number will influence the Sherwood number (Equation 2.23). From Equation 2.22, the aqueous feed mass transfer coefficient (k_f) can be calculated.

Some semi-empirical relationships for mass transfer coefficients in pipes and channels are given as shown in table 2.4

Table 2.4: Semi-empirical relationships for mass transfer coefficients

	Laminar	Turbulent
Tube	$Sh = k_c \, dh/D = 1.62(\mathrm{Re}.Sc.dh/L)^{0.33}$	$Sh = 0.04\,\mathrm{Re}^{0.75}\, Sc^{0.33}$
Channel	$Sh = 1.85(\mathrm{Re}.Sc.dh/L)^{0.33}$	$Sh = 0.04\,\mathrm{Re}^{0.75}\, Sc^{0.33}$

2.8 Feed Characteristics

2.8.1 Extractant Concentrations

For a given metal concentration in the aqueous phase, it is believed that the extraction coefficient will increase with an increase in extractant concentration. Extraction by a particular solvent, however, does not necessarily increase linearly with an increase in the extractant concentration; since the viscosity of the extractant increases with concentration. This may have an inhibiting influence on the carrier function that it must perform, during the transportation of metal species across the membrane. It is therefore necessary to evaluate each system, individually, in order to optimise the conditions for maximum results (Erlank, 1994:40).

Modern extractants make separation much faster, due to facilitated transport and being more selective, due to their chemical specificity. Because of small volumes of extractants and the possibility of conducting a continuous process, makes the SLM more attractive than classical ion exchange and solvent extraction technologies. Due to high diffusion coefficients in SLM, it is possible to have ion extraction, transport and re-extraction in one continuous technological step (Kocherginsky *et a*l, 2007:175).

2.8.2 Effect of pH

All chelating or acidic type extractants in counter-current mode extraction process liberate a hydrogen ion on the extraction of a metal ion:

$$M^{n-} + nHR \leftrightarrow MRn + nH^{-}$$

Equation 2.16

Thus, the greater the amount of metal extracted, the more hydrogen ions are produced and transferred to the feed side. This results in a decrease in pH of the feed side. The equilibrium will shift to the left and consequently results in a decrease in the amount of metal extracted (Erlank, 1994:40).

The pH of the system also affects both the metal ion and the extractant. If the pH on the feed side is increased, the metal will eventually hydrolyse and will not extract. A decrease in pH may result in the formation of non-extractable metal species, as a result of complexation.

At low pH values, all extractants suffer protonation. If the extractant is unable to ionise, it will not be able to form a complex with a metal ion; and extraction will not occur. Thus, it can be safely concluded that SLM extraction in this mode is pH-driven which implies the maintenance of a pH difference across the membrane for optimum results.

It can be seen from Fig. 2.3 that the copper ion transport rate increases with a decreasing pH of the feed phase (Ata, 2004:275).

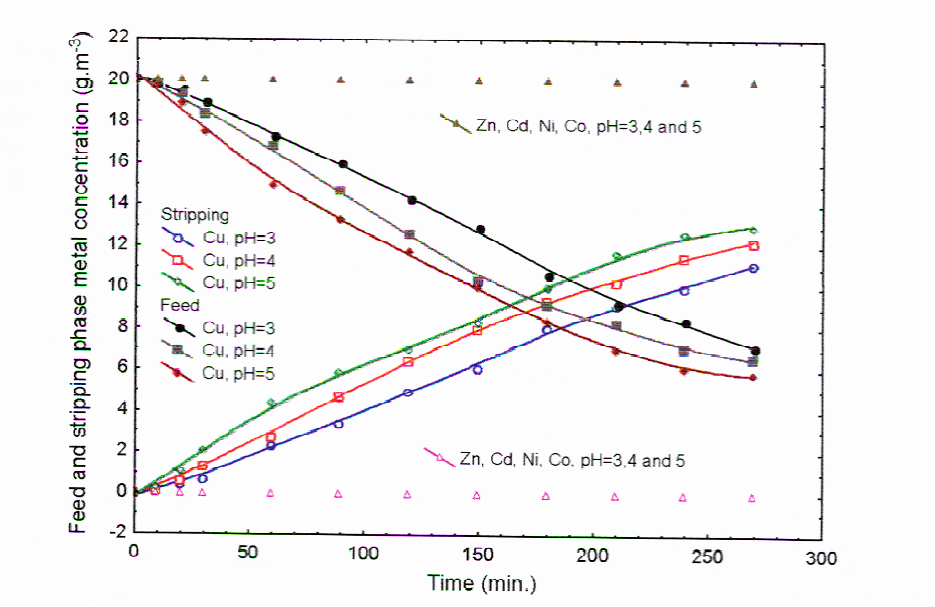

Figure 2.3: Concentration of copper at various pH conditions.

2.8.3 Aqueous phase composition

Extraction of metals is affected by the type and concentration of the ionic species present in the aqueous phase. Where the metal complex in the aqueous phase has a stability constant greater than that of the metal-extractant complex, it then can be predicted not to extract (Erlank, 1994:41).

If complexation of a metal in the aqueous phase produces a neutral species, it will not be extracted by an anionic or cationic extractant. The formation of a non-extractable metal ion or ion-associated complex in the aqueous phase is dependant on the ion and on its concentration, as well as chemical conditions such as pH.

Conversely, if the metal species in the aqueous phase is uncharged, then extraction with neutral or solvating extractants is more likely. However, increasing the ionic strength may seriously affect the extraction, either by the formation of stable metal complexes, or by the formation of unextractable charged species (Smit, 1997:12).

2.8.4 Metal Ion Concentration

If the metal ion concentration in the system is increased, all other conditions remaining constant, the concentration of free extractant will decrease. Thus, a relative decrease in

the extraction coefficient for that system could result in the limiting case of carrying capacity (Erlank, 1994:42).

Under certain controlled conditions, the extraction coefficient is independent of the metal ion concentration. This is not the case, however, at high metal concentrations. It must be kept in mind that activities were replaced by concentration for the sake of simplicity, but activities can change substantially with increasing concentration of reactants (Koekemoer, 2004:13).

2.8.5 Temperature Effect

The temperature of the process affects the mass transfer rate in the aqueous film and membrane and the chemical reactions occurring in the feed membrane and the stripping membrane interfaces. An increase in temperature results in an increase in mass transfer rate through the aqueous film at the side of the feed and stripping phases; and in the transport of the carrier and carrier-metal complex inside the support; and a decrease in the viscosity of the liquid inside the support (Ata *et al*, 2005:160).

Chemical reactions in high polymer substances are often considerably dependant on the mobility of the reactants, as well as the kinetics of the reaction itself (Crank, 1979:55).

2.8.6 Linear Velocity Effect

Linear velocity plays an important role in terms of gel layer formation, existence of the boundary layer and fouling of the membrane. It is important to keep it constant (Malherbe, 1993: 27).

The changing flow rate changes the thickness of the stagnant films in the feed-membrane and stripping-membrane sides. An increasing flow rate causes a decrease in the stagnant film and consequently, the mass transfer rate increases (Ata *et al*, 2005:160).

2.8.7 Viscosity

In liquids, the viscosity decreases with increasing temperature. Liquids are essentially incompressible; the viscosity is not affected by pressure.

2.9 LIX 984N-C

A 1:1 volume blend of LIX 860N-IC and LIX 84-IC is a mixture of 5-nonylsalicylaldoxime and 2-hydroxyl-5nonylacetonephenone oxime in a high flash point hydrocarbon diluent which forms water insoluble complexes with various metallic cations in a manner similar to that shown below for:

$$2RH_{(org)} + Cu^{+2}{}_{(aq)} \Leftrightarrow R_2Cu_{(org)} + 2H^{+}{}_{(aq)}$$

Equation 2.11

This extractant contains no added modifier. It may show advantages when used for Copper extraction from solutions containing soluble silica or finely divided solids (Cognis-us, 2002).

2.10 Membrane Material

Koch membrane systems Inc., 2007, has reported that Since the introduction of membrane treatment technology back in the 1970's, a variety of membrane types and configurations have been developed, including tubular membrane. Tubular membranes operate in tangential or cross-flow designs, where process fluid is pumped along the membrane surface in a sweeping type action.

There are many advantages of tubular membrane configurations. Besides their rugged construction, they have a distinct advantage of being able to process high suspended solids and concentrate product, successfully and repeatedly, to relatively high end point concentration levels, without plugging.

Tubular membranes are based on either PVDF (polyvinylidene fluoride) or PS (polysulfone). They are capable of continuous, reproducible processing cycles, which means they are cleanable, durable, easy to operate and a proven advance in technology.

Figure 2.4: Example of Tubular membranes (courtesy of Koch Membrane Systems Ltd)

2.10.1 Polyvinylidene flouride (PVDF)

The material is a popular choice for ultrafiltration and micro filtration membranes. It offers similar pH and temperature limits as polysulphone (allowing operation up to 80 ℃ and will tolerate a pH from 1.5-12 for cleaning), but has a higher tolerance to oxidising agents such as chlorine. It is available as an anisotropic membrane, formed by phase inversion (Scott *et al*, 1996:35).

The tortuosity factor plays a very important role in determining the mass transport mechanism. The larger the turtousity value, the lower the permeation flux (Srisurichan *et al*, 2005:189).

The images of the PVDF membrane analysed using an electron microscopic unit are shown in Fig. 2.5 to 2.7.

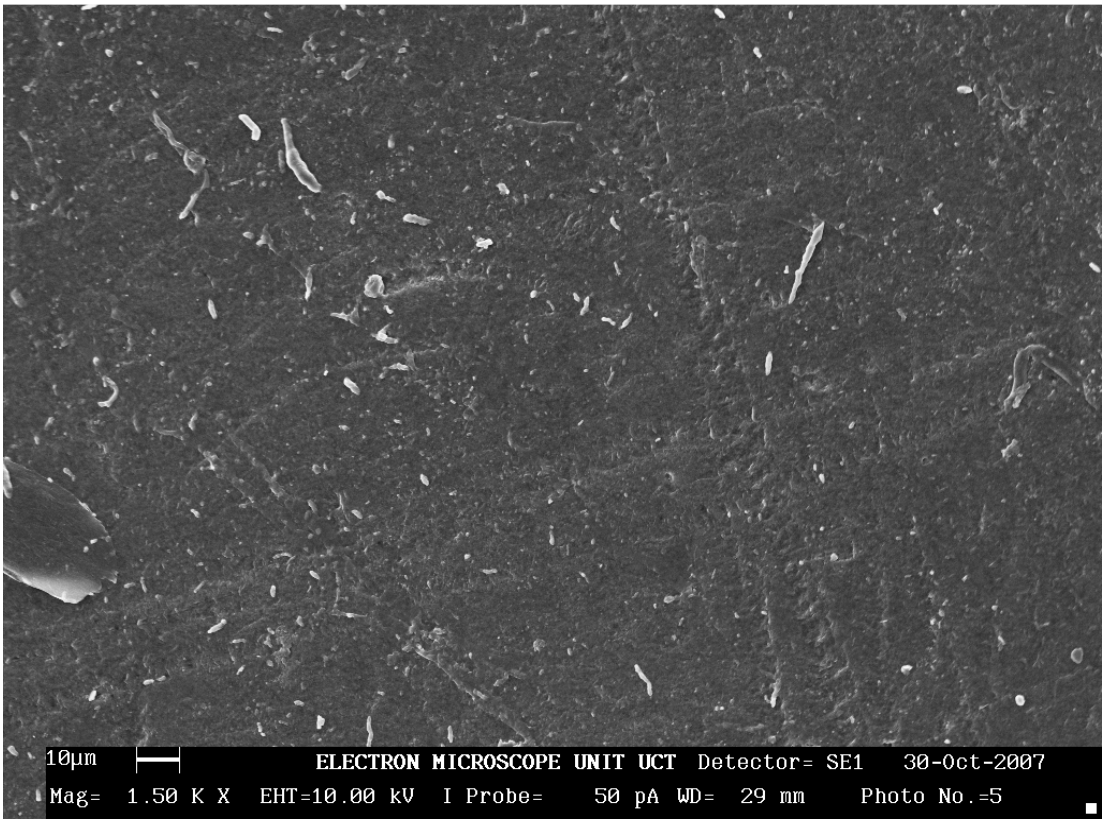

Figure 2.5: The images were analysed using the electron microscopic unit, this is the inner layer of the PVDF membrane magnified by 1500.

The separation characteristics are determined by the nature of membrane material or pore size; and the mass transport rate is determined mainly by the skin thickness (Biocompare, 2008).

The images were analysed using the electron microscopic unit. Fig. 2.5 shows the inner layer of the PVDF membrane.

The membrane material is affected by several factors, such as the pressure drop across the membrane, which increases beyond some minimum pressure Δp_{min}. The largest pores in the membrane become flooded with the non-wetting fluid; and the fuid flows through these penetrated pores. As the pressure drop is increased further, successively smaller pores become flooded until eventually, the entire membrane is flooded. Subsequent increases in pressure drop cause corresponding linear increases in flow (Mcguire *et al*,1994:127).

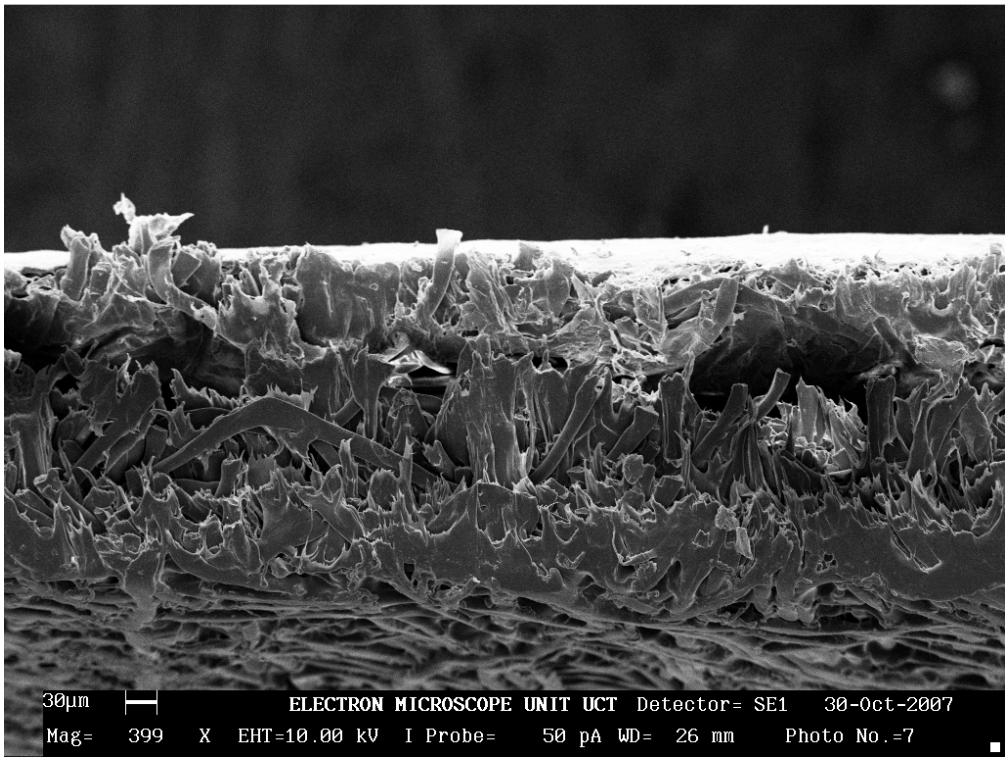

Figure 2.6: The cross sectional area of the tubular PVDF membrane magnified by 399.

The cross sectional area of the PVDF tubular membrane is shown in Fig. 2.6.According to literature, a thicker membrane results in lower flux, if the diffusion through the membrane is the rate controlling step. However, it also increases the capacity of the membrane to store the extractant solution and therefore, the stability of the membrane is improved. A higher porosity results in a lower tortuosity to the diffusing organo-metallic complex; and results in higher fluxes. The higher porosity also increases the capacity of the membrane, but this is countered by the lower support structure - there is a theoretical optimum porosity for optimum stability (Koekemoer, 2004:14).

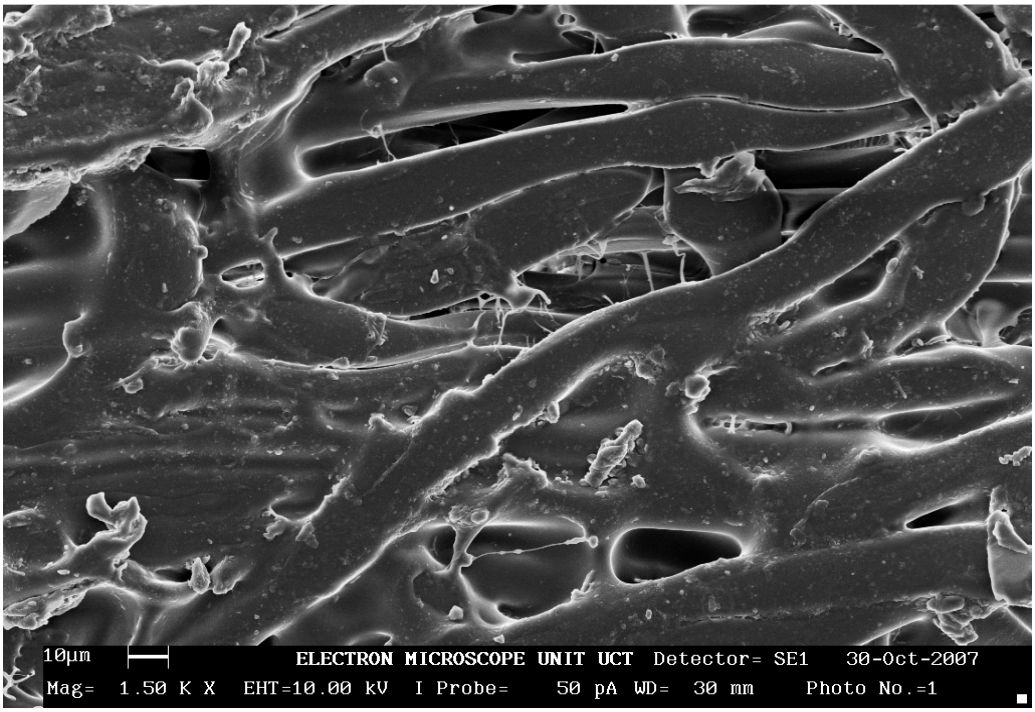

Figure 2.7: The outer layer of the PVDF membrane magnified by 1500.

The outer layer of the PVDF tubular membrane magnified by 1500 is shown in Fig. 2.7. The hydrophobic nature of the porous membrane prevents penetration of the aqueous solution into the membrane pores, resulting in gas/liquid or liquid/liquid interface at each pore entrance. It is estimated in the study done by Feng *et al*, 2006:55 ,that if a stronger hydrophobic membrane material with larger pores is selected, greater permeate flux will be expected under a high rejection coefficient.

CHAPTER THREE

3 Material and Method

This section provides a thorough description of the methodology and material used in this study. The experiments were divided into two sections: Equilibrium data and Kinetic data.

The first section was done in order to obtain the partition coefficients of the feed; and the strip for the copper metal ions.

3.1 The Equipment used for the Experiments.

- Automatic pH controller dosing pump (Hanna instruments)
- Double pipe bench scale Reactor system
- 2 Peristaltic pumps (Dune Engineering)
- 2 water baths (Buchi 461)
- 2 hot plate stirrers
- Separation flask
- Pipette

3.2 Material used

- Tubular PVDF Membrane(from Koch membranes)
- 25% Sulphuric Acid solution-Strippant
- LIX 984 N-C-Extractant (Cognis Corporation)
- Kerosene/Paraffin liquid (Kimix chemicals)
- 100ppm Copper sulphate solution
- Sodium Hydroxide solution- Base

3.3 Description of materials

3.3.1 Membrane

The membrane sample shown in Fig. 3.1 is discussed in depth in chapter two.

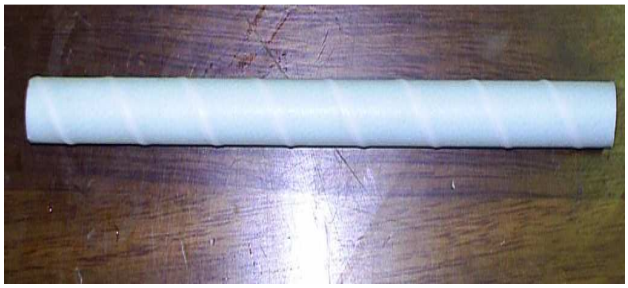

Figure 3.1: Tubular membrane

Table 3.1: Membrane dimensions

Polymeric material	PVDF
Fiber i.d.(cm)	1.1
Fiber o.d. (cm)	1.2
Membrane wall thickeness (cm)	0.5
Active membrane length (cm)	20
tortuosity	2.00
Porosity	0.6
Pore size (µm)	0.2
Cross sectional area (cm^2)	0.950

3.3.2 LIX 984N-C

The LIX 984N-C was supplied by Cognis corporation mining chemicals and this reagent is widely used in commercial copper solvent extraction circuits.

According to Cognis Corporation, 2002, LIX 984N-C, a 1:1 volume blend of LIX 860N-IC and LIX 84-IC is a mixture of 5-nonylsalicylaldoxime and 2-hydroxy-5-nonylacetophenone oxime in a high flash point hydrocarbon diluent, which forms water

insoluble complexes with various metallic cations, in a manner similar to that shown for copper below.

$$2RH_{(org)} + Cu^{2+}{}_{(aq)} \Leftrightarrow R_2Cu_{(org)} + 2H^+$$

Equation 3.1

3.3.3 Vacuum desiccator

Figure 3.2: A Vacuum desiccator

A Vacuum desiccator shown in Fig 3.2 is used to impregnate the pores of the liquid membrane with the extractant, LIX 984N-C, dissolved in kerosene.

3.3.4 Loading of membrane with carrier(20% LIX 984N-C)

A polyvinyldene-flouride tubular membrane module was used to prepare the system as discussed in the experimental section.
The walls of the tube were impregnated with liquid membrane phase by pumping an organic (20% LIX 984-NC dissolved in Kerosene) through the module using a Vacuum desiccator and a peristaltic pump for 1hour. Then, the membrane was taken out from the organic phase and the excess organic liquid was washed out by de-ionized water.
The membrane pores impregnated by organic solution acts as a barrier to avoid the direct contact of the feed and the stripping acid.

3.3.5 Sulphuric Acid

Sulfuric (or Sulphuric) acid, H_2SO_4 is a strong mineral acid, soluble in water at all concentrations. The acid has a density of 1.834 at 25℃ and freezes at 10.5℃. It is an important industrial commodity, used extensively in petroleum refining and in the manufacture of fertilizers, paints, pigments, dyes, and explosives. It reacts with most metals upon heating to produce sulfur dioxide. It ionises in aqueous solution and hence conducts electricity. (Henly, 1983:81)

3.3.6 Copper Sulphate

Copper (II) sulfate ($CuSO_4$), is a salt that exists as a series of compounds that differ in their degree of hydration. Copper and its alloys constitute one of the major groups of commercial metals. They are widely used because of the excellent electrical and thermal and thermal conductivities, outstanding resistance to corrosion, and ease of fabrication, together with good strength and fatigue resistance. Copper alloys are used in many applications that require service for extended periods in environments that can be aggressive to other metals.

Copper metals are used in equipment for handling salt solutions of various kinds; particulary those that are nearly neutral, among these are nitrates, sulfates and chlorides of sodium and potassium. (Boyer *et al*, 1984:7)

3.3.7 Reactor system

A Counter-current, double pipe Perspex bench-scale reactor with diameter of 30 mm, consisting of a single hydrophobic PVDF tubular membrane, mounted vertically inside it by epoxy quickset glue, was used for the test work as shown in Fig. 3.3. The membrane was impregnated with the LIX 984N-C dissolved in kerosene. This organic phase acts as the transport medium inside the membrane. Dilute Copper solution passed through the centre pipe and sulphuric acid, as strippant passed through the shell side.

Figure 3.3: A Counter-current, double pipe Perspex bench-scale reactor

3.3.8 Pumps used

The peristaltic-type pump from Dune Engineering, offers a low cost method of automatic fluid delivery. It has the advantage of being self-priming and has a disposable fluid path, which consists simply of special tubing.

3.3.9 Process Control

The temperature of the feed and strip solutions was controlled using the water bath and thermometer as a measuring device. As shown in Fig. 3.4

The pH of the feed solution was controlled using an automatic pH controller dosing pump. This controller has a proportional unit which assists in the pump dosing, slowing down when the measured pH level approaches the set value, thus ensuring the precise dosage; and avoiding costly waste of chemicals, as a result of over-dosage.

A sodium hydroxide (NaOH) solution was used as a dosing agent.

Figure 3.4: Water baths used for temperature control

3.3.10 Analytical Methods

Samples of the bulk feed and strip solutions were collected at predetermined time intervals and concentrations of metal ion were measured using a Varian Techtron AA-1275 Atomic Absorption spectrophotometer. The metal solution was diluted with de-ionized water so as to coincide with the measuring range of the AA.

An automatic pH controller in conjunction with a pH meter was used to measure and control the pH of the feed solution.

3.4 Experimental description

3.4.1 Solvent extraction

10ml of Copper sulphate solution (100ppm) was prepared and combined with equal volumes of extracted LIX 984N-C dissolved in Kerosene, using a stirrer for 20 minutes and then separated using a separation flask, is shown in Fig. 3.5. From separation, a 1ml volume sample was taken from a feed solution and the remaining LIX984N-C solution was combined with equal volume of Strippant (25% Sulphuric acid) and stirred for 20minutes. A sample was taken on the strip phase after separation. Both the feed and the strip samples were analysed for the copper ion concentration.
The results from the solvent extraction were used to determine the partition coefficient of copper metal ion, at varying extraction conditions.

Figure 3.5: The separation process for the solvent and the feed solution

3.4.2 Tubular supported liquid membrane experimental work

The 20cm long tubular membrane type from Koch membrane systems was impregnated with a carrier consisting of an extractant (20% LIX 984N-C), dissolved in organic diluent kerosene, a flammable hydrocarbon liquid, using a vacuum desiccator. The membrane was then fixed inside the SLM reactor as shown in Fig. 3.6.

The feed solution was a synthetic solution of Copper Sulphate at a 100ppm concentration; and the strip was made of 25% Sulphuric acid. The total volume in the strip and feed phases was 200ml each. The feed solution was pumped through the lumen side of the hydrophobic micro-porous PVDF tubular membrane, whereas the strip solution was counter-currently fed in the shell side. The feed and strip solutions were pumped at the same volumetric flowrates. Counter-current flow was utilised, so as to increase the transfer of ions.

The pH of the feed solution was kept constant at pH5 and an Automatic pH controller pump was used to control the pH at a desired value. Batch experiments were conducted as shown in Table 3.2. The runs were performed in duplicates, in order to check the repeatability of the results.

Table 3.2: Experimental Matrix

Experiment name	Feed (tube side) $CuSO_4$(ppm)	pH constant	Membrane LIX984N-C (%)	Strip (shell side) H_2SO_4 solution	Process Conditions	
					Flowrate (ml/min)	Temperature (ºC)
1a-1c (Equipment testing)	100	5	20	25%	30-120	30
2a-2c	100	5	20	25%	30	21,30,40,50
3a-3c	100	5	20	25%	40	21,30,40,50
4a-4c	100	5	20	25%	50	21,30,40,50
5a-5c	100	5	20	25%	60	21,30,40,50
6a-6c	100	5	20	25%	70	21,30,40,50
7a-7c	100	5	20	25%	80	21,30,40,50
8a-8c	100	5	20	25%	90	21,30,40,50
9a-9c	100	5	20	25%	100	21,30,40,50
10a-10c	100	5	20	25%	120	21,30,40,50

Discrete flow rates and temperatures were chosen for each test varying between 30 and 120ml.min^{-1} and 21 and 50 ℃ respectively, as shown in the exp eriment matrix Table 3.2.

3.5 The calculation for density and viscosity

The density and viscosity of the metal ion solution was taken from the water properties because it was prepared at such low concentrations, 100ppm.

Density of water at 21℃ which is 294K

$$[(294-290)/295-290)x(998-999)]+999=998.2kg/m^3=9.982x10^{-1}g/cm^3$$

Viscosity of water at 21℃

$$[(294-290)/295-290)x(959-1080)]+1080=992.2x10^{-6}N.s.m^{-2}=9.922x10^{-3}g/cm.s$$

The same interpolation was used to obtain the density and viscosity values at 30-50 ºC, Table 3.3 shows the obtained values.

Table 3.3: Density and Viscosity values

Temperature (K)	294	303	313	323
μ (g/cm.s)	9.92E-03	8.03E-03	6.57E-03	5.47E-03
ρ (g/cm^3)	9.98E-01	9.96E-01	9.92E-01	9.88E-01

These values were used to calculate the Reynolds number using equation 2.24 and the Schmidt's number using equation 2.25

Re = (9.98x10^{-1} g.cm^{-3}x 1.1cm x 0.007cm.s^{-1})/ (9.92x10^{-3} g.cm^{-1}.s^{-1})

= (7.6846x10^{-3} g.cm^{-1}.s^{-1})/ (9.92x10^{-3} g.cm^{-1}.s^{-1})

=0.77465

Sc = (9.92x 10^{-3} g.cm^{-1}.s^{-1})/ (9.98x10^{-1}g.cm^{-3} x 5x10^{-5} cm^2.s^{-1})

= 1.99x10^2

The associated Schmidt's and Reynold's numbers were calculated and shown in Table 3.4.

Table 3.4: Experiment parameters

Temperature →	**21.0 deg**	**30.0 deg**	**40.0 deg**	**50.0 deg**
Flow rates				
↓				
30 ml/min	0.80	0.99	1.20	1.44
40 ml/min	1.07	1.32	1.60	1.92
50ml/min	1.33	2.00	2.00	2.40
60 ml/min	1.60	1.97	2.40	2.87
70 ml/min	1.87	2.80	2.80	3.35
80 ml/min	2.13	2.63	3.21	3.83
90 ml/min	2.40	3.61	3.61	4.31
100 ml/min	2.67	3.29	4.01	4.79
120 ml/min	3.20	4.81	4.81	5.75
Schmidt No. →	198.80	161.36	132.40	110.73

Reynold's No. ↓

At the commencement of the experimental planning, batch experiments were performed for equipment testing at pH5 and 30℃. Each run consisted of three days and samples were sent to the laboratory for the analysis of the copper. The results were used to determine how much extraction occurs after what period of time. This also assisted in setting up the duration for the experimental runs to be performed, which further ensured that system stability could be checked.

The samples were taken for analyses of copper using the Atomic Absorption Spectrometer.

3.5 The Process Flow Diagram

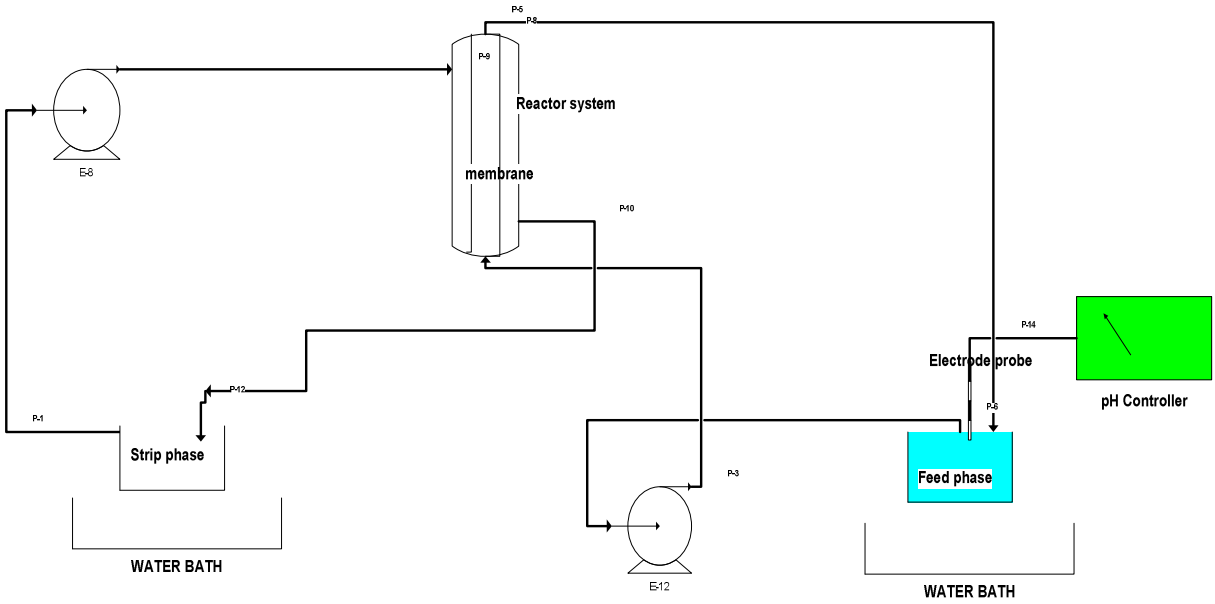

Figure 3.6: The representation of the set-up used for the test work: Two water baths (Buchi 461), feed and strip solutions, pH controller pump and electrode probe (Hanna instruments), (E-8&E-12) two peristaltic pumps (Dune Engineering), membrane supporting system (Double pipe perspex bench scale reactor) and (P-9) PVDF tubular membrane (Koch membrane systems).

3.6 Problems Encountered During Experimental Work

- Due to power failure, experimental time increased.
- Leakages on the piping - the piping used for transporting both solutions needed to be changed after a certain period of operating.
- Acid penetration on the O-rings - since sulphuric acid is used, it damages the O-rings and these had to be changed after a certain period of time.
- Pressure balancing between the strip and feed on the piping.

In order to reduce the problems encountered on the system, the piping on the system had to be changed for every new experiment, especially on the strip side of the system. Equal volumetric flowrates between feed and strip were used, so as to retain the organic solvent in the solid structure of the membrane.

3.7 Calculations used for obtaining Mass transfer coefficient on the feed-side, k_f

3.7.1 Area of the membrane

$$A = \pi * d * l$$

Equation 3.2

A = π (1.1) (20)

A = 69.12 cm^2

3.7.2 Change in Concentration

$$\Delta Cu = C_{bulk}(t + \Delta t) - C_{bulk}(t)$$

Equation 3.3

ΔCu = (1.65x10^{-5} -1.5x10^{-5})

= 1.48x10^{-6} mol.cm^{-3}

No of moles (n) = concentration x volume

Equation 3.4

n = (1.48x10^{-6} mol.cm^{-3})*(200 cm^3)

= 2.96x10^{-4} mol

3.7.3 Mass flux of the copper ion

$$N_{Cu} = n/(Area * time)$$

Equation 3.5

N_{cu} = (2.96 x10^{-4} mol)/ (69.12 cm^2 *****3600s)

N_{cu} = 1.19x10^{-9} mol.$cm^{-2}.s^{-1}$

3.7.4 Mass transfer coefficient

$$k_f = \frac{Ncu}{C_{bulk,\,Average}}$$

Equation 3.6

$C_{bulk,\,average} = ½(C_{bulk}\,(t+\Delta t) + C_{bulk}\,(t))$

Equation 3.7

$= ½(1.65\text{x}10^{-5}+1.5\text{x}10^{-5})$

$= 1.58\text{x}10^{-5}$ mol.cm^{-3}

Therefore

$k_f = (1.19\text{x}10^{-9}$ mol.cm^{-2}.s$^{-1})/ (1.58\text{x}10^{-5}$ mol.cm$^{-3})$

$k_f = 7.53\text{x}10^{-5}$ cm.s^{-1}

CHAPTER FOUR

4 Results

4.1 Introduction

This chapter presents the equilibrium data in the form of measured partition ratios, which confirms the tendency for the copper ions passing to the organic phase; in addition to the kinetic data from the tubular supported liquid membrane experimental work.

The primary purpose for the equilibrium data being done before the kinetic data was to confirm what is already known from literature, i.e. LIX 984N-C does extract copper ions in a solution.

4.2 Equilibrium data obtained from solvent extraction

The copper extraction is shown by Fig. 4.1. At initial conditions, 100% copper ions existed in the aqueous phase. Initially, there were no copper ions in the organic phase, equations; A.1 and A.2 were used as shown in Table A.1 in appendix A, hence the line on the y-axis. After mixing the two phases, organic and aqueous, the copper ions shifted completely to the organic phase.

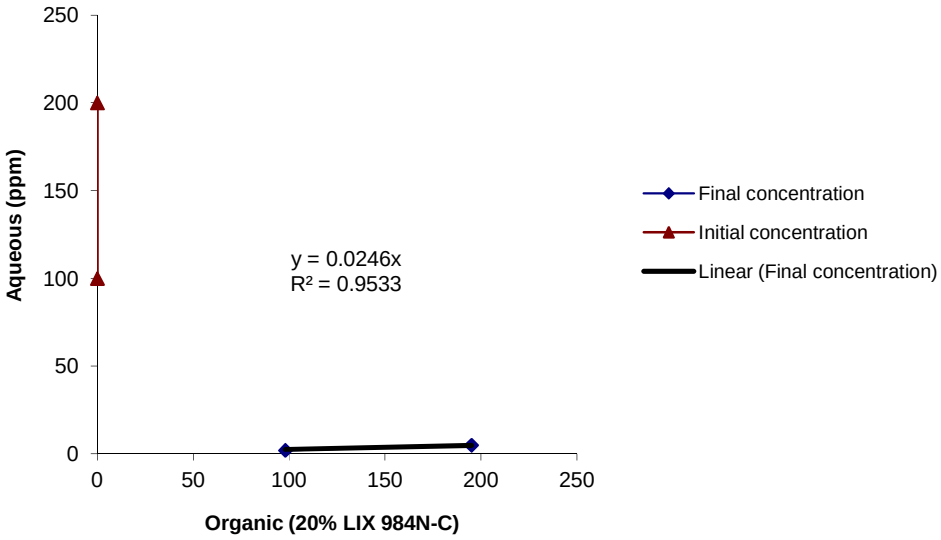

Figure 4.1: Copper on the equilibrium curve

The Partition coefficient of copper is equal to 0.98, shown in Table 4.1. This means that copper is successfully extracted by the extractant LIX984N-C, even if the concentration of copper is increased from 100ppm to 200ppm. The extraction of copper occurs despite the different feed concentration, using the same solvent concentration.

The copper concentration in Fig. 4.2 is shown first in the initial, organic, phase. Thereafter, it is stripped by the Sulphuric acid, reported by the final concentration line on the y-axis.

These results confirm the work done by many researchers like Aminian e*t al*, 2000, whereby LIX 984-NC is confirmed as a very effective Copper (II) extractant.

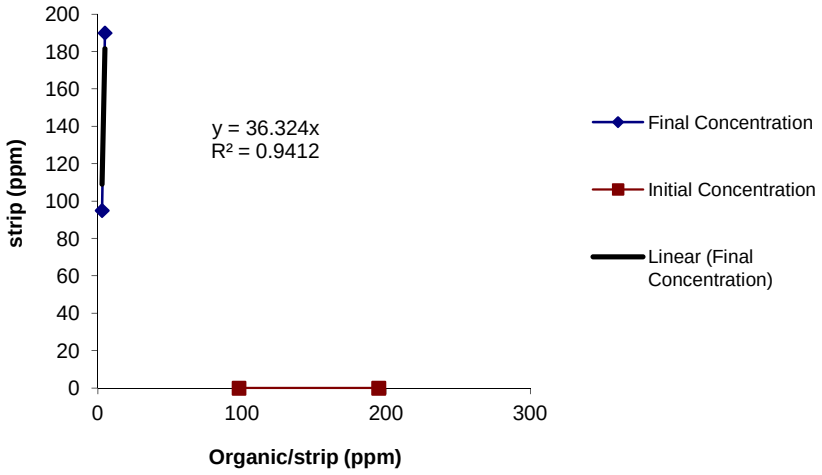

Figure 4.2: Partition coefficient on the strip side

The partition coefficient of copper from organic to strip is 0.97, shown in Table 4.1. This shows that copper is successfully stripped from LIX984N-C by a strippant.

The primary phenomenon is the mass transfer of copper between the aqueous and organic solutions. The mass transfer of copper is based on cation exchange reaction, whereby copper forms a chelate with LIX984N-C molecules. The equilibrium of this cation exchange reaction can be affected by the acidity of the aqueous solution. Hence constant pH was utilised on the feed phase. A complete transport of copper ions to the strippant is shown in table 4.1

Table 4.1: Partition coefficients of the metal ions

Feed Conc.(	Metal	Aqueous before	Aqueous after	Organic	Dcu(f)	Strip phase	Organic	Dcu (s)
100.00	Cu	100	2	98	0.98	95	3	0.97
200.00	Cu	200	5	195	0.98	190	5	0.97

The metal ion concentrations in the organic phase were calculated from the difference between the metal ion concentrations in the aqueous phase before and after extraction. The results are generally expressed as a percentage metal extraction.

These experiments were done in duplicates in order to confirm the repeatability of the results under varying parameters of the system.

4.3 Kinetic results obtained from Tubular Supported Liquid Membrane Experiments

The extraction of copper in the equilibrium test work shows that it is possible to extract this metal ion using LIX 984N-C as a carrier - as described by many researchers, such as Danesi, Ata, Breembroek, etc. The equipment used for kinetic tests was tested for stability and reliability.

4.3.1 Results obtained from equipment testing

The results obtained from the equipment testing shown in Fig. 4.3, confirm that the transport of copper ions from feed phase to strip phase occurs in a tubular supported liquid membrane system, from the initial stages of the experimental run; and a significant amount of ions are transported in a short period of time.

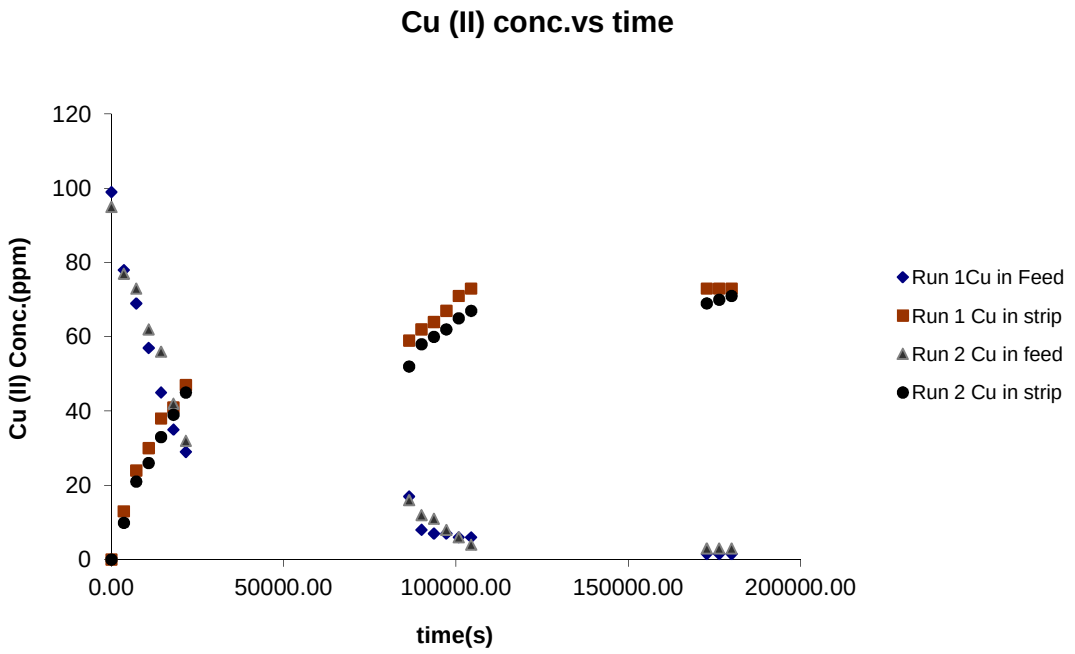

Figure 4.3: Copper extracted during the system testing.

One major objective of this study was to determine the effect of the feed characteristics on the boundary layer of the membrane and also on the recovery of the copper ion to the strip side. It can be seen from Fig 4.3, that more copper decreases during the first day of the extraction.

On the same graph, equilibrium is reached on the third day of the experiment the copper concentration has dropped to below 10% and also on the strip side; the copper concentration is above 70%.

Hence, from the satisfactory results obtained in Fig. 4.3, it was then decided that each experiment should run for the first six hours.

The system used to obtain the kinetic data was stable and reliable. This was a further confirmation that this system can be used for this study.

4.3.2 Effect of temperature on Copper extraction

The results shown in Fig. 4.4 indicates that more copper ions are extracted between the temperature of 30 and 40 ℃, however, at a temperat ure of 50℃, there is a significant copper ion decrease from the feed phase; and the copper concentration increases on the strip phase, as shown in Fig. 4.5.

Although the flowrate in Fig 4.4 is constant at 30ml.min^{-1}, for varying temperature conditions, it can be seen that there is a faster copper removal at the initial stages of the experiment.

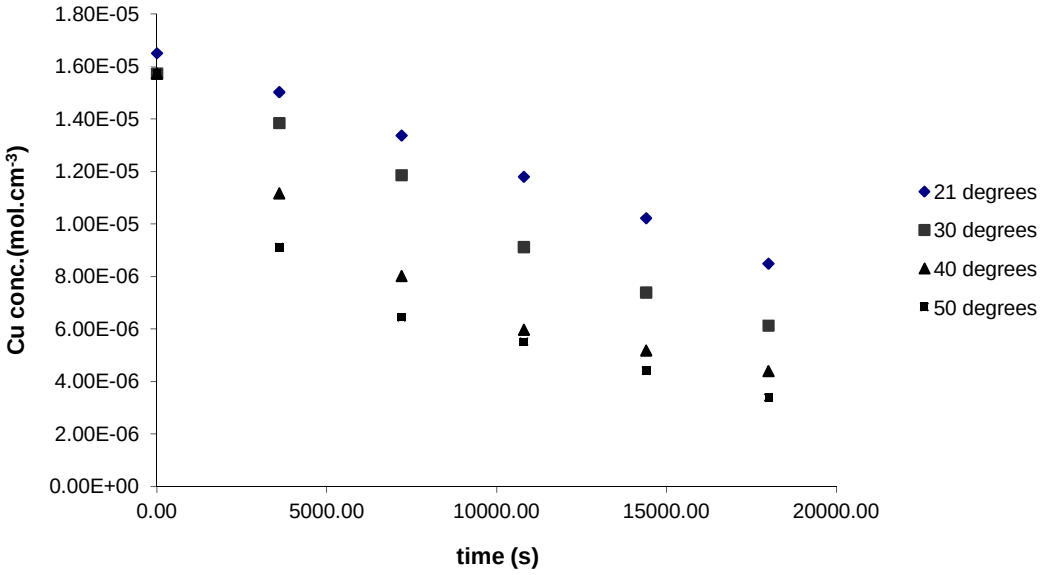

Figure 4.4: Copper ion decrease at varying feed temperature

Usually a decrease of copper mass in the feed side in the time interval dt, is slightly larger than corresponding increase in the strip side. According to Yang *et al*, 2007, this can be understood based on the fact that mass of copper is transferred from feed to strip phases but some still stays in the complex with carrier in the membrane phase.

As expected, the copper ions from the feed phase have been transported to the strip phase, shown in Fig. 4.5.

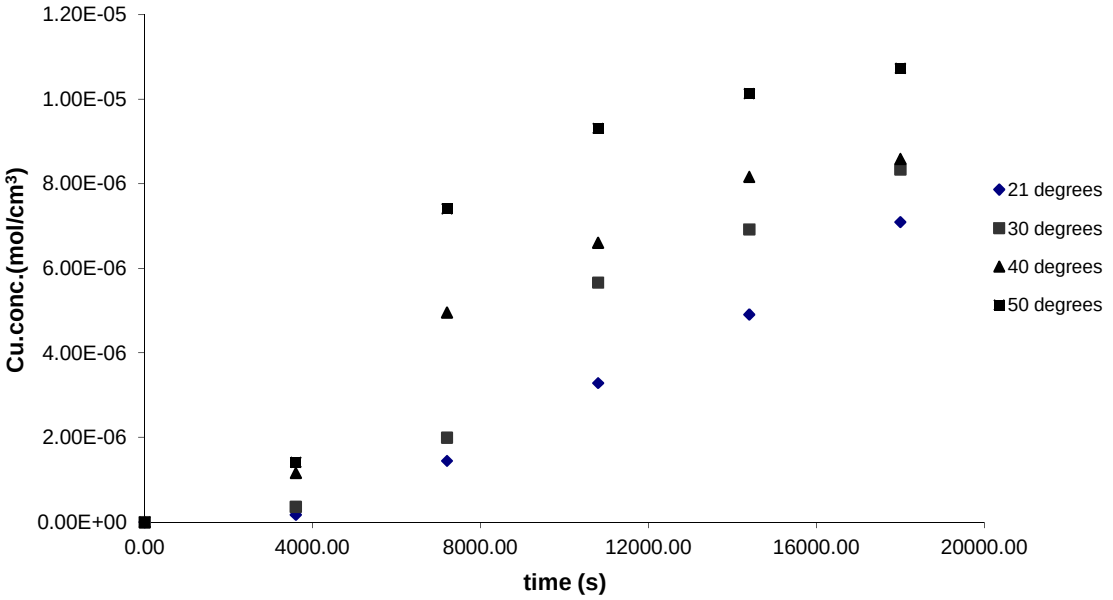

Figure 4.5: Copper ion increase on the strippant at varying feed temperature

Foremost, Fig. 4.5 concludes that the higher the temperatures on the system, the more copper ions are extracted. This is noted by the difference in extracted copper ions between the temperature values of 21 and 50 ℃. The concentration moved from $6.5x10^{-6}$ to $1.2x10^{-5}$ $mol.cm^{-3}$. This is a significant increase in a relatively short period of time.

Fig 4.5 shows that with time, copper concentration in the strip phase could be higher than in the feed phase. This evidently demonstrates the possibility of the carrier facilititated transport according to the work done by Yang *et al*, 2007.

4.3.3 Effect of feed flowrate on the copper extraction system

As expected, the copper concentration in the feed solution decreased during each run as shown in Fig. 4.6. At the lowest flow rate, i.e. 30ml.min^{-1}, the smallest drop in copper concentration was recorded i.e. 45%, implying that the lowest amount of copper was extracted under these circumstances, while at higher flowrates, the copper concentration in the feed decreased by approximately 65%.This appears to indicate a strong correlation between the rate of extraction and flow rate, which is strong evidence that assuming a laminar layer controlling mechanism is the correct approach.

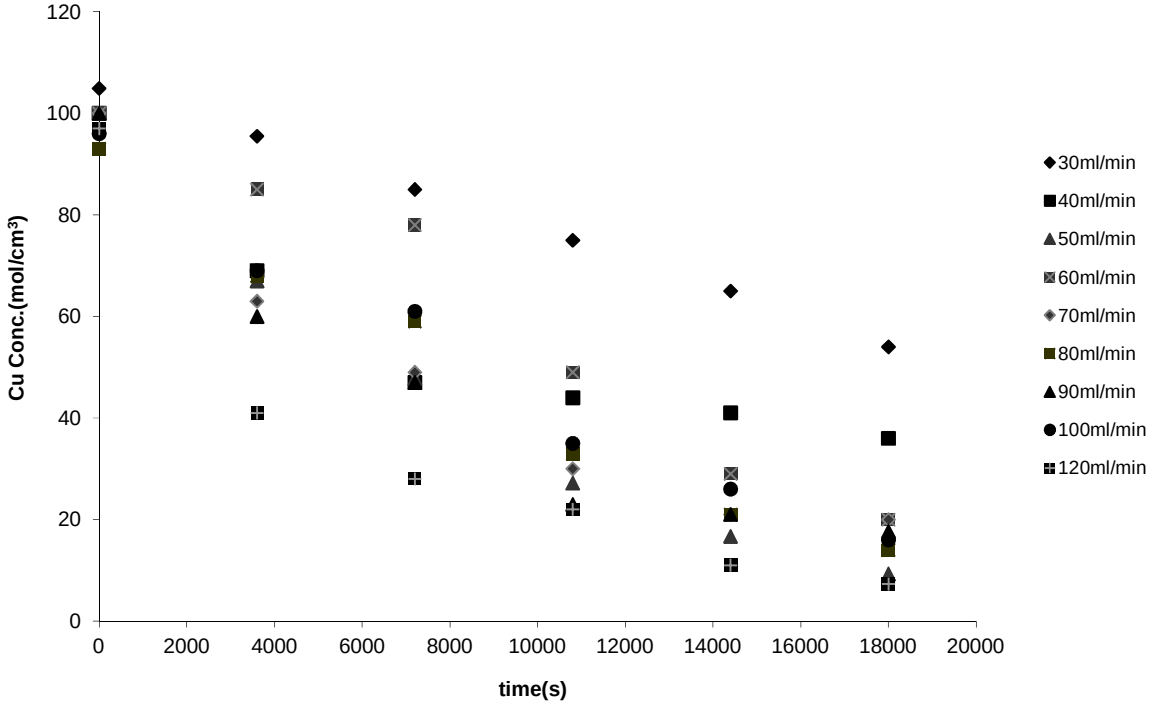

Figure 4.6: Copper decrease at varied flowrate values

The copper reports to the stripping side as expected (Fig. 4.7) and the mass transfer balances satisfactory.

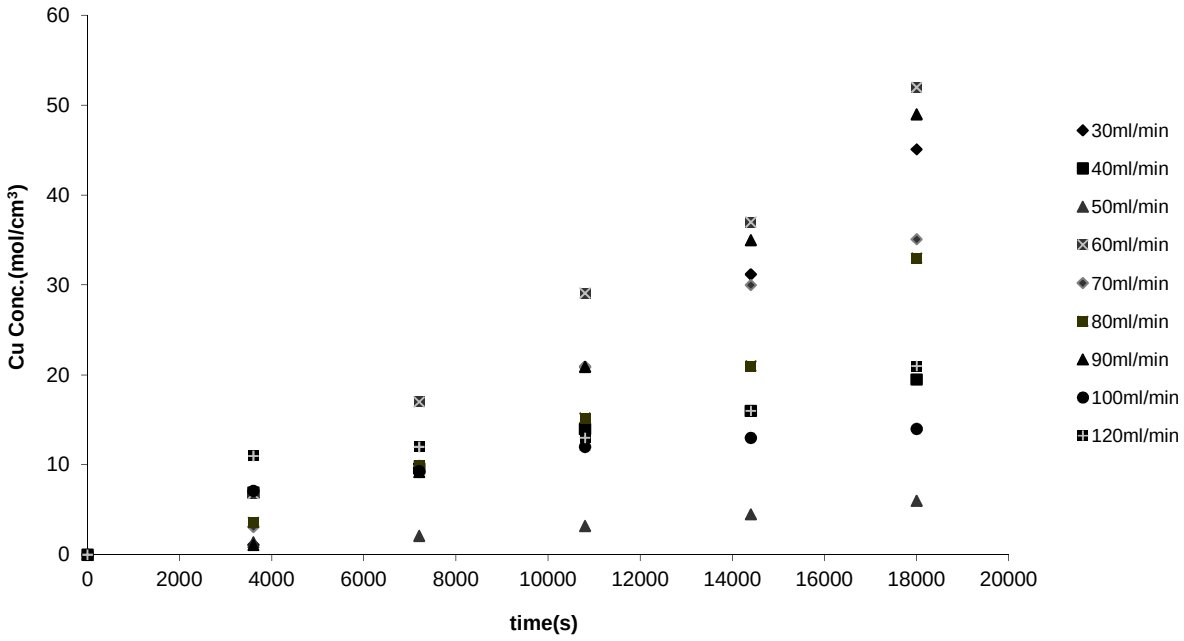

Figure 4.7: Copper gradually increases on the Strip side at varied flowrate conditions

It was observed from Fig 4.7, a volumetric flowrate of 60 ml.min^{-1} at a feed temperature of 30 ºC gave an extraction of copper ions at 52%.Therefore, a volumetric flowrate of 60ml.min^{-1} is optimal for this study.

4.4 The copper flux at 30 ml.min^{-1}

The mass flux of copper ions was calculated using first principles, Fick's law shown in Equation 2.14, chapter two. This flux was calculated from the change in bulk copper concentration over a time interval. A detailed calculation of the flux is shown in section 3.7 for a flowrate of 30ml.min^{-1}. This flux of copper ions was then used to calculate the mass transfer coefficient on the feed side of the membrane, using Equation 2.1.

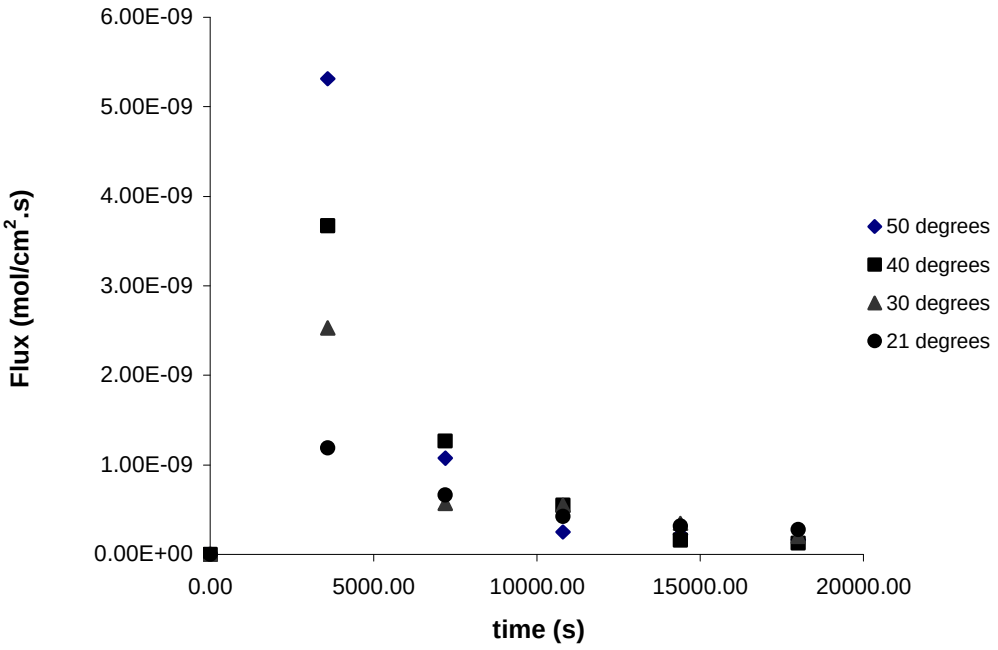

Figure 4.8: Mass flux at varying temperature

The mass flux of copper ions in the tubular supported liquid membrane system is shown in Fig. 4.8 for a constant flowrate of 30ml.min^{-1}. Flux decreases with both time and feed temperature. The flux values obtained at the beginning of the experiment are shown to be high, at approximately 2.53x10^{-9} mol.cm^{-2}s^{-1}; and slightly decreases with time to approximately 2.02x10^{-10} mol.cm^{-2}s^{-1} at the feed temperature of 30℃. At a feed solution temperature of 50 ℃, the mass flux started at 5.31 x10^{-9} mol.cm^{-2}s^{-1}; and significantly decreased to 1.64x10^{-10} mol.cm^{-2}s^{-1}.

The calculated copper ion flux for flow rates of 40 to 120 ml.min^{-1} are shown in Appendix C.

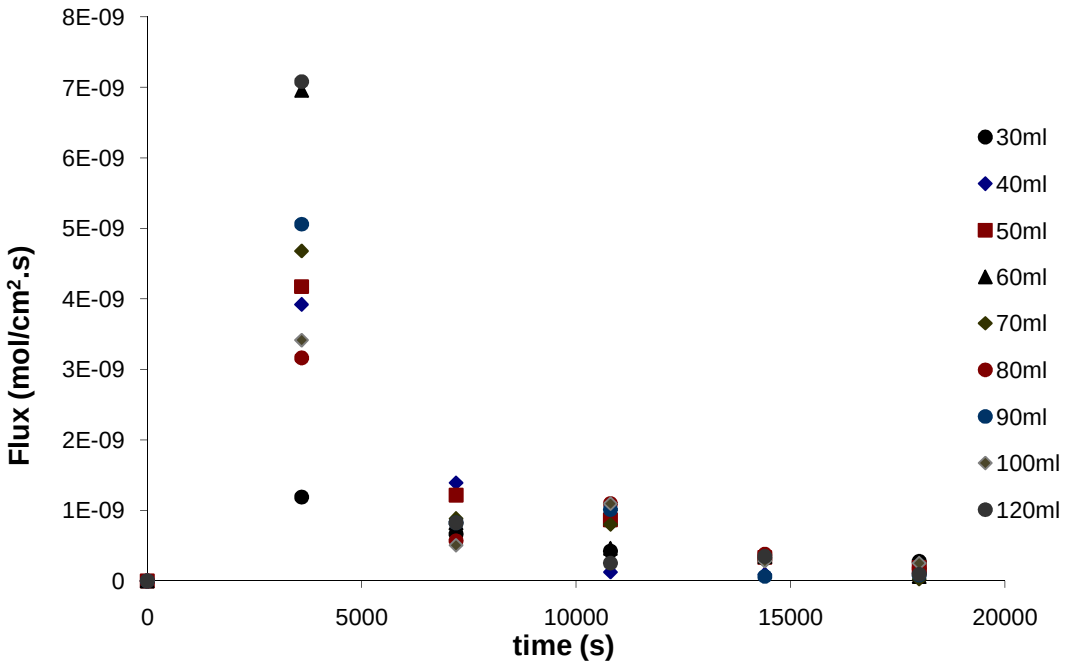

Figure 4.9: Mass Flux at varying feed flowrate

Fig. 4.9 shows the flux of copper ion as a function of flowrate at a time interval. The mass flux decreases with time and increases as the flowrate of the system increases.

According to the study done by Koekermoer, as the flowrate increases on the feed side, the flux increases.

CHAPTER FIVE

5 Interpretation of Results

5.1 Introduction

This chapter represents the interpretation of results as mentioned in the previous chapter.

5.2 Mass transfer coefficient on the feed side

An important focus of this study was to determine the mass transfer coefficient on the feed side of the membrane, this value represents the dimensionless form; and is used to calculate the Sherwood number. The mass transfer coefficient (k_f) on the feed side was calculated from the kinetic data using equation 3.6 as shown in section 3.7.

The mass transfer coefficients were calculated for the system, at varying flowrate and temperature, a whole set of experimental results is shown in Table 5.1

It can be seen from Table 5.1 the mass transfer coefficient on the feed side, k_f is affected by both varying temperature and flowrate of the system.

What is also revealed in Table 5.1, as flowrate of the feed phase increases, the mass transfer coefficient increases, at a higher flow rate of 120ml.min^{-1}, the mass transfer coefficient ranges between 7.54x10^{-5} cm.s^{-1} and 2.50x10^{-4} cm.s^{-1}.At a lower feed flow rate of 30ml.min^{-1}, the mass transfer coefficient ranges between 4.44 x10^{-5} cm.s^{-1} and 1.39x10^{-4} cm.s^{-1}.

The results shown in Table 5.1 correlate well with the research done by Ata *et al*, 2005 and Mokrani, 2000, which discusses the effect of flowrate on the mass transfer coefficient.

Table 5.1: Mass transfer coefficient

Flowrate (ml/min)										
Temperature (ºC)	30	40	50	60	70	80	90	100	120	k_f
21	7.54E-05	2.95E-04	3.18E-04	1.30E-04	3.65E-04	2.50E-04	4.02E-04	2.63E-04	6.52E-04	
	4.68E-05	1.52E-04	1.34E-04	3.45E-05	1.00E-04	5.70E-05	9.77E-05	4.95E-05	1.51E-04	
	4.15E-05	1.77E-05	1.47E-04	1.22E-04	1.29E-04	1.51E-04	1.84E-04	1.45E-04	6.43E-05	
	2.87E-05	1.42E-05	9.61E-05	1.03E-04	7.09E-05	8.93E-05	1.83E-05	5.93E-05	1.34E-04	
	2.97E-05	2.09E-05	9.15E-05	5.91E-05	7.84E-06	6.43E-05	2.74E-05	7.66E-05	6.50E-05	
Average k_f	**4.44E-05**	**1.00E-04**	**1.57E-04**	**8.99E-05**	**1.35E-04**	**1.22E-04**	**1.46E-04**	**1.19E-04**	**2.13E-04**	
30	1.79E-04	3.89E-04	5.43E-04	1.69E-04	3.53E-04	4.38E-04	3.58E-04	3.18E-04	1.64E-04	
	4.79E-05	1.39E-04	2.30E-04	3.74E-05	8.32E-05	1.20E-04	7.97E-05	5.93E-05	3.17E-05	
	5.40E-05	1.94E-05	1.85E-04	2.19E-04	1.70E-04	1.74E-04	2.12E-05	1.52E-04	9.00E-05	
	4.21E-05	2.68E-05	2.63E-04	8.67E-05	7.93E-05	5.61E-05	4.93E-05	8.34E-05	4.28E-05	
	2.99E-05	4.15E-05	5.85E-06	6.82E-05	1.98E-05	2.96E-05	5.84E-05	3.07E-05	4.34E-05	
Average k_f	**7.05E-05**	**1.23E-04**	**2.45E-04**	**1.16E-04**	**1.41E-04**	**1.63E-04**	**1.13E-04**	**1.29E-04**	**7.45E-05**	
40	2.73E-04	5.10E-04	7.92E-04	4.80E-04	4.80E-04	1.96E-04	5.36E-04	2.51E-04	6.25E-04	
	1.32E-04	1.78E-04	4.59E-04	1.37E-04	1.10E-04	2.89E-05	1.14E-04	3.44E-05	1.27E-04	
	7.83E-05	1.14E-04	1.61E-04	1.56E-04	2.09E-04	1.30E-04	1.24E-04	1.97E-04	1.94E-04	
	2.83E-05	9.81E-05	6.01E-05	5.43E-05	3.65E-05	4.84E-05	5.77E-05	8.67E-05	1.00E-04	
	2.64E-05	9.23E-05	2.84E-05	7.57E-05	1.11E-05	3.50E-05	2.00E-05	2.23E-04	9.19E-05	
Average k_f	**1.07E-04**	**1.99E-04**	**3.00E-04**	**1.81E-04**	**1.69E-04**	**8.76E-05**	**1.70E-04**	**1.58E-04**	**2.28E-04**	
50	4.27E-04	6.57E-04	9.44E-04	6.10E-04	6.73E-04	8.87E-04	5.65E-04	3.91E-04	7.74E-04	
	1.38E-04	2.04E-04	4.33E-04	1.36E-04	1.51E-04	2.70E-04	9.56E-05	5.36E-05	1.83E-04	
	4.15E-05	1.69E-04	1.05E-05	1.11E-04	7.66E-05	2.48E-04	1.08E-04	8.93E-05	2.20E-04	
	4.45E-05	9.57E-05	5.43E-06	1.41E-04	4.58E-05	3.42E-05	3.48E-05	1.80E-05	5.46E-05	
	4.21E-05	5.40E-05	6.75E-06	4.34E-05	5.27E-05	7.35E-05	8.72E-05	6.60E-05	1.69E-05	
Average k_f	**1.39E-04**	**2.36E-04**	**2.80E-04**	**2.08E-04**	**2.00E-04**	**3.03E-04**	**1.78E-04**	**1.24E-04**	**2.50E-04**	

In line with the study done by Mokrani, 2000, it was found that the mass transfer coefficient increased with increasing liquid flow rate. That means the feed liquid boundary layer has an important role in mass transfer, and by increasing the flow rate of the liquid, the resistance in the boundary layer is reduced and that gives rise to an increase in the mass transfer rate.

The flowrate of the feed affect the mass transfer in the stagnant layer .According to Ata *et al*, 2005, increasing flowrate causes a decrease in the thickness of the stagnant film and consequently, both mass transfer rate and the mass transfer coefficient increase.

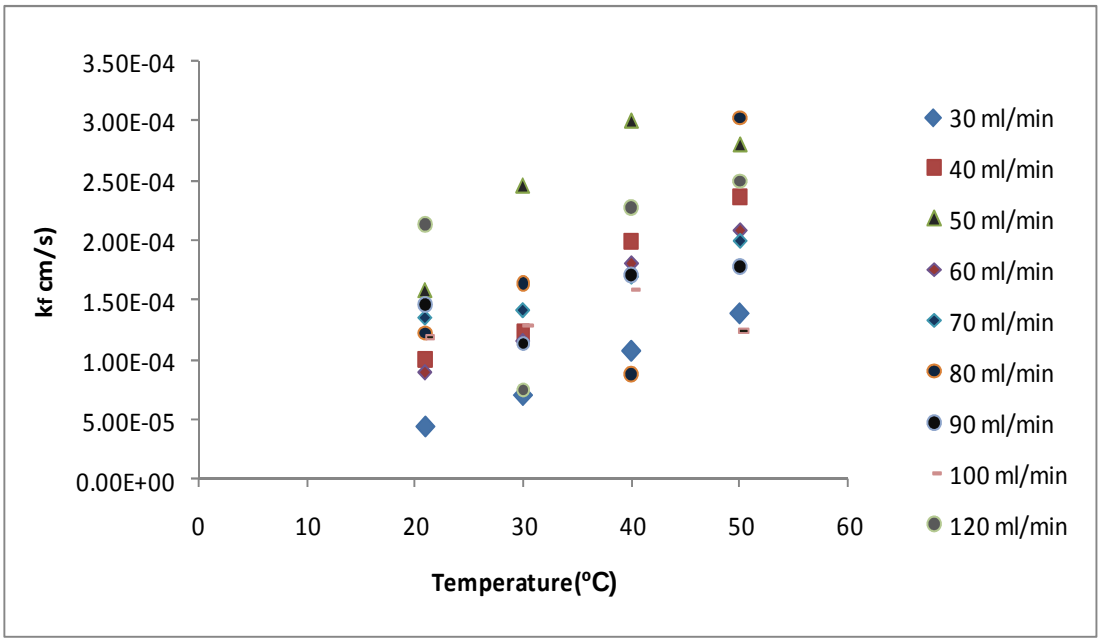

Figure 5.1: Average k_f vs. Temperature

It can be seen in Fig. 5.1 that the mass transfer coefficient appears to increase with increasing flowrate, once again indicating that the laminar layer has a strong effect on the mechanism of mass transfer.

Fig 5.1 shows that temperature of the feed solution has a significant effect on the mass transfer coefficient. As the temperature of the feed solution increases, the mass transfer coefficient increases, this correlates with the results obtained by Ata, 2005.

The study done by Ata *et al*, 2005, discovered that an increase in temperature of the feed will increase the mass transfer rate in the aqueous film at the feed and stripping phases and results in a decrease in viscosity of the liquid phases and the liquid membrane inside the support.

At feed temperature of 50 ºC, k_f values ranges between 1.39×10^{-4} and 3.03×10^{-4} $cm.s^{-1}$, at feed temperature of 30 ºC, k_f values ranges between 4.44×10^{-5} and 2.13×10^{-4} $cm.s^{-1}$.

The mass transfer coefficient on the feed side of the membrane was used to calculate the Sherwood's numbers, using Equation 2.22.

5.1 The Sherwood number

As stated in chapter two, one of the functions for the dimensionless numbers is to determine the relationship between feed parameters. The Sherwood number was calculated using Equation 2.22 in Chapter 2.

$$Sh = \frac{k_f di}{Dcu}$$

= (7.53x10^{-5} cm.s^{-1} x 1.1 cm)/ (5x10^{-5}cm^2.s^{-1})

= 1.66

The Sherwood number calculated for all experiments is shown in the appendix, Table D.42 and it increases with an increasing in flow rate, as shown in Fig. 5.2.

Fig.5.2 shows an increase in the Sherwood number from 1.66 to 19.80, with increasing feed flow rate from, 0.007 cm.s^{-1} to 0.029 cm.s^{-1}. This increase was expected based on the obtained mass transfer coefficient which is used to calculate the Sherwood number.

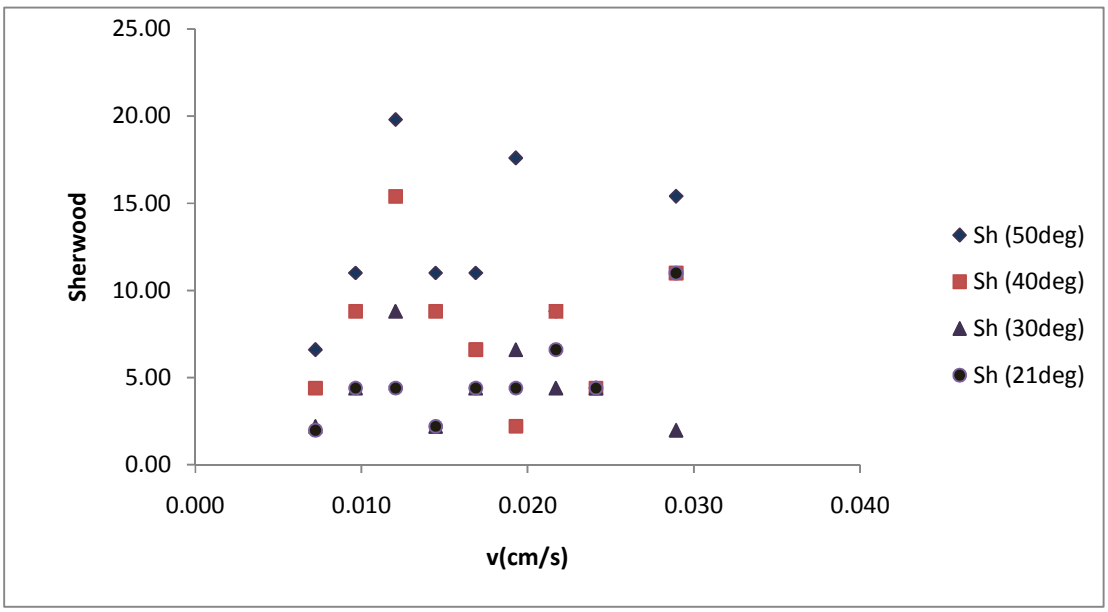

Figure 5.2: Sherwood number vs. the feed velocity

The Sherwood number increases with the increasing Re number by increasing the inlet velocity, as shown in Table 5.2.

In the research done by Mbulawa, 2005, considers the relationship of Sherwood number and Reynolds number, Sherwood number has a mass transfer component and Reynolds number has a viscosity component.

Increasing Reynolds number by decreasing viscosity should increase the mass transfer coefficient, this study concludes by saying that these effects might have a counter acting effect on the mass transfer.
The data shown in Table 5.2 correlates with research study done by Mbulawa, 2005; however the results are not very accurate most probably due to the influence of the inlet and outlet effects.

Table 5.2: The dimensionless numbers with the corresponding feed velocity

Flowrate-(ml/min)	Q(cm^3/s)	velocity(cm/s)	Re(21deg)	Sc(21deg)	Sh(21deg)
30	0.50	0.007	0.80	1.99E+02	1.14E+00
40	0.67	0.010	1.07	1.99E+02	2.20E+00
50	0.83	0.012	1.33	1.99E+02	3.46E+00
60	1.00	0.014	1.60	1.99E+02	1.98E+00
70	1.17	0.017	1.87	1.99E+02	2.96E+00
80	1.33	0.019	2.13	1.99E+02	2.69E+00
90	1.50	0.022	2.40	1.99E+02	3.21E+00
100	1.67	0.024	2.67	1.99E+02	2.61E+00
120	2.00	0.029	3.20	1.99E+02	4.70E+00

Table 5.2 shows that at constant Schmidt's number, the Reynolds number and the Sherwood number increases.

5.2 The Sherwood number vs. the Reynolds number

To correlate the present data using dimensionless equation, the Sherwood number was plotted against Reynolds number.

The coefficient of determination R^2 is a measure of how well the regression line represents the data.

A strong correlation between Sh and Re is observed in Fig. 5.3. The power law shown in Equation 5.2 represents the strong correlation between Re no. and Sh no.

The coefficient of determination represents the percent of the data that is the closest to the line of best fit. In Fig 5.3, $R^2 = 0.912$, this means that 91% of the total variation in Sh can be explained by the linear relationship between Re and Sh. The other 9% of the total variation in Re remains unexplained.

$$Sh = \mathrm{Re}^{0.912} + 1.1597$$

Equation 5.2

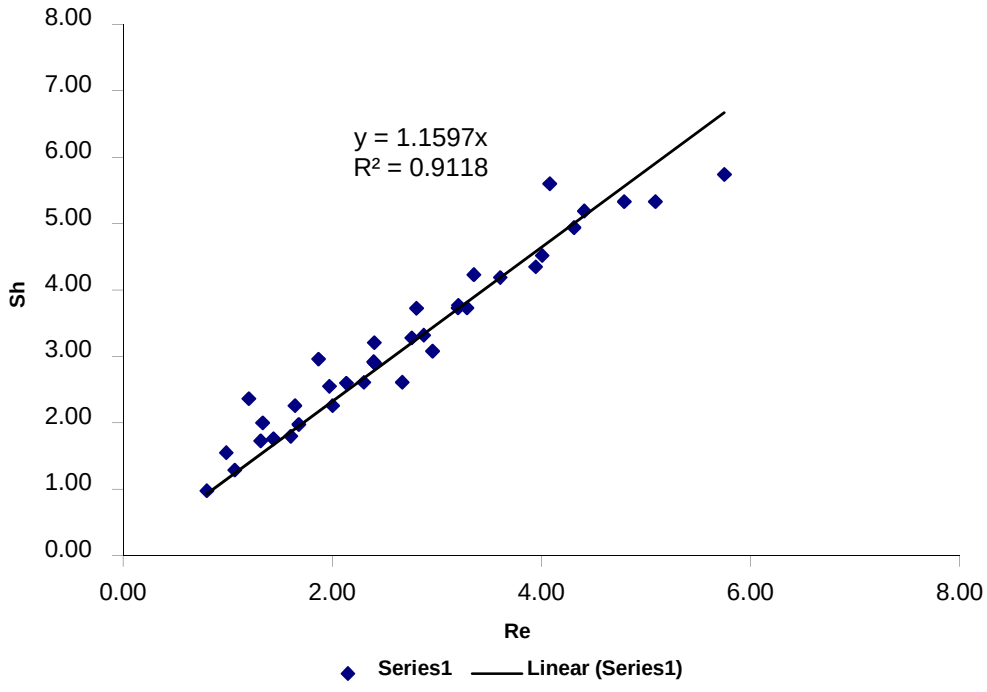

Figure 5.3: The Sherwood vs. Reynolds

In this study, Log Sherwood number was plotted against Log Reynolds and the graph is shown in appendix D and it shows a correlation with R^2 equal to 0.75.The same correlation was obtained between the plot of Ln Sherwood vs Ln Reynolds.

The research study done by Mubarak *et al*, 2004, a log Sh versus log Re was plotted in order to correlate the obtained data using the dimensionless equation and a linear relationship was found, Sh increases with the 0.537 power of Reynolds.

5.3 The empirical model

The Reynold's and the Schmidt's numbers were calculated, as shown in appendix D. Equation 2.24 and Equation 2.25 were used. The Sherwood number was calculated as shown in Appendix C; Equation 2.22 was used.

A traditional log-log relationship between our dimensionless numbers was employed to determine the model parameters through a curve fitting process. The final model is given in Equation 5.2.

$$Sh = 0.1634\,\mathrm{Re}^{0.69}\,Sc^{0.33}$$

Equation 5.2

The obtained values, where C equals 0.1634, n equals 0.69 and m equals 0.33.

Fig. 5.4 compares the model prediction to the measured data. A parity line has also been introduced. A linear regression fit of the data achieved an R^2 of 0.971, which falls directly on the parity line for this data.

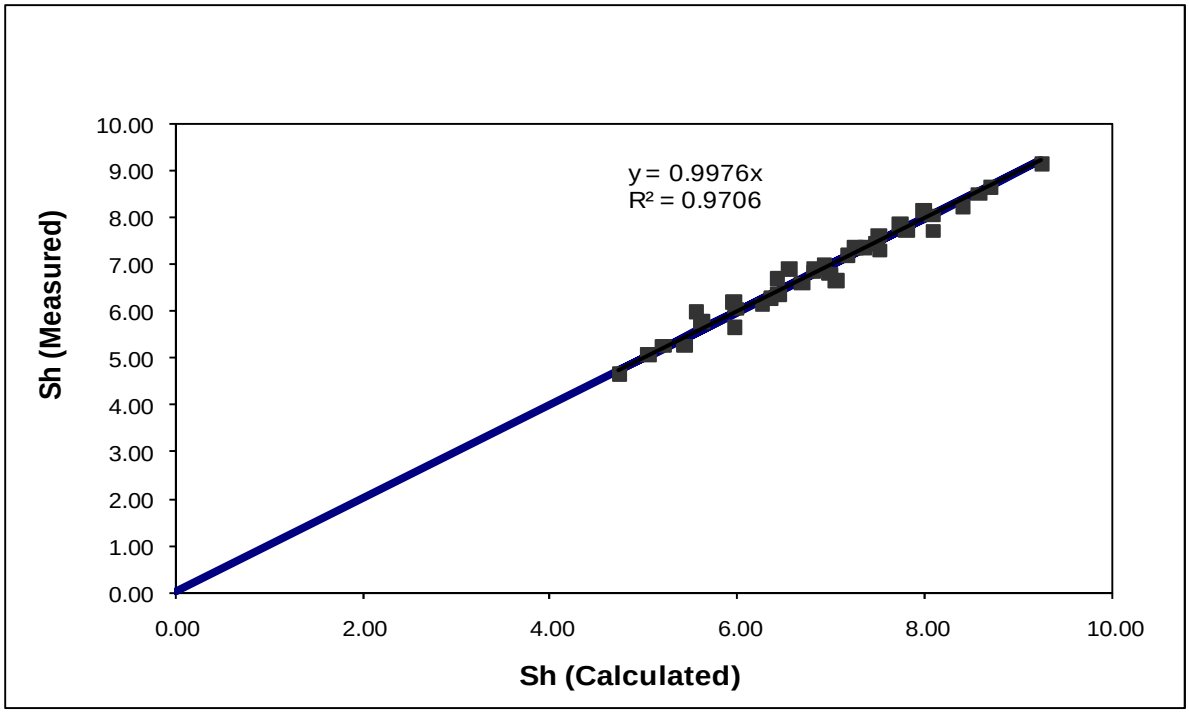

Figure 5.4: Parity graph for Sherwood number

The mass transfer coefficient data of the side of the feed phase were correlated by Ata *et al*, 2005, in the form of $Sh = 0.0047\ Re^{1.349}\ Sc^{0.333}$

The correlation obtained from this data, $Sh = 0.1634\ Re^{0.69}\ Sc^{0.33}$, is not far off from what is obtained in literature.

The correlation obtained by Yang *et al*, 1986 was, $Sh = 1.38\ Re^{0.4}Sc^{0.33}$

Wickramasighe *et al*, found that the liquid mass transfer coefficient could be represented by the correlation, $Sh = 0.8\ Re^{0.47}\ Sc^{0.33}$

5.4 Comparing the empirical models

These correlations were plotted against each other, so to observe the comparison.

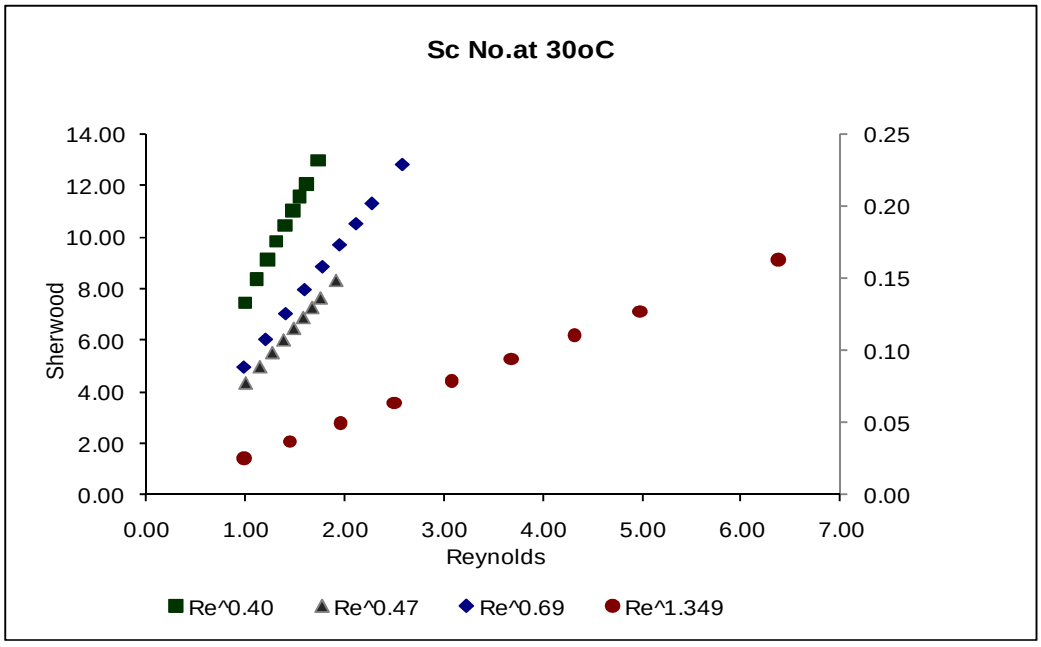

Figure 5.5: The graph for the different correlations

The Reynolds number from both the correlations done by Yang *et al*, 1986 and Wickramasighe *et al*, 2002 both are more or less the same as shown in Fig 5.5; this is because hollow fibre membrane modules were used and the flow is very laminar.

For this study a tubular membrane was used and the Reynolds number slightly decreased compared to the hollow fibre modules but still the flow is laminar and the tube internal diameter was 1.1cm. Also the Sherwood number is much smaller compared to the rest of the correlations.

And lastly, Ata *et al*, 2005 has used a flat-sheet module and the flow is very laminar, hence this is a bit off compared to the other three correlations.

CHAPTER SIX

6 Conclusion

6.1 Overall Conclusion and Recommendation

This chapter contains the overall conclusion of this research study, starting by mentioning the objectives.

The objectives of this study were to:

- Extract metal ions from low concentration metal solution, using TSLM and LIX 984N-C dissolved in Kerosene; and using a bench-scale apparatus system.
- Determine the partition coefficients across the membrane.
- Evaluate the effect of the feed characteristics (viscosity, density, pH, temperature and velocity) on the resistance of the laminar layer of the aqueous feed side of TSLM.
- Utilise the permeation on the TSLM to determine a mass transport relationship, using the dimensionless numbers.

The equilibrium data obtained in this study shows that copper ions are successfully transported to LIX984N-C at a diffusion coefficient of 0.98 at the feed-organic phase; and at 0.97 at the organic-strip phase.

The kinetic data obtained from this study shows that copper ions can be extracted by this system and in addition a high level of repeatability was achieved.

A credible and repeatable relationship between the Sherwood, Schmidt's and Reynold's numbers was achieved, as witnessed by the goodness of fit in Fig. 5.4.

$Sh = 0.1634\ Re^{0.69}\ Sc^{0.33}$

From this study, it can be concluded that the extraction of copper ions on the tubular supported liquid membrane system is significantly affected by mass transfer coefficient. The feed properties of the system, the flow rate, temperature as well as the viscosity and density of the system, significantly impact on the rate of the mass transfer.

The mass transfer rate is low compared to other mass transport unit operations, with k_f value ranges from $4.44x10^{-5}$ to $3.03x10^{-4}$ $cm.s^{-1}$

I recommend that a broader data search area i.e. more to higher Reynolds numbers, specifically Re to turbulent with addition to see how it will affect the mass transfer coefficient on the feed side of the membrane.

References

1. Aminian, H., Bazin, C., 2000.Solvent extraction equilibria in copper (II)-iron (III)-LIX984 system. *Minerals Engineering*, 13:667-672.
2. Ata, O.N., 2004. Modelling of copper ion through supported liquid membrane containing LIX 984. *Hydrometallurgy*, 77:269-277.
3. Ata, O.N., Çolak, S., 2005. Modelling of zinc transport through a supported liquid. *Hydrometallurgy,*80:155-162
4. Alguacil, F.J., Coedo, A.G., Dorado, M.T., 2000. Transport of chromium (VI) through a Cyanex 923-xylene flat-sheet supported liquid membrane. *Hydrometallurgy*, 57: 51– 56.
5. Alhusseini, A., Ajbar, A., 2000. Mass transfer in supported liquid membranes: a rigorous model. *Mathematical and Computer Modelling*, 32:465– 480.
6. Aziz, M & Mneno, S. 2005. The recovery of Copper by tubular supported liquid membrane. Paper presented at the 6th annual conference of the Water of Southern Africa (WISA), Membrane Technology Division, Wilderness,13-15 March 2005.[not published]
7. Baker, R.W. 2004. *Membrane technology and Applications*. 2nd edition, California, John Wiley and Sons, (Ltd).
8. Barrow, G.M.1996. *Physical Chemistry*, 6th edition, North America, McGraw-Hill.
9. Benzal, G., Kumar,A., Delshams, A.&Sastre, M.A,2004. Mathematical modelling and simulation of co-transport phenomena through flat sheet-supported liquid membranes. *Hydrometallurg*,74:117-130
10. Boyer, E.H. &Gall, T.L. 1984. *Metals Handbook*. Desk Edition, Metals Park, American Society for Metals.

11. Breembroek,G.R.M,van Straalen,A.,Witkamp,G.J &van Rosmalen,G.M ,1998. Extraction of cadmium and copper using hollow fiber supported liquid membranes. *Journal of Membrane Science*,146:185-195
12. Crank J. 1979. *Mathematics of diffusion.* Second Edition, United States, Oxford University press
13. Danesi, P.R, Harwitz, E.P Vandegrift, G.F& Chiarizia, R., 1981. Mass transfer rate through liquid membrane. *Separation Science and Technology,*16:201-211
14. Danesi, P.R, 1984. A simplified model for the coupled transport of metal ions through hollow fiber supported liquid membrane. *Journal of Membrane Science*,20:231-248
15. Deorkar, N.V., Tavlarides, L.L., 1997. Zinc, cadmium, and lead separation from aqueous streams using solid-phase extractants, *Industrial & Engineering Chemistry Research,* 36**:**399– 406.
16. Dho, N.Y., Lee, S.R., 2003. Effect of temperature on single and competitive adsorptions of Cu (II) and Zn (II) onto natural clays, *Environmental Monitoring and Assessment,* 83: 177- 203.
17. Erlank, S.N.1994.*The application of supported liquid membranes (SLM) and doubt salt precipitation (DSP) for demineralization of calcium and nickel in aqueous solution.* Potchefstroom: PU for CHE.
18. Feng, C., Wang, R., Shi, B., Li, G. & Wu, Y. 2006. Factors affecting pore structure and performance of poly (vinylidenefluoride-cohexafluoro propylene) asymmetric porous membrane. *Journal of Membrane Science,*277:55-64
19. Geankoplis, C.J.1983. *Transport processes: momentum, heat and mass*.USA.Allyn and Bacon, INC.
20. Geankoplis, C.J.2003. *Transport processes and Separation Process Principles*.4th edition, USA, Prentice Hall.

21. Gherrou, A., Kerdjoudj, Molinari, R. &Drioli, E., 2002. Removal of Silver and Copper ions from acidic thiourea solutions with a Supported liquid membrane containing DE2HPA as carrier. *Journal of Membrane Science*, 28:235-244
22. Gill, J.S., Singh, H. & Gupta, C.K., 2000. Studies on supported liquid membrane for simultaneous separation of Fe (III),Cu(II) and Ni(II) from dilute feed.*Hydrometallurgy*,5:113-116
23. Henly R.L. 1983. *Chemistry for Today.* Mount Temple Comprehensive School.Folens.
24. Hoffman D.L, .1991. *Development and modification of supported liquid membrane extraction system for the recovery of cesium, strontium and uranium*.Potchefstroom:PU vir CHP.(Thesis-PhD) 337
25. Kamiƞski, W.&Kwapiƞski,W. 2000. Applicability of liquid membranes in enviromental protection.*Journal of Enviromental Studies*, 9:37-43
26. Kargari, A. Kaghazchi, T &Soleimani, M., 2004. Mass transfer investigation of liquid membrane transport of gold (III) by methyl iso-butyl ketone mobile carrier, *Journal of Chemical Engineering & Technology*, 27:1014– 1018.
27. Keane, M. A., 1998. The removal of copper and nickel from aqueous solution using Y zeolite ion exchangers, *Colloids Surfaces A,* 138**:**11-20.
28. Kocherginsky,N.M., & Yang ,Q., 2007. Big carrousel mechanism of copper removal from ammoniacal wastewater through supported liquid membrane. *Journal of Membrane Science* ,54: 104-116
29. Kocherginsky, N.M., Yang , Q& Seelam, L.,2007. Recent advances in supported liquid membrane technology.*Separation and Purification Technology*,153:171-177
30. Koekermoer, L.R. 2004. *The evaluation of the mechanisms involved in the extraction of nickel from low concentration effluents by means of supported liquid*

membranes. Unpublished PhD Thesis, University.Potchestroom Campus, Northwest

31. Levine, I.N.1995. *Physical Chemistry*, 4th edition. North America, McGraw-Hill.
32. Liu, J.S., Chen, H., Chen, X.Y., Guo, Z.L., Hu, Y.C., Liu, C.P. & Sun, Y.Z., 2006. Extraction and separation of In(III), Ga(III) and Zn(II) from sulfate solution using extraction resin, *Hydrometallurgy,* 82**:**137-143.
33. Malherbe, G.F. 1993. *Development and application of ultrafiltration and reverse osmosis membranes*. Unpublished M-Tech thesis, Cape Technikon, Cape Town.
34. Marchese, J., Campderros, M.E., Acosta, A., 1993. Mechanistic study of cobalt, nickel and copper transfer across a supported liquid membrane. *Journal of Chemical Technology & Biotechnology*. 57: 37– 42.
35. Mbulawa, X.P. 2005. *Development and Evaluation of silicone membrane as aerators for membrane bioreactors.* Unpublished M-Tech thesis, Durban University of Technology, Durban
36. McGuire, K.S., Lawson, K.W. & Lloyd, R.D.1994. Pore size distribution determination from liquid permeation through micro porous membranes. *Journal of Membrane Science,*99:127-137
37. Mollah, M.Y.A., Schennach, R., Parga, J.R. & Cocke D.L., 2001. Electrocoagulation (EC)—science and applications, *Journal Hazardous Materials,* B84**:**29–41.
38. Mokrani, T. 2000. *Transport of gases across membranes.* Unpublished M-Tech thesis, Cape Peninsula University of Technology. Bellville Campus, Cape Town
39. Mubarak, A.A., El-Shazly, A.H. & Konsowa, A.H. 2004. Recovery of copper from industrial waste solution by cementation on reciprocating horizontal perforated zinc disc. *Desalination*, 167:127-133.

40. Mulder, M. 1996. *Basic principles of membrane technology.2nd edition*.Netherlands.Kluwer academic publishers.
41. Ravanchi, M.T., Kaghazchi, T., & Kargari, A. 2009. Application of membrane separation processes in petrochemical industry: a review. *Desalination*, 239:199-244
42. Richardson J.F., Harker J.H. & Backhurst J.R. 2002. *Chemical Engineering*. Vol. 2,5th edition. Amsterdam. . Butterworth Heinemann.
43. Ruey-Shin, J., juin-Dong, C., Huey-Chyng, H., 2000. Dispersion free membrane extraction: case studies of metal ion and organic acid extraction. *Journal of Membrane Science*, 165: 59– 73.
44. Saleem, M., Afzal, M., Qadeer, R., Hanif, J., 1992. Selective adsorption of uranium on activated-charcoal rom electrolytic aqueous solutions, *Separation Science and Technology.* 27:239–253.
45. Sastre, A., Madi, A., Cortina, J.L., Miralles, N., 1998. Modelling of mass transfer in facilitated supported liquid membrane transport of gold (III) using phospholene derivatives as carriers. *Journal of Membrane Science*, 139:57-65
46. Schoeman, J.J., Steyn, A., Slabbert, J.L & Venter, E.A. 2003. *Treatment of landfill leachate from hazardous and municipal solid waste*.WRC.Report no.1167/1/03.
47. Scott K. & Hughes K. 1996. *Industrial Membrane Separation Technology.*London.Chapman & Hall.
48. Sherwood,L. 2006. *Fundamentals of Physiology:A human perspective*,3rd edition.United States of America,Thomson Learning.
49. Smit J.J., & Koekemoer, L.R.1996. The extraction of Nickel with the use of Supported Liquid Membrane Capsules. *Water S.A,22:249*

50. Smit J.J. 1997. *The extraction of Nickel with the use of Supported Liquid Membrane (SLM)*, WRC Report No.617/1/97.Department of Chemical Engineering Potchefstroom University for CHE.
51. Srisurichan, S., Jiraratananon, R., & Fane, A.G.2005. Mass transfer mechanism and transport resistances in direct contact membrane distillation process. *Journal of Membrane Science,* 277:186-194
52. Tan, X., Tan, S.P., Teo, W.K., & Li, K., 2005. Polyvinylidene fluoride (PVDF) hollow fibre membranes for ammonia removal from water. *Journal of Membrane Science*,271:59-68
53. Treybal, R.E. 1986. *Mass transfer operations*. 3rd edition. McGraw-Hill.
54. Unlu, N., Ersoz, M., 2006. Adsorption characteristics of heavy metal ions onto a low cost biopolymeric sorbent from aqueous solutions, *Journal of Hazard Materials,* 136**:**272-280.
55. Valenzuela,F.,Vega,M.A, 2002. Application of mathematical model for copper permeation from Chilean mine water through a hollow fiber-type supported liquid membrane. *Journal of Membrane Science*,204:385-400
56. Wang, W.M., Fthenakis, V., 2005. Kinetics study on separation of cadmium from tellurium in acidic solution media using ion-exchange resins, *Journal Hazardous Materials,* 125:80-88.
57. Welty, J., Wicks, C.E., Wilson, R.E., & Rorrer, G.L. 2001. *Fundamentals of momentum, heat, and mass transfer*, 4th Edition. New York, John Wiley & Sons, Inc.
58. Yang, M.C& Cussler, E.L., 1986. Designing hollow-fiber contactors. *AIChE Journal*, 2:1910-1916

59. Yang, Q. & Korcherginsky, N.M., 2007. Copper removal from ammonicial wastewater through a hollow fiber supported liquid membrane system: modeling and experimental verification. *Journal of Membrane Science*,297:121-129
60. Yang, Q. 2007. *Copper Recovery and spent etchant regeneration based on supported liquid membrane technology*. Unpublished PhD Thesis, National University of Singapore, Singapore
61. Zeman, L.J., &Zydney, A.L.1996. *Microfiltration and Ultrafiltration: Principles and Applications.* New York. Marcel Dekker.INC.
62. Biocompare. 2008. *Types of Membranes*. http://www.biocompare.com/forums/ViewThread.aspx?threadid=3355 [25 May 2008]
63. Cognis Corporation. 2002. *LIX 984N-C Material Safety Data Sheet*.http://www.cognis-us.com/company/Businesses/Lubricants/Our+Products/Product+Catalog/[15 July 2006]
64. Copper development centre. 2004. *Copper Research*. http://www.copper.com.au/cdc/article.asp?CID=59&AID=213 [21 August 2007]
65. Fuelcellknowledge.2002.*Heat and Mass transfer*. http://www.fuelcellknowledge.org/research_and_analysis/heat_and_mass_transfer/index.html [08 March 2007]
66. Koch Membrane Systems. 2004. *Tubular Membranes-Overview*. http://www.kochmembrane.com/prod_tubular.html [21 August 2007]
67. Lenntech Water Treatment & Air purification Holding B.V.2008.*Chemical Properties of Nickel.* http://www.lenntech.com/periodic-chart-element/Ni-en.htm [22 March 2008]
68. The Chamber of Mines South Africa.2007. *Education-Base metals and minerals*.

http://www.bullion.org.za/Education/Base.htm [9 January 2007]

List of Appendices

Appendix A: Calculations for Partition Coefficient

$$D_{CU(f)} = \frac{[Cu^{2+}]_{organic}}{[Cu^{2+}]_{aqueous}}$$ **Equation A.1**

= (98ppm)/ (100ppm)

= 0.98

$$D_{CU(s)} = \frac{[Cu^{2+}]_{strip}}{[Cu^{2+}]_{organic}}$$ **Equation A.2**

= (95ppm/98 ppm)

= 0.97

Table A.1

feed conc.(ppm)	metal	Aqueous befo	Aqueous after	Organic (after	Dcu(f)	Strip phase	org	Dcu (s)	org(in)	Strip(in)
100.00	Cu	100	2	98	0.98	95	3	0.97	0	0
200.00	Cu	200	5	195	0.98	190	5	0.97	0	0
100.00	Zn	100	98	2	0.02	1.2	0.8	0.60	0	0
200.00	Zn	200	199	1	0.01	1	0	1.00	0	0
100.00	Ni	100	99	1	0.01	1	0	1.00	0	0
200.00	Ni	200	199	1	0.01	1	0	1.00	0	0

Appendix B: Equipment Testing Data

Table B.1 Equipment testing data

Time (hr)	Time(s)	Cu(ppm)	%	strip (ppm)	%
0	0	9.9	99	0	0
1	3600	7.8	78	1.3	13
2	7200	5.7	57	2.4	24
3	10800	4	40	3	30
4	14400	3.2	32	3.8	38
5	18000	2.5	25	4.1	41
6	21600	2	20	4.7	47
24	86400	0.9	9	5.9	59
25	90000	0.8	8	6.2	62
26	93600	0.4	4	6.4	64
27	97200	0.3	3	6.7	67
28	100800	0.25	2.5	7.1	71
29	104400	0.2	2	7.3	73
48	172800	0.17	1.7	7.8	78
49	176400	0.15	1.5	7.9	79
50	180000	0.15	1.5	7.9	79

Tubular supported liquid membrane dimensions

Table B.2 Membrane dimensions

Polymeric material	PVDF
Fiber i.d.(cm)	1.1
Fiber o.d. (cm)	1.2
Membrane wall thickeness (cm)	0.5
Active membrane length (cm)	20
tortuosity	2.00
Porosity	0.6
Pore size (μm)	0.2
Cross sectional area (cm^2)	69.115
Volume of feed and strip soln (cm^3)	200.00

Table B. 3: System material

Name	**Material**	**Quantity**
Feed	$CuSO_4$	200ml
Strip	H_2SO_4	25%
Solvent	LIX984N-C	20%
Diluent	Kerosene	80%
pH		5
Mr Cu	Copper	63.546

Appendix C: Data for varying Flowrates

Flowrate of 30 $ml.min^{-1}$

Mass flux of the copper ion

Area of the membrane

$$A = \pi * d * l$$

Equation 3.2

A = π (1.1) (20)

A = 69.12 cm^2

Change in Concentration

$$\Delta Cu = C_{bulk}(t + \Delta t) - C_{bulk}(t)$$

Equation 3.3

ΔCu = (1.65×10^{-5} - 1.5×10^{-5})

= 1.48×10^{-6} mol.cm^{-3}

No of moles (n) = concentration x volume

Equation 3.4

n = (1.48×10^{-6} mol.cm^{-3})*(200 cm^3)

= 2.96×10^{-4} mol

Mass flux of the copper ion

$$N_{Cu} = n/(Area * time)$$

Equation 3.5

N_{cu} = (2.96 $\times 10^{-4}$ mol)/ (69.12 cm^2 *****3600s)

N_{cu} = 1.19×10^{-9} mol.$cm^{-2}.s^{-1}$

Mass transfer coefficient

The mass transfer coefficient on the feed side of the membrane was calculated from the kinetic data. Equation 3.5 was used as shown below.

$$k_f = \frac{Ncu}{C_{bulk,\,Average}}$$

Equation 3.6

$C_{bulk,\,average} = ½(C_{bulk}\,(t+\Delta t) + C_{bulk}\,(t))$

$= ½(1.65\text{x}10^{-5}+1.5\text{x}10^{-5})$

$= 1.58\text{x}10^{-5}$ mol.cm^{-3}

Therefore,

$k_f = (1.19\text{x}10^{-9}$ mol.cm^{-2}.s^{-1})/ ($1.58\text{x}10^{-5}$ mol.cm^{-3})

$k_f = 7.53\text{x}10^{-5}$ cm.s^{-1}

Sherwood number

The diffusion coefficient of copper was taken from the study done by Valenzuela *et al*, 2002.

$$Sh = \frac{k_f di}{Dcu}$$

Equation 2.22

= (7.53x10^{-5} cm.s^{-1} x 1.1 cm)/ (5x10^{-5}cm^2.s^{-1})

= 1.66

The same method shown by the equations 3.2-3.6 and 2.22 was used for the flowrates of 40-120 ml.min^{-1}.

Table C.2: Kinetic results for copper extraction at 21 ºC

Time(min)	Time(s)	feed	(mg/L)	strip	(mg/L)	[feed](mol/cm^3)	[cu] (mole)	[strip](mol/cm3)	ΔC	$C_{bulk,average}$	Moles	Ncu(mol/cm^{2}s)	k_f	Sh
0.00	0.00	10.49	104.90	0.00	0.00	1.65E-05	3.30E-03	0.00E+00	0.00E+00	1.65077E-05	0.00E+00	0.00E+00	0.00E+00	0.00E+00
1.00	3600.00	9.55	95.50	0.11	1.10	1.50E-05	3.01E-03	1.73E-07	1.48E-06	1.58E-05	2.96E-04	1.19E-09	7.54E-05	1.66
2.00	7200.00	8.50	85.00	0.92	9.20	1.34E-05	2.68E-03	1.45E-06	1.65E-06	1.42E-05	3.30E-04	6.64E-10	4.68E-05	1.03
3.00	10800.00	7.50	75.00	2.09	20.90	1.18E-05	2.36E-03	3.29E-06	1.57E-06	1.26E-05	3.15E-04	4.22E-10	3.35E-05	0.74
4.00	14400.00	6.50	65.00	3.12	31.20	1.02E-05	2.05E-03	4.91E-06	1.57E-06	1.10E-05	3.15E-04	3.16E-10	2.87E-05	0.63
5.00	18000.00	5.40	54.00	4.51	45.10	8.50E-06	1.70E-03	7.10E-06	1.73E-06	9.36E-06	3.46E-04	2.78E-10	2.97E-05	0.65
24.00	86400.00	5.00	50.00	5.48	54.80	7.87E-06	1.57E-03	8.62E-06	6.29E-07	8.18E-06	1.26E-04	2.11E-11	2.58E-06	0.06
25.00	90000.00	3.90	39.00	5.32	53.20	6.14E-06	1.23E-03	8.37E-06	1.73E-06	7.00E-06	3.46E-04	5.57E-11	7.95E-06	0.17
26.00	93600.00	3.70	37.00	5.37	53.70	5.82E-06	1.16E-03	8.45E-06	3.15E-07	5.98E-06	6.29E-05	9.73E-12	1.63E-06	0.04
27.00	97200.00	3.30	33.00	5.86	58.60	5.19E-06	1.04E-03	9.22E-06	6.29E-07	5.51E-06	1.26E-04	1.87E-11	3.40E-06	0.07

Table C.3: Kinetic results for copper extraction at 30 ºC

Time(min)	Time(s)	feed	(mg/L)	strip	(mg/L)	[feed](mol/cm^3)	[cu] (mole)	[strip](mol/cm^3)	ΔC	$C_{bulk,average}$	Moles	Ncu(mol/cm^{2}s)	k_f	Sh
0.00	0.00	10.00	100.00	0.00	0.00	1.57E-05	3.15E-03	0.00E+00	0.00E+00	1.57E-05	0.00E+00	0.00E+00	0.00E+00	0.00E+00
1.00	3600.00	8.80	80.00	0.23	2.30	1.26E-05	2.52E-03	3.62E-07	3.15E-06	1.42E-05	6.29E-04	2.53E-09	1.79E-04	3.93
2.00	7200.00	7.54	71.00	1.27	12.70	1.12E-05	2.23E-03	2.00E-06	1.42E-06	1.19E-05	2.83E-04	5.69E-10	4.79E-05	1.05
3.00	10800.00	5.80	58.00	3.60	36.00	9.13E-06	1.83E-03	5.67E-06	2.05E-06	1.02E-05	4.09E-04	5.48E-10	5.40E-05	1.19
4.00	14400.00	4.70	47.00	4.40	44.00	7.40E-06	1.48E-03	6.92E-06	1.73E-06	8.26E-06	3.46E-04	3.48E-10	4.21E-05	0.93
5.00	18000.00	3.90	39.00	5.30	53.00	6.14E-06	1.23E-03	8.34E-06	1.26E-06	6.77E-06	2.52E-04	2.02E-10	2.99E-05	0.66
24.00	86400.00	3.00	30.00	5.60	56.00	4.72E-06	9.44E-04	8.81E-06	1.42E-06	5.43E-06	2.83E-04	4.74E-11	8.74E-06	0.19
25.00	90000.00	2.50	25.00	5.90	59.00	3.93E-06	7.87E-04	9.28E-06	7.87E-07	4.33E-06	1.57E-04	2.53E-11	5.85E-06	0.13
26.00	93600.00	2.00	20.00	6.30	63.00	3.15E-06	6.29E-04	9.91E-06	7.87E-07	3.54E-06	1.57E-04	2.43E-11	6.87E-06	0.15
27.00	97200.00	1.50	15.00	6.70	67.00	2.36E-06	4.72E-04	1.05E-05	7.87E-07	2.75E-06	1.57E-04	2.34E-11	8.51E-06	0.19

Table C.4: Kinetic results for copper extraction at 40 ºC

Time(min)	Time(s)	feed	(mg/L)	strip	(mg/L)	[feed](mol/cm^3)	[cu] (mole)	[strip](mol/cm^3)	ΔC	$C_{bulk,average}$	Moles	Ncu(mol/cm^{2}s)	k_f	Sh
0.00	0.00	10.00	100.00	0.00	0.00	1.57E-05	3.15E-03	0.00E+00	0.00E+00	1.57E-05	0.00E+00	0.00E+00	0.00E+00	0.00E+00
1.00	3600.00	7.10	71.00	0.74	7.40	1.12E-05	2.23E-03	1.16E-06	4.56E-06	1.35E-05	9.13E-04	3.67E-09	2.73E-04	6.00
2.00	7200.00	5.10	51.00	3.15	31.50	8.03E-06	1.61E-03	4.96E-06	3.15E-06	9.60E-06	6.29E-04	1.26E-09	1.32E-04	2.90
3.00	10800.00	3.80	38.00	4.20	42.00	5.98E-06	1.20E-03	6.61E-06	2.05E-06	7.00E-06	4.09E-04	5.48E-10	7.83E-05	1.72
4.00	14400.00	3.30	33.00	5.19	51.90	5.19E-06	1.04E-03	8.17E-06	7.87E-07	5.59E-06	1.57E-04	1.58E-10	2.83E-05	0.62
5.00	18000.00	2.80	28.00	5.46	54.60	4.41E-06	8.81E-04	8.59E-06	7.87E-07	4.80E-06	1.57E-04	1.26E-10	2.64E-05	0.58
24.00	86400.00	1.20	12.00	7.10	71.00	1.89E-06	3.78E-04	1.12E-05	2.52E-06	3.15E-06	5.04E-04	8.43E-11	2.68E-05	0.59
25.00	90000.00	0.56	5.60	7.50	75.00	8.81E-07	1.76E-04	1.18E-05	1.01E-06	1.38E-06	2.01E-04	3.24E-11	2.34E-05	0.51
26.00	93600.00	0.13	1.30	8.20	82.00	2.05E-07	4.09E-05	1.29E-05	6.77E-07	5.43E-07	1.35E-04	2.09E-11	3.85E-05	0.85
27.00	97200.00	0.11	1.10	8.40	84.00	1.73E-07	3.46E-05	1.32E-05	3.15E-08	1.89E-07	6.29E-06	9.37E-13	4.96E-06	0.11

Table C.5: Kinetic results for copper extraction at 50 ºC

Time(min)	Time(s)	feed	(mg/L)	strip	(mg/L)	[feed](mol/cm^3)	[cu] (mole)	[strip](mol/cm^3)	ΔC	$C_{bulk,average}$	Moles	Ncu(mol/cm^{2}s)	k_f	Sh
0.00	0.00	10.00	100.00	0.00	0.00	1.57E-05	3.15E-03	0.00E+00	0.00E+00	1.57E-05	0.00E+00	0.00E+00	0.00E+00	0.00E+00
1.00	3600.00	5.80	58.00	0.90	9.00	9.13E-06	1.83E-03	1.42E-06	6.61E-06	1.24E-05	1.32E-03	5.31E-09	4.27E-04	9.40
2.00	7200.00	4.10	41.00	4.71	47.10	6.45E-06	1.29E-03	7.41E-06	2.68E-06	7.79E-06	5.35E-04	1.08E-09	1.38E-04	3.04
3.00	10800.00	3.51	35.10	5.92	59.20	5.52E-06	1.10E-03	9.32E-06	9.28E-07	5.99E-06	1.86E-04	2.49E-10	4.15E-05	0.91
4.00	14400.00	2.81	28.10	6.44	64.40	4.42E-06	8.84E-04	1.01E-05	1.10E-06	4.97E-06	2.20E-04	2.21E-10	4.45E-05	0.98
5.00	18000.00	2.16	21.60	6.82	68.20	3.40E-06	6.80E-04	1.07E-05	1.02E-06	3.91E-06	2.05E-04	1.64E-10	4.21E-05	0.93
24.00	86400.00	1.43	14.30	8.10	81.00	2.25E-06	4.50E-04	1.27E-05	1.15E-06	2.82E-06	2.30E-04	3.85E-11	1.36E-05	0.30
25.00	90000.00	0.29	2.90	8.20	82.00	4.56E-07	9.13E-05	1.29E-05	1.79E-06	1.35E-06	3.59E-04	5.77E-11	4.26E-05	0.94
26.00	93600.00	0.22	2.20	8.60	86.00	3.46E-07	6.92E-05	1.35E-05	1.10E-07	4.01E-07	2.20E-05	3.41E-12	8.49E-06	0.19
27.00	97200.00	0.12	1.20	8.80	88.00	1.89E-07	3.78E-05	1.38E-05	1.57E-07	2.68E-07	3.15E-05	4.68E-12	1.75E-05	0.39

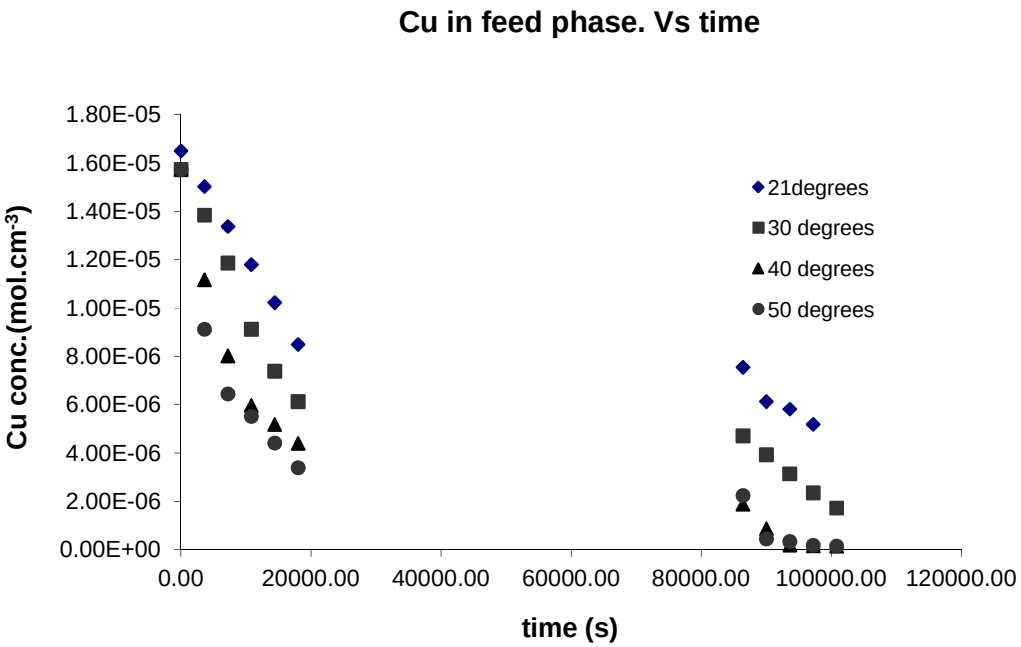

Figure C.1: Copper decrease at 30ml.min^{-1} and varying temperatures

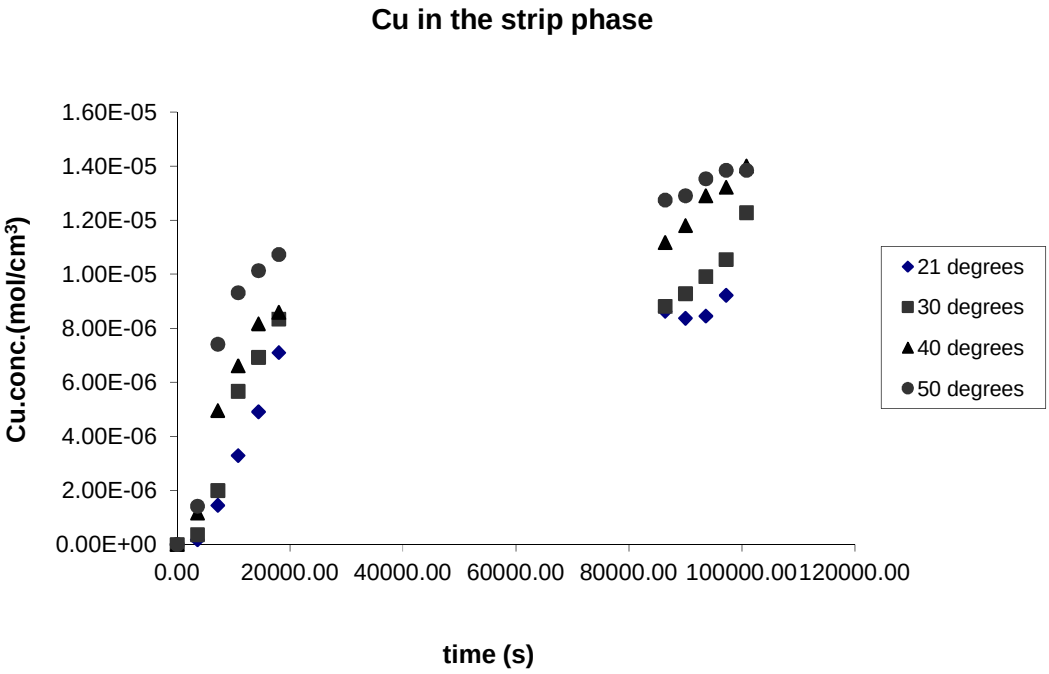

Figure C.2: Copper increase at 30 ml.min^{-1} and varying temperatures

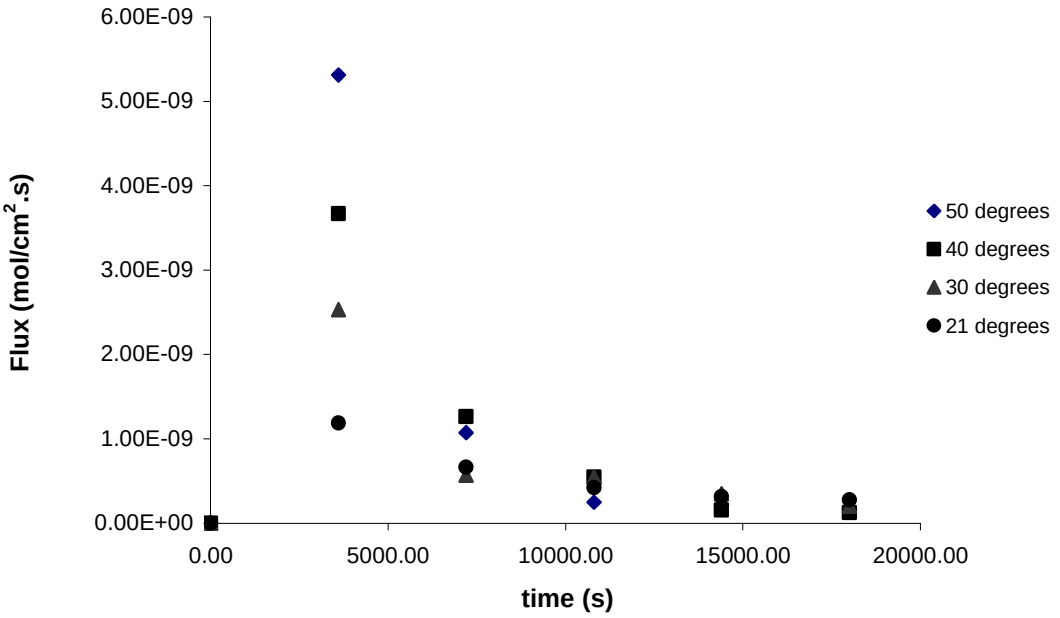

Figure C.3: Mass flux of copper ion at 30 ml.min^{-1} and varying temperatures

Flowrate of 40 $ml.min^{-1}$

Table C. 6: Kinetic results for copper extraction at 21 ºC

Time(min)	Time(s)	feed	(mg/L)	strip	(mg/L)	[feed](mol/cm^3)	[cu] (mole)	[strip](mol/cm^3)	ΔC	$C_{bulk,average}$	Moles	Ncu(mol/cm^{2}s)	k_f	Sh
0.00	0.00	10.00	100.00	0.00	0.00	1.57E-05	3.15E-03	0.00E+00	0.00E+00	1.57E-05	0.00E+00	0.00E+00	0.00E+00	0.00
1.00	3600.00	6.90	69.00	0.69	6.90	1.09E-05	2.17E-03	1.09E-06	4.88E-06	1.33E-05	9.76E-04	3.92E-09	2.95E-04	6.49
2.00	7200.00	4.70	47.00	0.96	9.60	7.40E-06	1.48E-03	1.51E-06	3.46E-06	9.13E-06	6.92E-04	1.39E-09	1.52E-04	3.35
3.00	10800.00	4.40	44.00	1.40	14.00	6.92E-06	1.38E-03	2.20E-06	4.72E-07	7.16E-06	9.44E-05	1.26E-10	1.77E-05	0.39
4.00	14400.00	4.10	41.00	1.60	16.00	6.45E-06	1.29E-03	2.52E-06	4.72E-07	6.69E-06	9.44E-05	9.49E-11	1.42E-05	0.31
5.00	18000.00	3.60	36.00	1.95	19.50	5.67E-06	1.13E-03	3.07E-06	7.87E-07	6.06E-06	1.57E-04	1.26E-10	2.09E-05	0.46
24.00	86400.00	1.50	15.00	5.00	50.00	2.36E-06	4.72E-04	7.87E-06	3.30E-06	4.01E-06	6.61E-04	1.11E-10	2.76E-05	0.61
25.00	90000.00	1.30	13.00	5.30	53.00	2.05E-06	4.09E-04	8.34E-06	3.15E-07	2.20E-06	6.29E-05	1.01E-11	4.59E-06	0.10
26.00	93600.00	1.20	12.00	5.60	56.00	1.89E-06	3.78E-04	8.81E-06	1.57E-07	1.97E-06	3.15E-05	4.87E-12	2.47E-06	0.05
27.00	97200.00	1.00	10.00	6.00	60.00	1.57E-06	3.15E-04	9.44E-06	3.15E-07	1.73E-06	6.29E-05	9.37E-12	5.41E-06	0.12

Table C.7: Kinetic results for copper extraction at 30 ºC

Time(min)	Time(s)	feed	(mg/L)	strip	(mg/L)	[feed](mol/cm^3)	[cu] (mole)	[strip](mol/cm^3)	ΔC	$C_{bulk,average}$	Moles	Ncu(mol/cm^{2}s)	k_f	Sh
0.00	0.00	10.00	100.00	0.00	0.00	1.57E-05	3.15E-03	0.00E+00	0.00E+00	1.57E-05	0.00E+00	0.00E+00	0.00E+00	0.00E+00
1.00	3600.00	6.10	61.00	0.90	9.00	9.60E-06	1.92E-03	1.42E-06	6.14E-06	1.27E-05	1.23E-03	4.93E-09	3.89E-04	8.57
2.00	7200.00	4.30	43.00	1.20	12.00	6.77E-06	1.35E-03	1.89E-06	2.83E-06	8.18E-06	5.67E-04	1.14E-09	1.39E-04	3.06
3.00	10800.00	4.00	40.00	1.70	17.00	6.29E-06	1.26E-03	2.68E-06	4.72E-07	6.53E-06	9.44E-05	1.26E-10	1.94E-05	0.43
4.00	14400.00	3.50	35.00	2.00	20.00	5.51E-06	1.10E-03	3.15E-06	7.87E-07	5.90E-06	1.57E-04	1.58E-10	2.68E-05	0.59
5.00	18000.00	2.70	27.00	2.50	25.00	4.25E-06	8.50E-04	3.93E-06	1.26E-06	4.88E-06	2.52E-04	2.02E-10	4.15E-05	0.91
24.00	86400.00	1.00	10.00	5.40	54.00	1.57E-06	3.15E-04	8.50E-06	2.68E-06	2.91E-06	5.35E-04	8.96E-11	3.08E-05	0.68
25.00	90000.00	0.74	7.40	5.80	58.00	1.16E-06	2.33E-04	9.13E-06	4.09E-07	1.37E-06	8.18E-05	1.32E-11	9.61E-06	0.21
26.00	93600.00	0.67	6.70	6.20	62.00	1.05E-06	2.11E-04	9.76E-06	1.10E-07	1.11E-06	2.20E-05	3.41E-12	3.07E-06	0.07
27.00	97200.00	0.52	5.20	6.50	65.00	8.18E-07	1.64E-04	1.02E-05	2.36E-07	9.36E-07	4.72E-05	7.03E-12	7.51E-06	0.17

Table C.8: Kinetic results for copper extraction at 40 ºC

Time(min)	Time(s)	feed	(mg/L)	strip	(mg/L)	[feed](mol/cm^3)	[cu] (mole)	[strip](mol/cm^3)	∆C	$C_{bulk,average}$	Moles	Ncu(mol/cm^{2}s)	k_f	Sh
0.00	0.00	10.00	100.00	0.00	0.00	1.57E-05	3.15E-03	0.00E+00	0.00E+00	1.57E-05	0.00E+00	0.00E+00	0.00E+00	0.00E+00
1.00	3600.00	5.18	51.80	0.99	9.90	8.15E-06	1.63E-03	1.56E-06	7.59E-06	1.19E-05	1.52E-03	6.10E-09	5.10E-04	11.23
2.00	7200.00	3.30	33.00	1.79	17.90	5.19E-06	1.04E-03	2.82E-06	2.96E-06	6.67E-06	5.92E-04	1.19E-09	1.78E-04	3.92
3.00	10800.00	2.14	21.40	2.30	23.00	3.37E-06	6.74E-04	3.62E-06	1.83E-06	4.28E-06	3.65E-04	4.89E-10	1.14E-04	2.51
4.00	14400.00	1.30	13.00	2.70	27.00	2.05E-06	4.09E-04	4.25E-06	1.32E-06	2.71E-06	2.64E-04	2.66E-10	9.81E-05	2.16
5.00	18000.00	0.72	7.20	3.30	33.00	1.13E-06	2.27E-04	5.19E-06	9.13E-07	1.59E-06	1.83E-04	1.47E-10	9.23E-05	2.03
24.00	86400.00	0.69	6.90	5.80	58.00	1.09E-06	2.17E-04	9.13E-06	4.72E-08	1.11E-06	9.44E-06	1.58E-12	1.43E-06	0.03
25.00	90000.00	0.60	6.00	6.20	62.00	9.44E-07	1.89E-04	9.76E-06	1.42E-07	1.02E-06	2.83E-05	4.55E-12	4.49E-06	0.10
26.00	93600.00	0.58	5.80	6.50	65.00	9.13E-07	1.83E-04	1.02E-05	3.15E-08	9.28E-07	6.29E-06	9.73E-13	1.05E-06	0.02
27.00	97200.00	0.40	4.00	6.90	69.00	6.29E-07	1.26E-04	1.09E-05	2.83E-07	7.71E-07	5.67E-05	8.43E-12	1.09E-05	0.24

Table C.9: Kinetic results for copper extraction at 50 ºC

Time(min)	Time(s)	feed	(mg/L)	strip	(mg/L)	[feed](mol/cm^3)	[cu] (mole)	[strip](mol/cm^3)	∆C	$C_{bulk,average}$	Moles	Ncu(mol/cm^{2}s)	k_f	Sh
0.00	0.00	10.00	100.00	0.00	0	1.57E-05	3.15E-03	0.00E+00	0.00E+00	1.57E-05	0.00E+00	0.00E+00	0.00E+00	0.00E+00
1.00	3600.00	4.20	42.00	0.23	2.3	6.61E-06	1.32E-03	3.62E-07	9.13E-06	1.12E-05	1.83E-03	7.34E-09	6.57E-04	14.45
2.00	7200.00	2.50	25.00	0.69	6.9	3.93E-06	7.87E-04	1.09E-06	2.68E-06	5.27E-06	5.35E-04	1.08E-09	2.04E-04	4.49
3.00	10800.00	1.30	13.00	1.20	12	2.05E-06	4.09E-04	1.89E-06	1.89E-06	2.99E-06	3.78E-04	5.06E-10	1.69E-04	3.72
4.00	14400.00	0.80	8.00	1.50	15	1.26E-06	2.52E-04	2.36E-06	7.87E-07	1.65E-06	1.57E-04	1.58E-10	9.57E-05	2.11
5.00	18000.00	0.57	5.70	1.70	17	8.97E-07	1.79E-04	2.68E-06	3.62E-07	1.08E-06	7.24E-05	5.82E-11	5.40E-05	1.19
24.00	86400.00	0.56	5.60	3.30	33	8.81E-07	1.76E-04	5.19E-06	1.57E-08	8.89E-07	3.15E-06	5.27E-13	5.93E-07	0.01
25.00	90000.00	0.50	5.00	3.50	35	7.87E-07	1.57E-04	5.51E-06	9.44E-08	8.34E-07	1.89E-05	3.04E-12	3.64E-06	0.08
26.00	93600.00	0.49	4.90	3.80	38	7.71E-07	1.54E-04	5.98E-06	1.57E-08	7.79E-07	3.15E-06	4.87E-13	6.25E-07	0.01
27.00	97200.00	0.43	4.30	3.90	39	6.77E-07	1.35E-04	6.14E-06	9.44E-08	7.24E-07	1.89E-05	2.81E-12	3.88E-06	0.09

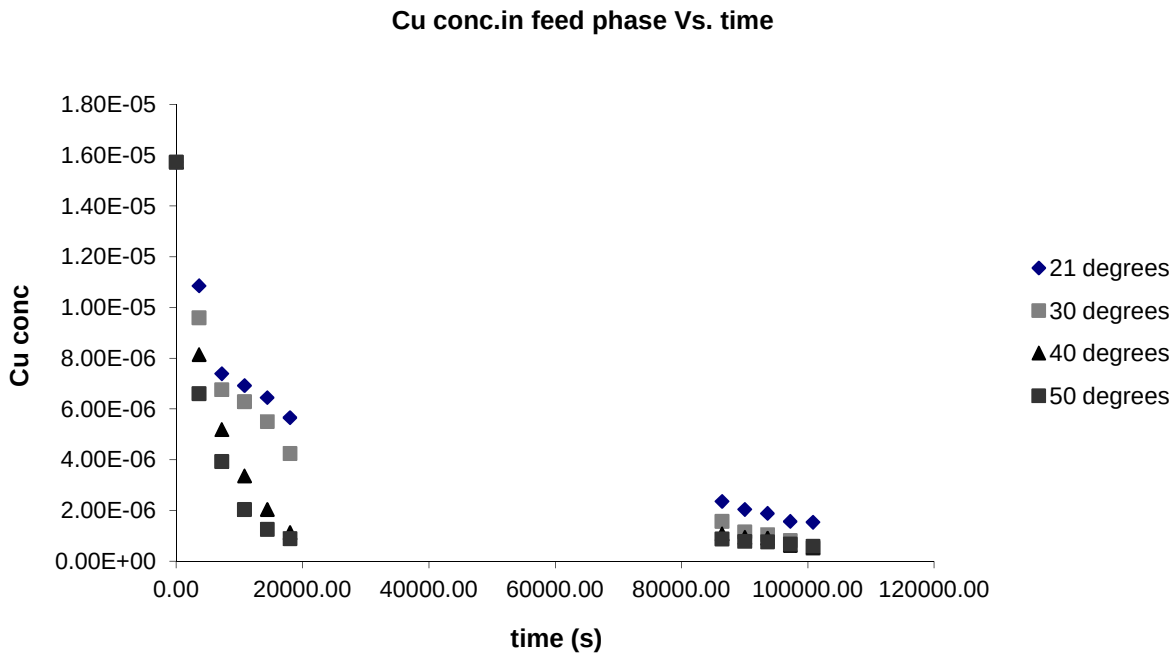

Figure C.4: Copper decrease at 40 ml.min^{-1} and varying temperatures

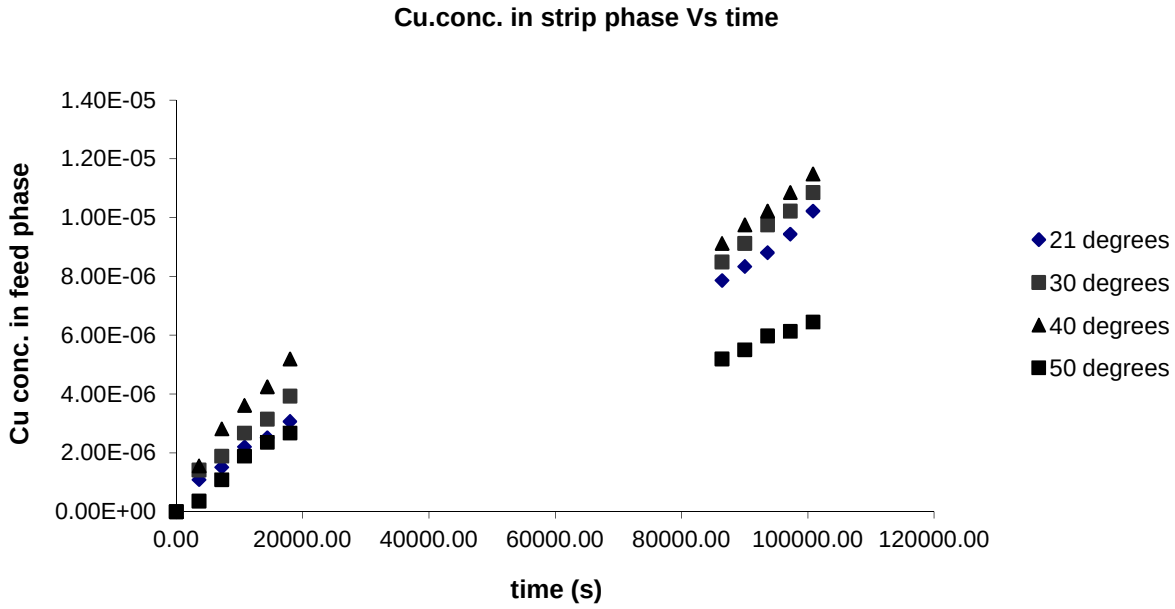

Figure C.5: Copper increase at 40 ml.min^{-1} and varying temperatures

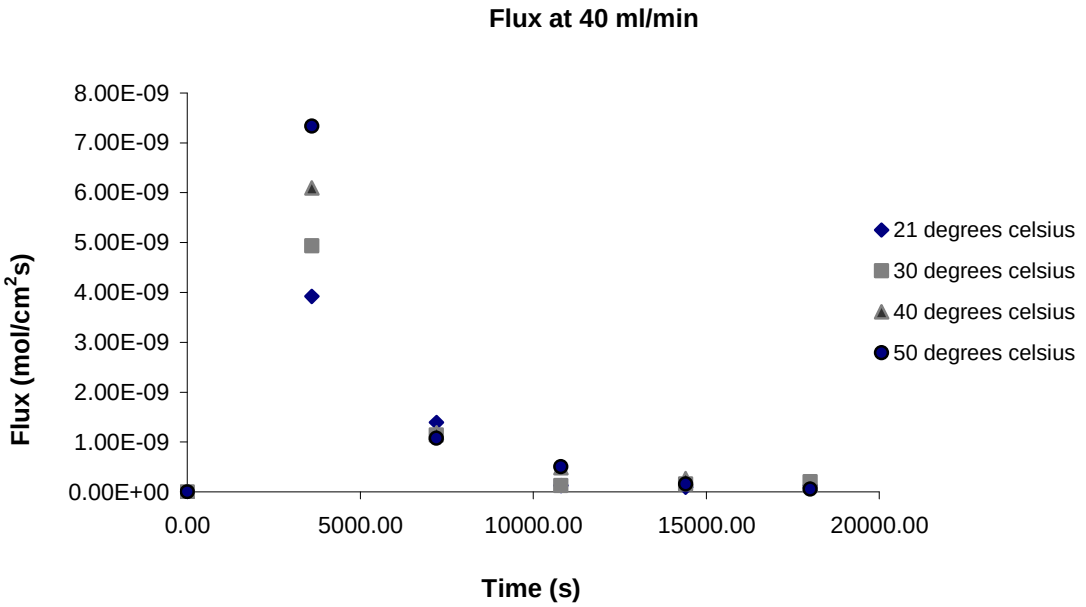

Figure C.6: Mass flux of copper ion at 40 ml.min^{-1} and varying temperatures

Flowrate of 50 $ml.min^{-1}$

Table C.10: Kinetic results for copper extraction at 21 ºC

Time(min)	Time(s)	feed	(mg/L)	strip	(mg/L)	[feed](mol/cm^3)	[cu] (mole)	[strip](mol/cm^3)	ΔC	$C_{bulk,average}$	Moles	Ncu(mol/cm^{2}s)	k_f	Sh
0.00	0.00	10.00	100.00	0.00	0.00	1.57E-05	3.15E-03	0.00E+00	0.00E+00	1.57E-05	0.00E+00	0.00E+00	0.00E+00	0.00E+00
1.00	3600.00	6.70	67.00	0.14	1.40	1.05E-05	2.11E-03	2.20E-07	5.19E-06	1.31E-05	1.04E-03	4.17E-09	3.18E-04	6.99
2.00	7200.00	4.78	47.80	0.21	2.10	7.52E-06	1.50E-03	3.30E-07	3.02E-06	9.03E-06	6.04E-04	1.21E-09	1.34E-04	2.96
3.00	10800.00	2.72	27.20	0.32	3.20	4.28E-06	8.56E-04	5.04E-07	3.24E-06	5.90E-06	6.48E-04	8.69E-10	1.47E-04	3.24
4.00	14400.00	1.67	16.70	0.45	4.50	2.63E-06	5.26E-04	7.08E-07	1.65E-06	3.45E-06	3.30E-04	3.32E-10	9.61E-05	2.11
5.00	18000.00	0.93	9.30	0.60	6.00	1.46E-06	2.93E-04	9.44E-07	1.16E-06	2.05E-06	2.33E-04	1.87E-10	9.15E-05	2.01
24.00	86400.00	0.46	4.60	1.90	19.00	7.24E-07	1.45E-04	2.99E-06	7.40E-07	1.09E-06	1.48E-04	2.48E-11	2.26E-05	0.50
25.00	90000.00	0.33	3.30	2.00	20.00	5.19E-07	1.04E-04	3.15E-06	2.05E-07	6.22E-07	4.09E-05	6.58E-12	1.06E-05	0.23
26.00	93600.00	0.15	1.50	2.40	24.00	2.36E-07	4.72E-05	3.78E-06	2.83E-07	3.78E-07	5.67E-05	8.76E-12	2.32E-05	0.51
27.00	97200.00	0.12	1.20	2.80	28.00	1.89E-07	3.78E-05	4.41E-06	4.72E-08	2.12E-07	9.44E-06	1.41E-12	6.62E-06	0.15

Table C. 11: Kinetic results for copper extraction at 30 ºC

Time(min)	Time(s)	feed	(mg/L)	strip	(mg/L)	[feed](mol/cm^3)	[cu] (mole)	[strip](mol/cm^3)	ΔC	$C_{bulk,average}$	Moles	Ncu(mol/cm^{2}s)	k_f	Sh
0.00	0.00	10.00	100.00	0.00	0.00	1.57E-05	3.15E-03	0.00E+00	0.00E+00	1.57E-05	0.00E+00	0.00E+00	0.00E+00	0.00E+00
1.00	3600.00	4.95	49.50	0.15	1.50	7.79E-06	1.56E-03	2.36E-07	7.95E-06	1.18E-05	1.59E-03	6.39E-09	5.43E-04	11.95
2.00	7200.00	2.75	27.50	0.35	3.50	4.33E-06	8.66E-04	5.51E-07	3.46E-06	6.06E-06	6.92E-04	1.39E-09	2.30E-04	5.05
3.00	10800.00	1.34	13.40	0.48	4.80	2.11E-06	4.22E-04	7.55E-07	2.22E-06	3.22E-06	4.44E-04	5.95E-10	1.85E-04	4.06
4.00	14400.00	0.28	2.80	0.63	6.30	4.41E-07	8.81E-05	9.91E-07	1.67E-06	1.27E-06	3.34E-04	3.35E-10	2.63E-04	5.79
5.00	18000.00	0.27	2.70	0.70	7.00	4.25E-07	8.50E-05	1.10E-06	1.57E-08	4.33E-07	3.15E-06	2.53E-12	5.85E-06	0.13
24.00	86400.00	0.25	2.50	2.00	20.00	3.93E-07	7.87E-05	3.15E-06	3.15E-08	4.09E-07	6.29E-06	1.05E-12	2.58E-06	0.06
25.00	90000.00	0.15	1.50	2.10	21.00	2.36E-07	4.72E-05	3.30E-06	1.57E-07	3.15E-07	3.15E-05	5.06E-12	1.61E-05	0.35
26.00	93600.00	0.13	1.30	2.30	23.00	2.05E-07	4.09E-05	3.62E-06	3.15E-08	2.20E-07	6.29E-06	9.73E-13	4.42E-06	0.10
27.00	97200.00	0.12	1.20	2.50	25.00	1.89E-07	3.78E-05	3.93E-06	1.57E-08	1.97E-07	3.15E-06	4.68E-13	2.38E-06	0.05

Table C.12: Kinetic results for copper extraction at 40 ºC

Time(min)	time(s)	feed	(mg/L)	strip	(mg/L)	[feed](mol/cm^3)	[cu] (mole)	[strip](mol/cm^3)	ΔC	$C_{bulk,average}$	Moles	Ncu(mol/cm^{2}s)	k_f	Sh
0.00	0.00	10.00	100.00	0.00	0.00	1.57E-05	3.15E-03	0.00E+00	0.00E+00	1.57E-05	0.00E+00	0.00E+00	0.00E+00	0.00E+00
1.00	3600.00	3.40	34.00	0.14	1.40	5.35E-06	1.07E-03	2.20E-07	1.04E-05	1.05E-05	2.08E-03	8.35E-09	7.92E-04	17.42
2.00	7200.00	0.93	9.30	0.22	2.20	1.46E-06	2.93E-04	3.46E-07	3.89E-06	3.41E-06	7.77E-04	1.56E-09	4.59E-04	10.09
3.00	10800.00	0.50	5.00	0.28	2.80	7.87E-07	1.57E-04	4.41E-07	6.77E-07	1.13E-06	1.35E-04	1.81E-10	1.61E-04	3.55
4.00	14400.00	0.37	3.70	0.40	4.00	5.82E-07	1.16E-04	6.29E-07	2.05E-07	6.85E-07	4.09E-05	4.11E-11	6.01E-05	1.32
5.00	18000.00	0.31	3.10	0.50	5.00	4.88E-07	9.76E-05	7.87E-07	9.44E-08	5.35E-07	1.89E-05	1.52E-11	2.84E-05	0.62
24.00	86400.00	0.30	3.00	1.80	18.00	4.72E-07	9.44E-05	2.83E-06	1.57E-08	4.80E-07	3.15E-06	5.27E-13	1.10E-06	0.02
25.00	90000.00	0.29	2.90	1.90	19.00	4.56E-07	9.13E-05	2.99E-06	1.57E-08	4.64E-07	3.15E-06	5.06E-13	1.09E-06	0.02
26.00	93600.00	0.23	2.30	2.00	20.00	3.62E-07	7.24E-05	3.15E-06	9.44E-08	4.09E-07	1.89E-05	2.92E-12	7.13E-06	0.16
27.00	97200.00	0.20	2.00	2.10	21.00	3.15E-07	6.29E-05	3.30E-06	4.72E-08	3.38E-07	9.44E-06	1.41E-12	4.15E-06	0.09

Table C.13: Kinetic results for copper extraction at 50 ºC

Time(min)	Time(s)	feed	(mg/L)	strip	(mg/L)	[feed](mol/cm^3)	[cu] (mole)	[strip](mol/cm^3)	ΔC	$C_{bulk,average}$	Moles	Ncu(mol/cm^{2}s)	k_f	Sh
0.00	0.00	10.00	100.00	0.00	0.00	1.57E-05	3.15E-03	0.00E+00	0.00E+00	1.57E-05	0.00E+00	0.00E+00	0.00E+00	0.00E+00
1.00	3600.00	2.60	26.00	0.10	1.00	4.09E-06	8.18E-04	1.57E-07	1.16E-05	9.91E-06	2.33E-03	9.36E-09	9.44E-04	20.77
2.00	7200.00	0.78	7.80	0.15	1.50	1.23E-06	2.45E-04	2.36E-07	2.86E-06	2.66E-06	5.73E-04	1.15E-09	4.33E-04	9.52
3.00	10800.00	0.75	7.50	0.26	2.60	1.18E-06	2.36E-04	4.09E-07	4.72E-08	1.20E-06	9.44E-06	1.26E-11	1.05E-05	0.23
4.00	14400.00	0.73	7.30	0.35	3.50	1.15E-06	2.30E-04	5.51E-07	3.15E-08	1.16E-06	6.29E-06	6.32E-12	5.43E-06	0.12
5.00	18000.00	0.70	7.00	0.45	4.50	1.10E-06	2.20E-04	7.08E-07	4.72E-08	1.13E-06	9.44E-06	7.59E-12	6.75E-06	0.15
24.00	86400.00	0.61	6.10	1.60	16.00	9.60E-07	1.92E-04	2.52E-06	1.42E-07	1.03E-06	2.83E-05	4.74E-12	4.60E-06	0.10
25.00	90000.00	0.51	5.10	1.70	17.00	8.03E-07	1.61E-04	2.68E-06	1.57E-07	8.81E-07	3.15E-05	5.06E-12	5.74E-06	0.13
26.00	93600.00	0.43	4.30	1.90	19.00	6.77E-07	1.35E-04	2.99E-06	1.26E-07	7.40E-07	2.52E-05	3.89E-12	5.26E-06	0.12
27.00	97200.00	0.40	4.00	2.00	20.00	6.29E-07	1.26E-04	3.15E-06	4.72E-08	6.53E-07	9.44E-06	1.41E-12	2.15E-06	0.05

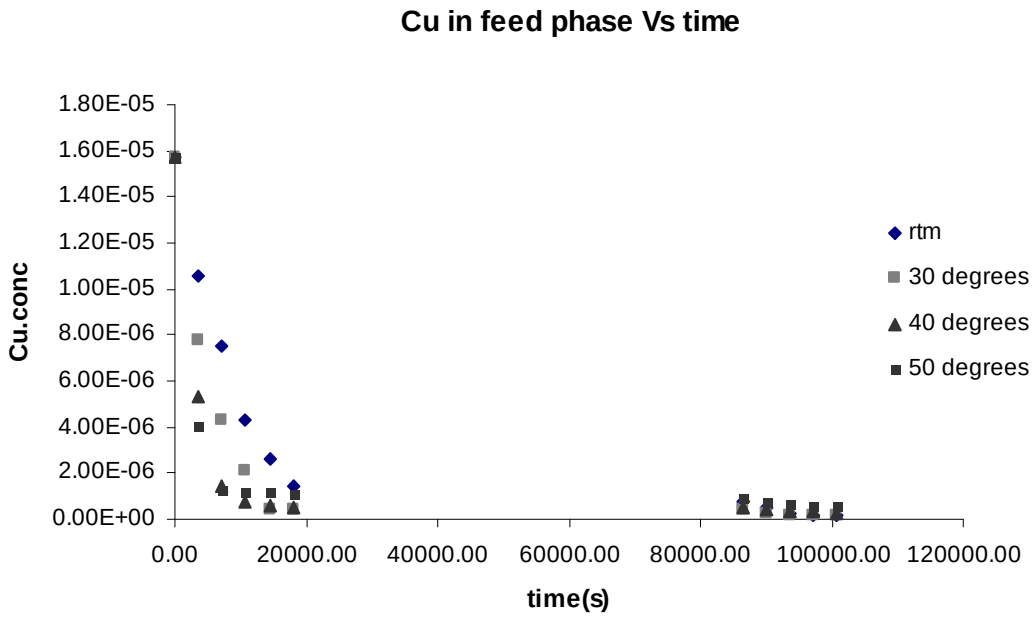

Figure C.7: Copper decrease at 50 ml.min^{-1} and varying temperatures

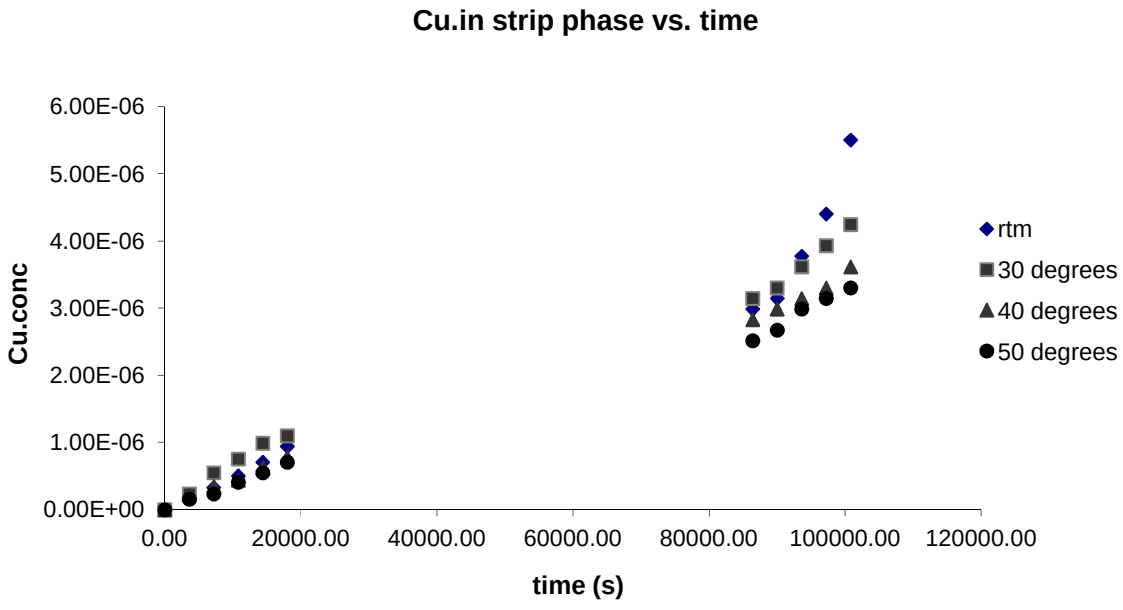

Figure C.8: Copper increase at 50 ml.min^{-1} and varying temperatures

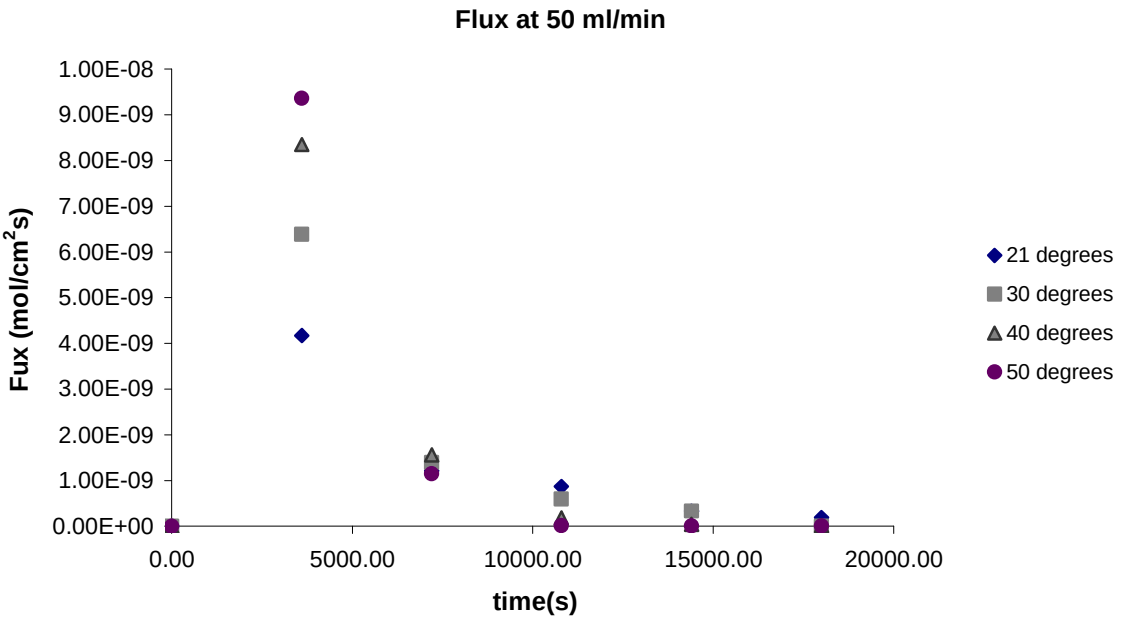

Figure C.9: Mass flux of copper ion at 50 ml.min^{-1} and varying temperatures

Flowrate of 60 $ml.min^{-1}$

Table C.14: Kinetic results for copper extraction at 21 ºC

Time(min)	Time(s)	feed	(mg/L)	strip	(mg/L)	[feed](mol/cm^3)	[cu] (mole)	[strip](mol/cm^3)	ΔC	$C_{bulk,average}$	Moles	Ncu(mol/cm^{2}s)	k_f	Sh
0.00	0.00	10.00	100.00	0.00	0.00	1.57E-05	3.15E-03	0.00E+00	0.00E+00	1.57E-05	0.00E+00	0.00E+00	0.00E+00	0.00E+00
1.00	3600.00	8.5	85.00	0.68	6.80	1.34E-05	2.68E-03	1.07E-06	2.36E-06	1.46E-05	4.72E-04	1.90E-09	1.30E-04	2.87
2.00	7200.00	7.8	78.00	1.7	17.00	1.23E-05	2.45E-03	2.68E-06	1.10E-06	1.28E-05	2.20E-04	4.43E-10	3.45E-05	0.76
3.00	10800.00	4.9	49.00	2.91	29.10	7.71E-06	1.54E-03	4.58E-06	4.56E-06	9.99E-06	9.13E-04	1.22E-09	1.22E-04	2.69
4.00	14400.00	2.9	29.00	3.7	37.00	4.56E-06	9.13E-04	5.82E-06	3.15E-06	6.14E-06	6.29E-04	6.32E-10	1.03E-04	2.27
5.00	18000.00	2	20.00	5.2	52.00	3.15E-06	6.29E-04	8.18E-06	1.42E-06	3.86E-06	2.83E-04	2.28E-10	5.91E-05	1.30

Table C. 15 : Kinetic results for copper extraction at 30 ºC

Time(min)	Time(s)	feed	(mg/L)	strip	(mg/L)	[feed](mol/cm^3)	[cu] (mole)	[strip](mol/cm^3)	ΔC	$C_{bulk,average}$	Moles	Ncu(mol/cm^{2}s)	k_f	Sh
0.00	0.00	10.00	100.00	0.00	0.00	1.57E-05	3.15E-03	0.00E+00	0.00E+00	1.57E-05	0.00E+00	0.00E+00	0.00E+00	0.00E+00
1.00	3600.00	8.10	81.00	0.93	9.30	1.27E-05	2.55E-03	1.46E-06	2.99E-06	1.42E-05	5.98E-04	2.40E-09	1.69E-04	3.71
2.00	7200.00	7.38	73.80	1.87	18.70	1.16E-05	2.32E-03	2.94E-06	1.13E-06	1.22E-05	2.27E-04	4.55E-10	3.74E-05	0.82
3.00	10800.00	3.10	31.00	3.60	36.00	4.88E-06	9.76E-04	5.67E-06	6.74E-06	8.25E-06	1.35E-03	1.80E-09	2.19E-04	4.81
4.00	14400.00	2.00	20.00	4.40	44.00	3.15E-06	6.29E-04	6.92E-06	1.73E-06	4.01E-06	3.46E-04	3.48E-10	8.67E-05	1.91
5.00	18000.00	1.30	13.00	6.50	65.00	2.05E-06	4.09E-04	1.02E-05	1.10E-06	2.60E-06	2.20E-04	1.77E-10	6.82E-05	1.50

Table C.16: Kinetic results for copper extraction at 40 ºC

Time(min)	Time(s)	feed	(mg/L)	strip	(mg/L)	[feed](mol/cm^3)	[cu] (mole)	[strip](mol/cm^3)	ΔC	$C_{bulk,average}$	Moles	Ncu(mol/cm^{2}s)	k_f	Sh
0.00	0.00	10.00	100.00	0.00	0.00	1.57E-05	3.15E-03	0.00E+00	0.00E+00	1.57E-05	0.00E+00	0.00E+00	0.00E+00	0.00E+00
1.00	3600.00	5.40	54.00	0.44	4.40	8.50E-06	1.70E-03	6.92E-07	7.24E-06	1.21E-05	1.45E-03	5.82E-09	4.80E-04	10.56
2.00	7200.00	3.83	38.30	1.15	11.50	6.03E-06	1.21E-03	1.81E-06	2.47E-06	7.26E-06	4.94E-04	9.93E-10	1.37E-04	3.01
3.00	10800.00	2.10	21.00	2.20	22.00	3.30E-06	6.61E-04	3.46E-06	2.72E-06	4.67E-06	5.44E-04	7.29E-10	1.56E-04	3.44
4.00	14400.00	1.60	16.00	3.19	31.90	2.52E-06	5.04E-04	5.02E-06	7.87E-07	2.91E-06	1.57E-04	1.58E-10	5.43E-05	1.19
5.00	18000.00	0.99	9.90	4.46	44.60	1.56E-06	3.12E-04	7.02E-06	9.60E-07	2.04E-06	1.92E-04	1.54E-10	7.57E-05	1.67

Table C.17: Kinetic results for copper extraction at 50 ºC

Time(min)	Time(s)	feed	(mg/L)	strip	(mg/L)	[feed](mol/cm^3)	[cu] (mole)	[strip](mol/cm^3)	ΔC	$C_{bulk,average}$	Moles	Ncu(mol/cm^{2}s)	k_f	Sh
0.00	0.00	10.00	100.00	0.00	0.00	1.57E-05	3.15E-03	0.00E+00	0.00E+00	1.57E-05	0.00E+00	0.00E+00	0.00E+00	0.00E+00
1.00	3600.00	4.50	45.00	0.30	3.00	7.08E-06	1.42E-03	4.72E-07	8.66E-06	1.14E-05	1.73E-03	6.96E-09	6.10E-04	13.42
2.00	7200.00	3.20	32.00	0.70	7.00	5.04E-06	1.01E-03	1.10E-06	2.05E-06	6.06E-06	4.09E-04	8.22E-10	1.36E-04	2.99
3.00	10800.00	2.10	21.00	1.30	13.00	3.30E-06	6.61E-04	2.05E-06	1.73E-06	4.17E-06	3.46E-04	4.64E-10	1.11E-04	2.45
4.00	14400.00	1.01	10.10	1.90	19.00	1.59E-06	3.18E-04	2.99E-06	1.72E-06	2.45E-06	3.43E-04	3.45E-10	1.41E-04	3.10
5.00	18000.00	0.77	7.70	2.30	23.00	1.21E-06	2.42E-04	3.62E-06	3.78E-07	1.40E-06	7.55E-05	6.07E-11	4.34E-05	0.95

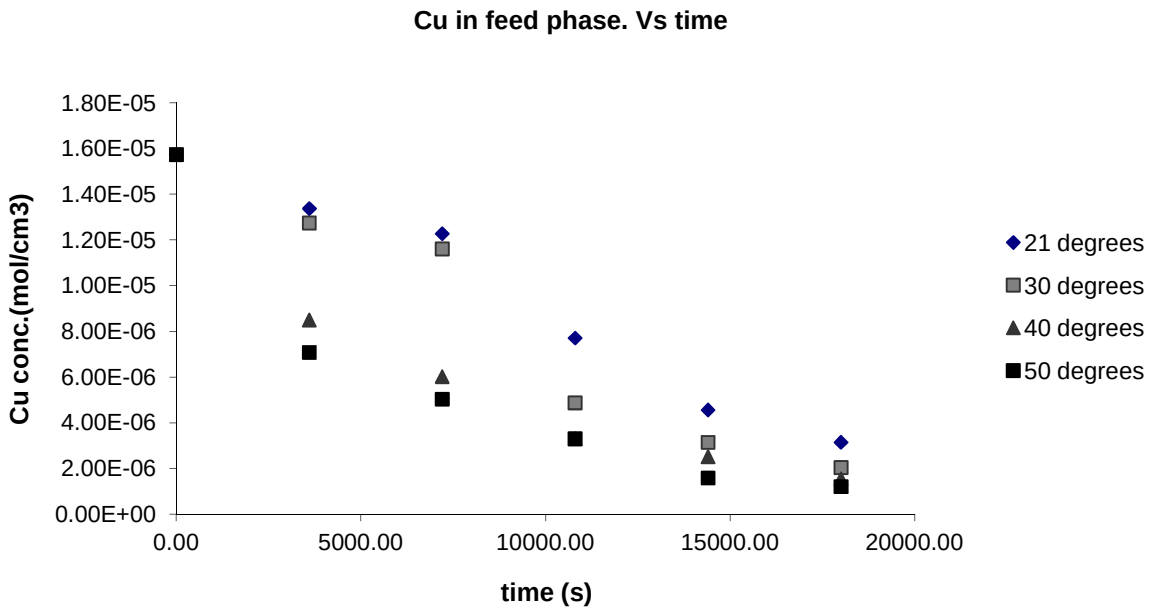

Figure C.10: Copper decrease at 60 ml.min^{-1} and varying temperatures

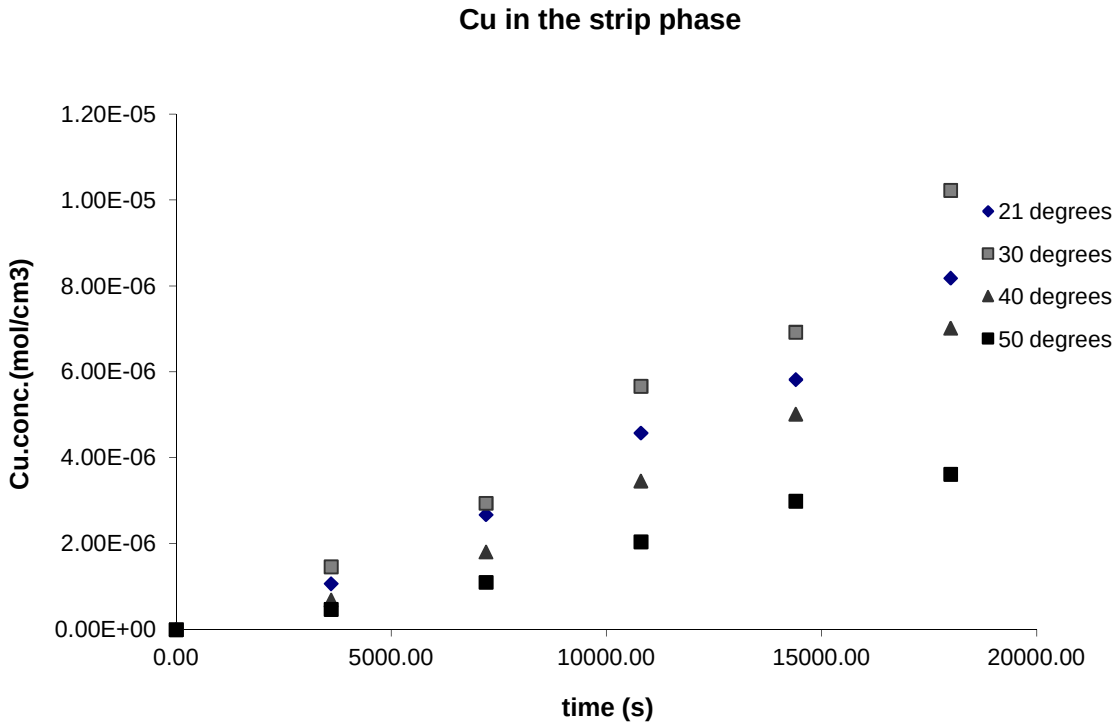

Figure C.11: Copper increase at 60 ml.min^{-1} and varying temperatures

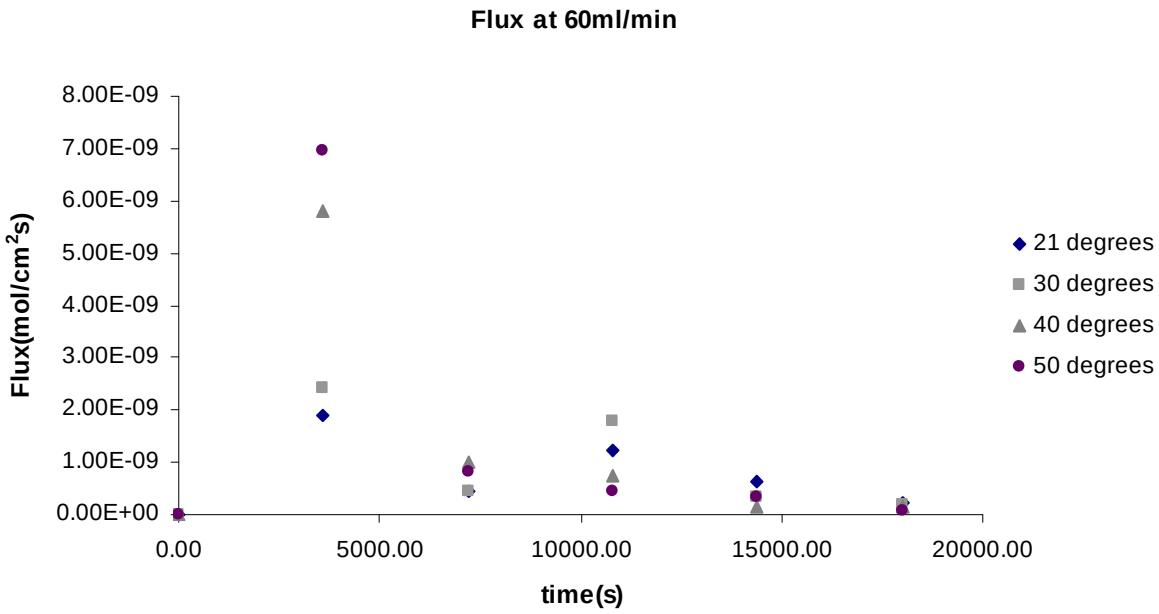

Figure C.12: Mass flux of copper ion at 60 ml.min^{-1} and varying temperatures

Flowrate of 70 $ml.min^{-1}$

Table C.18: Kinetic results for copper extraction at 21 ºC

Time(min)	Time(s)	feed	(mg/L)	strip	(mg/L)	[feed](mol/cm^3)	[cu] (mole)	[strip](mol/cm^3)	ΔC	$C_{bulk,average}$	Moles	Ncu(mol/cm^{2}s)	k_f	Sh
0.00	0.00	10.00	100.00	0.00	0.00	1.57E-05	3.15E-03	0.00E+00	0.00E+00	1.57E-05	0.00E+00	0.00E+00	0.00E+00	0.00E+00
1.00	3600.00	6.30	63.00	0.31	3.10	9.91E-06	1.98E-03	4.88E-07	5.82E-06	1.28E-05	1.16E-03	4.68E-09	3.65E-04	8.03
2.00	7200.00	4.90	49.00	0.99	9.90	7.71E-06	1.54E-03	1.56E-06	2.20E-06	8.81E-06	4.41E-04	8.85E-10	1.00E-04	2.21
3.00	10800.00	3.00	30.00	2.09	20.90	4.72E-06	9.44E-04	3.29E-06	2.99E-06	6.22E-06	5.98E-04	8.01E-10	1.29E-04	2.84
4.00	14400.00	2.10	21.00	3.00	30.00	3.30E-06	6.61E-04	4.72E-06	1.42E-06	4.01E-06	2.83E-04	2.85E-10	7.09E-05	1.56
5.00	18000.00	2.00	20.00	3.51	35.10	3.15E-06	6.29E-04	5.52E-06	1.57E-07	3.23E-06	3.15E-05	2.53E-11	7.84E-06	0.17

Table C.19: Kinetic results for copper extraction at 30 ºC

Time(min)	Time(s)	feed	(mg/L)	strip	(mg/L)	[feed](mol/cm^3)	[cu] (mole)	[strip](mol/cm^3)	ΔC	$C_{bulk,average}$	Moles	Ncu(mol/cm^{2}s)	k_f	Sh
0.00	0.00	10	100.00	0.00	0.00	1.57E-05	3.15E-03	0.00E+00	0.00E+00	1.57E-05	0.00E+00	0.00E+00	0.00E+00	0.00E+00
1.00	3600.00	6.4	64.00	0.53	5.30	1.01E-05	2.01E-03	8.34E-07	5.67E-06	1.29E-05	1.13E-03	4.55E-09	3.53E-04	7.76
2.00	7200.00	5.2	52.00	1.41	14.10	8.18E-06	1.64E-03	2.22E-06	1.89E-06	9.13E-06	3.78E-04	7.59E-10	8.32E-05	1.83
3.00	10800.00	2.7	27.00	2.41	24.10	4.25E-06	8.50E-04	3.79E-06	3.93E-06	6.22E-06	7.87E-04	1.05E-09	1.70E-04	3.73
4.00	14400.00	1.81	18.10	3.2	32.00	2.85E-06	5.70E-04	5.04E-06	1.40E-06	3.55E-06	2.80E-04	2.81E-10	7.93E-05	1.74
5.00	18000.00	1.6	16.00	3.8	38.00	2.52E-06	5.04E-04	5.98E-06	3.30E-07	2.68E-06	6.61E-05	5.31E-11	1.98E-05	0.44

Table C.20: Kinetic results for copper extraction at 40 ºC

Time(hr)	Time(s)	feed	(mg/L)	strip	(mg/L)	[feed](mol/cm^3)	[cu] (mole)	[strip](mol/cm^3)	ΔC	$C_{bulk,average}$	Moles	Ncu(mol/cm^{2}s)	k_f	Sh
0.00	0.00	10.00	100.00	0.00	0.00	1.57E-05	3.15E-03	0.00E+00	0.00E+00	1.57E-05	0.00E+00	0.00E+00	0.00E+00	0.00E+00
1.00	3600.00	5.40	54.00	0.24	2.40	8.50E-06	1.70E-03	3.78E-07	7.24E-06	1.21E-05	1.45E-03	5.82E-09	4.80E-04	10.56
2.00	7200.00	4.10	41.00	0.95	9.50	6.45E-06	1.29E-03	1.49E-06	2.05E-06	7.47E-06	4.09E-04	8.22E-10	1.10E-04	2.42
3.00	10800.00	1.80	18.00	1.80	18.00	2.83E-06	5.67E-04	2.83E-06	3.62E-06	4.64E-06	7.24E-04	9.70E-10	2.09E-04	4.60
4.00	14400.00	1.50	15.00	2.60	26.00	2.36E-06	4.72E-04	4.09E-06	4.72E-07	2.60E-06	9.44E-05	9.49E-11	3.65E-05	0.80
5.00	18000.00	1.40	14.00	3.20	32.00	2.20E-06	4.41E-04	5.04E-06	1.57E-07	2.28E-06	3.15E-05	2.53E-11	1.11E-05	0.24

Table C.21: Kinetic results for copper extraction at 50 ºC

Time(hr)	Time(s)	feed	(mg/L)	strip	(mg/L)	[feed](mol/cm^3)	[cu] (mole)	[strip](mol/cm^3)	ΔC	$C_{bulk,average}$	Moles	Ncu(mol/cm^{2}s)	k_f	Sh
0.00	0.00	10.00	100.00	0.00	0.00	1.57E-05	3.15E-03	0.00E+00	0.00E+00	1.57E-05	0.00E+00	0.00E+00	0.00E+00	0.00E+00
1.00	3600.00	4.10	41.00	0.08	0.80	6.45E-06	1.29E-03	1.26E-07	9.28E-06	1.11E-05	1.86E-03	7.46E-09	6.73E-04	14.80
2.00	7200.00	2.80	28.00	0.71	7.10	4.41E-06	8.81E-04	1.12E-06	2.05E-06	5.43E-06	4.09E-04	8.22E-10	1.51E-04	3.33
3.00	10800.00	2.10	21.00	1.52	15.20	3.30E-06	6.61E-04	2.39E-06	1.10E-06	3.86E-06	2.20E-04	2.95E-10	7.66E-05	1.68
4.00	14400.00	1.67	16.70	2.34	23.40	2.63E-06	5.26E-04	3.68E-06	6.77E-07	2.97E-06	1.35E-04	1.36E-10	4.58E-05	1.01
5.00	18000.00	1.20	12.00	2.72	27.20	1.89E-06	3.78E-04	4.28E-06	7.40E-07	2.26E-06	1.48E-04	1.19E-10	5.27E-05	1.16

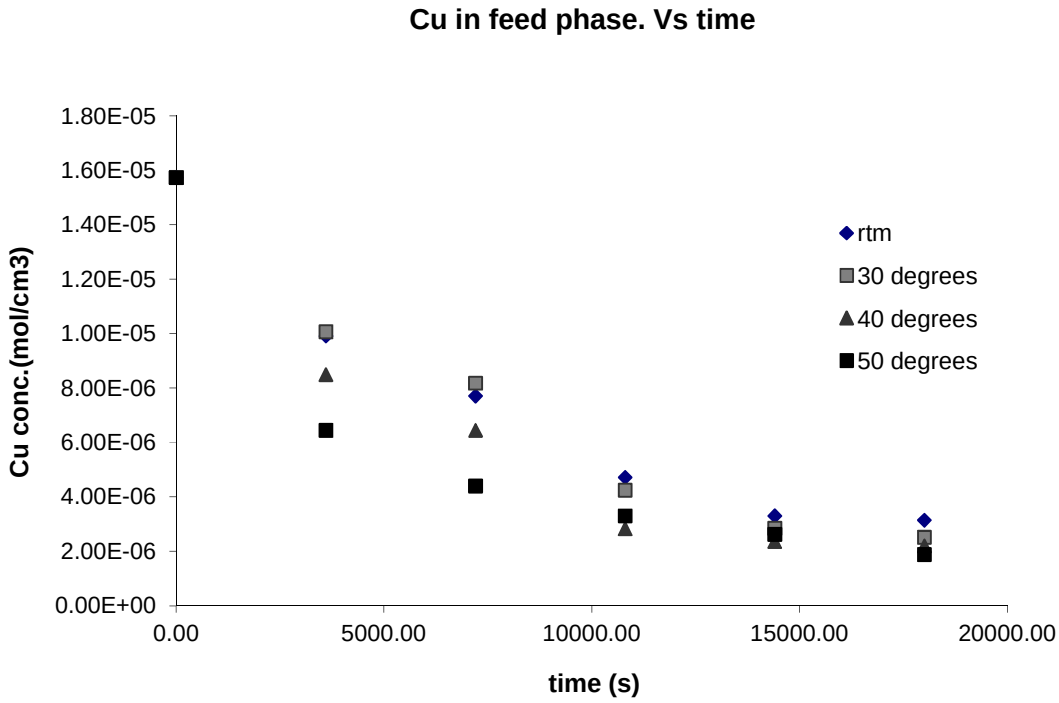

Figure C.13: Copper decrease at 70 ml.min^{-1} and varying temperatures

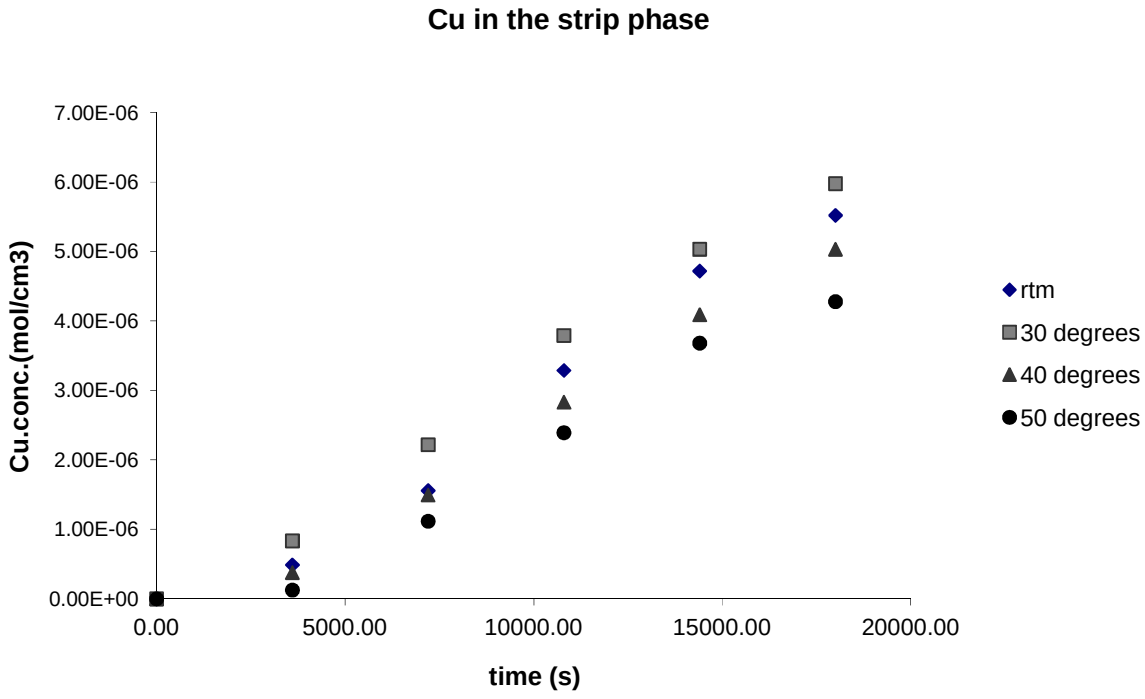

Figure C.14: Copper increase at 70 ml.min^{-1} and varying temperatures

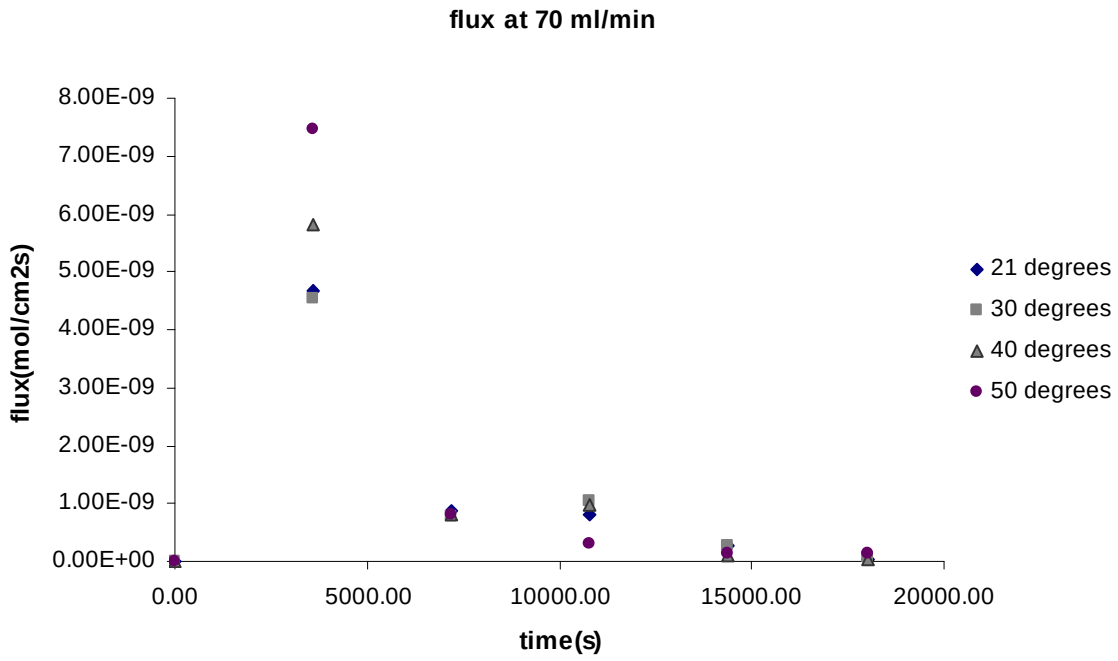

Figure C.15: Mass flux of copper ion at 70 ml.min^{-1} and varying temperatures

Flowrate of 80 $ml.min^{-1}$

Table C.22: Kinetic results for copper extraction at 21 ºC

Time(hr)	time(s)	feed	(mg/L)	strip	(mg/L)	[feed](mol/cm^3)	[cu] (mole)	[strip](mol/cm^3)	ΔC	$C_{bulk,average}$	Moles	Ncu(mol/cm^{2}s)	k_f	Sh
0.00	0.00	9.3	93.00	0	0.00	1.46E-05	2.93E-03	0.00E+00	0.00E+00	1.46E-05	0.00E+00	0.00E+00	0.00E+00	0.00E+00
1.00	3600.00	6.8	68.00	0.36	3.60	1.07E-05	2.14E-03	5.67E-07	3.93E-06	1.27E-05	7.87E-04	3.16E-09	2.50E-04	5.49
2.00	7200.00	5.9	59.00	0.99	9.90	9.28E-06	1.86E-03	1.56E-06	1.42E-06	9.99E-06	2.83E-04	5.69E-10	5.70E-05	1.25
3.00	10800.00	3.3	33.00	1.52	15.20	5.19E-06	1.04E-03	2.39E-06	4.09E-06	7.24E-06	8.18E-04	1.10E-09	1.51E-04	3.33
4.00	14400.00	2.1	21.00	2.1	21.00	3.30E-06	6.61E-04	3.30E-06	1.89E-06	4.25E-06	3.78E-04	3.79E-10	8.93E-05	1.96
5.00	18000.00	1.4	14.00	3.3	33.00	2.20E-06	4.41E-04	5.19E-06	1.10E-06	2.75E-06	2.20E-04	1.77E-10	6.43E-05	1.41

Table C. 23: Kinetic results for copper extraction at 30 ºC

Time(hr)	time(s)	feed	(mg/L)	strip	(mg/L)	[feed](mol/cm^3)	[cu] (mole)	[strip](mol/cm^3)	ΔC	$C_{bulk,average}$	Moles	Ncu(mol/cm^{2}s)	k_f	Sh
0.00	0.00	9.44	94.40	0.00	0.00	1.49E-05	2.97E-03	0.00E+00	0.00E+00	1.49E-05	0.00E+00	0.00E+00	0.00E+00	0.00E+00
1.00	3600.00	5.4	54.00	0.77	7.70	8.50E-06	1.70E-03	1.21E-06	6.36E-06	1.17E-05	1.27E-03	5.11E-09	4.38E-04	9.63
2.00	7200.00	4	40.00	1.36	13.60	6.29E-06	1.26E-03	2.14E-06	2.20E-06	7.40E-06	4.41E-04	8.85E-10	1.20E-04	2.63
3.00	10800.00	2.04	20.40	2.12	21.20	3.21E-06	6.42E-04	3.34E-06	3.08E-06	4.75E-06	6.17E-04	8.26E-10	1.74E-04	3.83
4.00	14400.00	1.54	15.40	2.5	25.00	2.42E-06	4.85E-04	3.93E-06	7.87E-07	2.82E-06	1.57E-04	1.58E-10	5.61E-05	1.23
5.00	18000.00	1.28	12.80	3.3	33.00	2.01E-06	4.03E-04	5.19E-06	4.09E-07	2.22E-06	8.18E-05	6.58E-11	2.96E-05	0.65

Table C. 24: Kinetic results for copper extraction at 40 ºC

Time(hr)	time(s)	feed	(mg/L)	strip	(mg/L)	[feed](mol/cm^3)	[cu] (mole)	[strip](mol/cm^3)	ΔC	$C_{bulk,average}$	Moles	Ncu(mol/cm^{2}s)	k_f	Sh
0.00	0.00	9.2	92.00	0.00	0.00	1.45E-05	2.90E-03	0.00E+00	0.00E+00	1.45E-05	0.00E+00	0.00E+00	0.00E+00	0.00E+00
1.00	3600.00	7.2	72.00	0.34	3.40	1.13E-05	2.27E-03	5.35E-07	3.15E-06	1.29E-05	6.29E-04	2.53E-09	1.96E-04	4.31
2.00	7200.00	6.7	67.00	0.78	7.80	1.05E-05	2.11E-03	1.23E-06	7.87E-07	1.09E-05	1.57E-04	3.16E-10	2.89E-05	0.64
3.00	10800.00	4.09	40.90	1.28	12.80	6.44E-06	1.29E-03	2.01E-06	4.11E-06	8.49E-06	8.21E-04	1.10E-09	1.30E-04	2.85
4.00	14400.00	3.21	32.10	2.07	20.70	5.05E-06	1.01E-03	3.26E-06	1.38E-06	5.74E-06	2.77E-04	2.78E-10	4.84E-05	1.07
5.00	18000.00	2.58	25.80	3.11	31.10	4.06E-06	8.12E-04	4.89E-06	9.91E-07	4.56E-06	1.98E-04	1.59E-10	3.50E-05	0.77

Table C.25: Kinetic results for copper extraction at 50 ºC

Time(hr)	time(s)	feed	(mg/L)	strip	(mg/L)	[feed](mol/cm^3)	[cu] (mole)	[strip](mol/cm^3)	∆C	$C_{bulk,average}$	Moles	Ncu(mol/cm^{2}s)	k_f	Sh
0.00	0.00	9.7	97.00	0.00	0.00	1.53E-05	3.05E-03	0.00E+00	0.00E+00	1.53E-05	0.00E+00	0.00E+00	0.00E+00	0.00E+00
1.00	3600.00	2.8	28.00	0.12	1.20	4.41E-06	8.81E-04	1.89E-07	1.09E-05	9.84E-06	2.17E-03	8.73E-09	8.87E-04	19.52
2.00	7200.00	1.39	13.90	0.41	4.10	2.19E-06	4.37E-04	6.45E-07	2.22E-06	3.30E-06	4.44E-04	8.92E-10	2.70E-04	5.95
3.00	10800.00	0.51	5.10	1	10.00	8.03E-07	1.61E-04	1.57E-06	1.38E-06	1.49E-06	2.77E-04	3.71E-10	2.48E-04	5.46
4.00	14400.00	0.43	4.30	1.44	14.40	6.77E-07	1.35E-04	2.27E-06	1.26E-07	7.40E-07	2.52E-05	2.53E-11	3.42E-05	0.75
5.00	18000.00	0.27	2.70	2.4	24.00	4.25E-07	8.50E-05	3.78E-06	2.52E-07	5.51E-07	5.04E-05	4.05E-11	7.35E-05	1.62

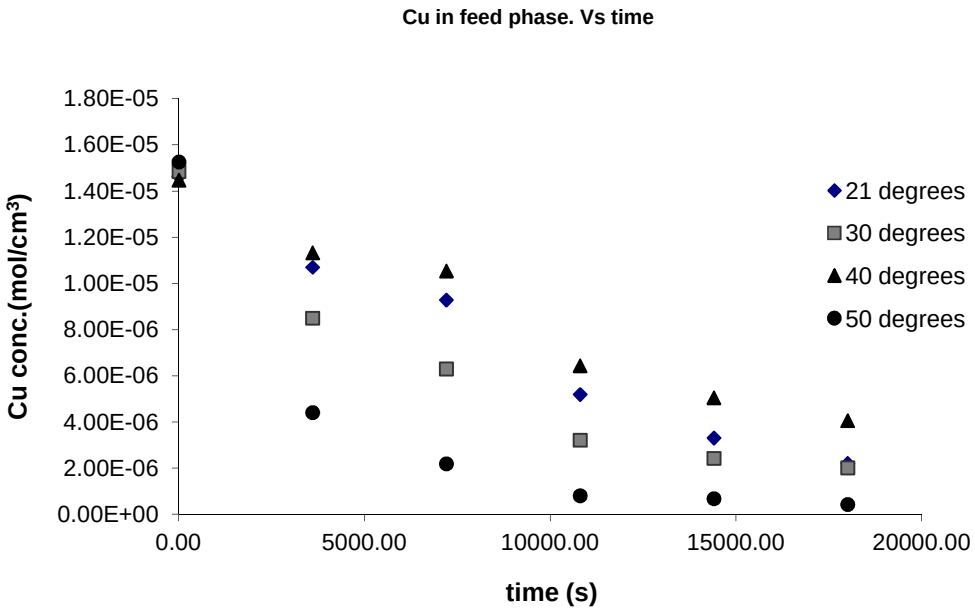

Figure C.16: Copper decrease at 80 ml.min^{-1} and varying temperatures

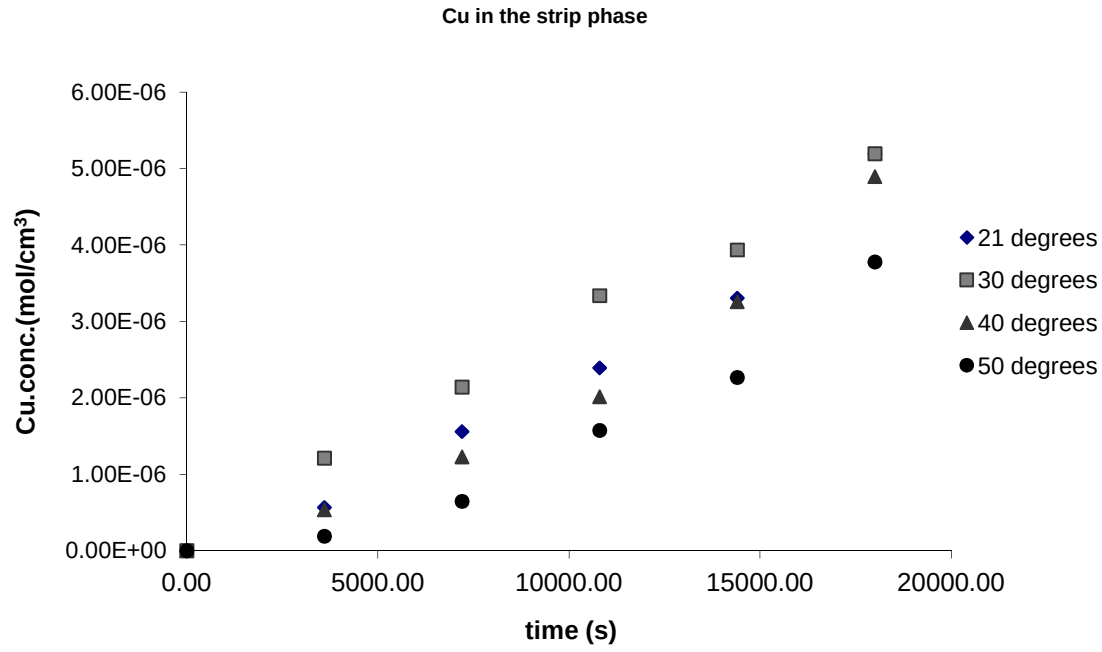

Figure C.17: Copper increase at 80 ml.min^{-1} and varying temperatures

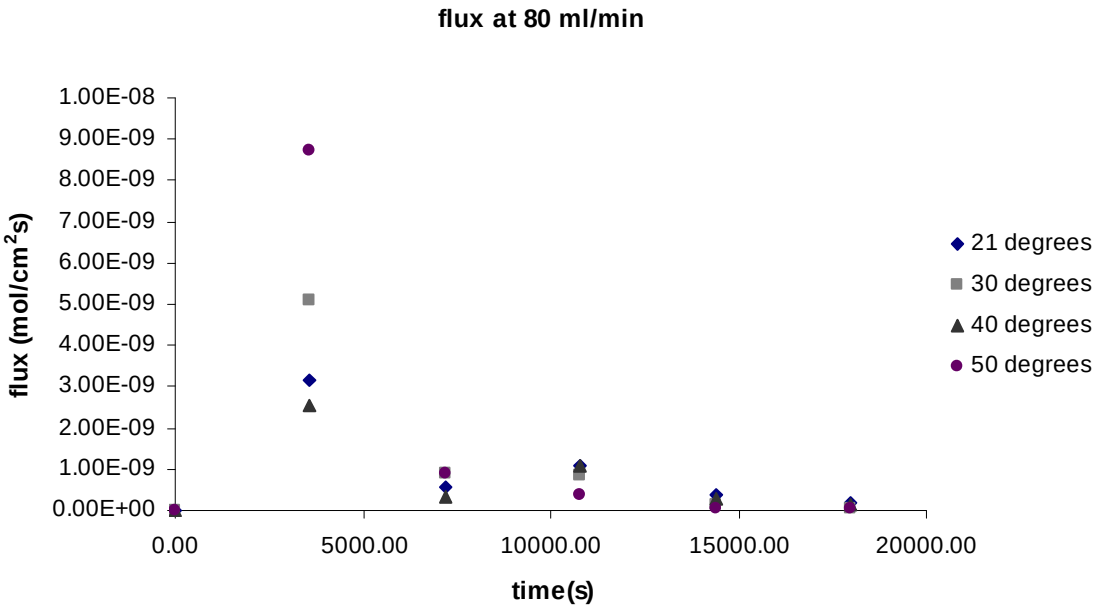

Figure C.18: Mass flux of copper ion at 80 ml.min^{-1} and varying temperatures

Flowrate of 90 ml.min^{-1}

Table C. 26: Kinetic results for copper extraction at 21 ºC

Time(hr)	time(s)	feed	(mg/L)	strip	(mg/L)	[feed](mol/cm^3)	[cu] (mole)	[strip](mol/cm^3)	∆C	$C_{bulk,average}$	Moles	Ncu(mol/cm^{2}s)	k_f	Sh
0.00	0.00	10.00	100.00	0.00	0.00	1.57E-05	3.15E-03	0.00E+00	0.00E+00	1.57E-05	0.00E+00	0.00E+00	0.00E+00	0.00E+00
1.00	3600.00	6.00	60.00	0.11	1.10	9.44E-06	1.89E-03	1.73E-07	6.29E-06	1.26E-05	1.26E-03	5.06E-09	4.02E-04	8.84
2.00	7200.00	4.70	47.00	0.92	9.20	7.40E-06	1.48E-03	1.45E-06	2.05E-06	8.42E-06	4.09E-04	8.22E-10	9.77E-05	2.15
3.00	10800.00	2.30	23.00	2.09	20.90	3.62E-06	7.24E-04	3.29E-06	3.78E-06	5.51E-06	7.55E-04	1.01E-09	1.84E-04	4.04
4.00	14400.00	2.10	21.00	3.50	35.00	3.30E-06	6.61E-04	5.51E-06	3.15E-07	3.46E-06	6.29E-05	6.32E-11	1.83E-05	0.40
5.00	18000.00	1.77	17.70	4.90	49.00	2.79E-06	5.57E-04	7.71E-06	5.19E-07	3.05E-06	1.04E-04	8.35E-11	2.74E-05	0.60

Table C.27: Kinetic results for copper extraction at 30 ºC

Time(hr)	time(s)	feed	(mg/L)	strip	(mg/L)	[feed](mol/cm^3)	[cu] (mole)	[strip](mo	∆C	$C_{bulk,average}$	Moles	Ncu(mol/cm^{2}s)	k_f	Sh
0.00	0.00	9.6	96.00	0.00	0.00	1.51E-05	3.02E-03	0.00E+00	0.00E+00	1.51E-05	0.00E+00	0.00E+00	0.00E+00	0.00E+00
1.00	3600.00	6.1	61.00	0.47	4.70	9.60E-06	1.92E-03	7.40E-07	5.51E-06	1.24E-05	1.10E-03	4.43E-09	3.58E-04	7.88
2.00	7200.00	5	50.00	1.96	19.60	7.87E-06	1.57E-03	3.08E-06	1.73E-06	8.73E-06	3.46E-04	6.96E-10	7.97E-05	1.75
3.00	10800.00	4.62	46.20	2.52	25.20	7.27E-06	1.45E-03	3.97E-06	5.98E-07	7.57E-06	1.20E-04	1.60E-10	2.12E-05	0.47
4.00	14400.00	3.61	36.10	3.7	37.00	5.68E-06	1.14E-03	5.82E-06	1.59E-06	6.48E-06	3.18E-04	3.19E-10	4.93E-05	1.09
5.00	18000.00	2.5	25.00	3.9	39.00	3.93E-06	7.87E-04	6.14E-06	1.75E-06	4.81E-06	3.49E-04	2.81E-10	5.84E-05	1.29

Table C. 28: Kinetic results for copper extraction at 40 ºC

Time(hr)	time(s)	feed	(mg/L)	strip	(mg/L)	[feed](mol/cm^3)	[cu] (mole)	[strip](mol/cm^3)	ΔC	$C_{bulk,average}$	Moles	Ncu(mol/cm^{2}s)	k_f	Sh
0.00	0.00	10.2	102.00	0.00	0.00	1.61E-05	3.21E-03	0.00E+00	0.00E+00	1.61E-05	0.00E+00	0.00E+00	0.00E+00	0.00E+00
1.00	3600.00	5.1	51.00	0.34	3.40	8.03E-06	1.61E-03	5.35E-07	8.03E-06	1.20E-05	1.61E-03	6.45E-09	5.36E-04	11.79
2.00	7200.00	3.83	38.30	0.5	5.00	6.03E-06	1.21E-03	7.87E-07	2.00E-06	7.03E-06	4.00E-04	8.03E-10	1.14E-04	2.51
3.00	10800.00	2.39	23.90	1.78	17.80	3.76E-06	7.52E-04	2.80E-06	2.27E-06	4.89E-06	4.53E-04	6.07E-10	1.24E-04	2.73
4.00	14400.00	1.79	17.90	2.67	26.70	2.82E-06	5.63E-04	4.20E-06	9.44E-07	3.29E-06	1.89E-04	1.90E-10	5.77E-05	1.27
5.00	18000.00	1.58	15.80	2.71	27.10	2.49E-06	4.97E-04	4.26E-06	3.30E-07	2.65E-06	6.61E-05	5.31E-11	2.00E-05	0.44

Table C. 29: Kinetic results for copper extraction at 50 ºC

Time(hr)	time(s)	feed	(mg/L)	strip	(mg/L)	[feed](mol/cm^3)	[cu] (mole)	[strip](mol/cm^3)	ΔC	$C_{bulk,average}$	Moles	Ncu(mol/cm^{2}s)	k_f	Sh
0.00	0.00	10.00	100.00	0.00	0.00	1.57E-05	3.15E-03	0.00E+00	0.00	1.57E-05	0.00E+00	0.00E+00	0.00E+00	0.00E+00
1.00	3600.00	4.80	48.00	0.78	7.80	7.55E-06	1.51E-03	1.23E-06	0.00	1.16E-05	1.64E-03	6.58E-09	5.65E-04	12.43
2.00	7200.00	3.78	37.80	1.65	16.50	5.95E-06	1.19E-03	2.60E-06	0.00	6.75E-06	3.21E-04	6.45E-10	9.56E-05	2.10
3.00	10800.00	2.51	25.10	2.92	29.20	3.95E-06	7.90E-04	4.60E-06	0.00	4.95E-06	4.00E-04	5.35E-10	1.08E-04	2.38
4.00	14400.00	2.11	21.10	2.44	24.40	3.32E-06	6.64E-04	3.84E-06	0.00	3.64E-06	1.26E-04	1.26E-10	3.48E-05	0.77
5.00	18000.00	1.21	12.10	2.82	28.20	1.90E-06	3.81E-04	4.44E-06	0.00	2.61E-06	2.83E-04	2.28E-10	8.72E-05	1.92

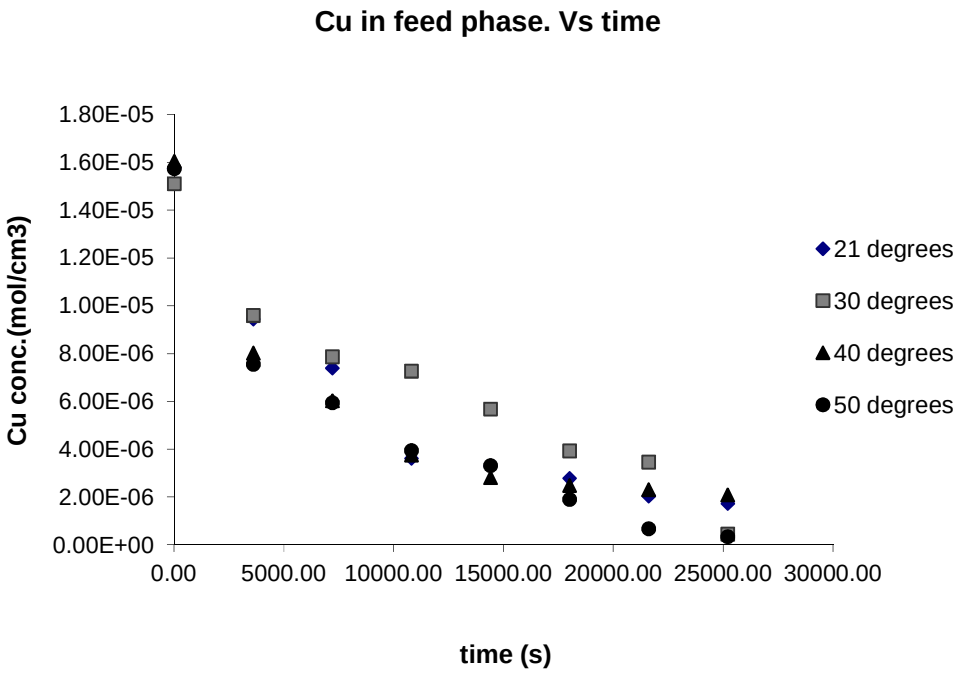

Figure C.19: Copper decrease at 90 ml.min^{-1} and varying temperatures

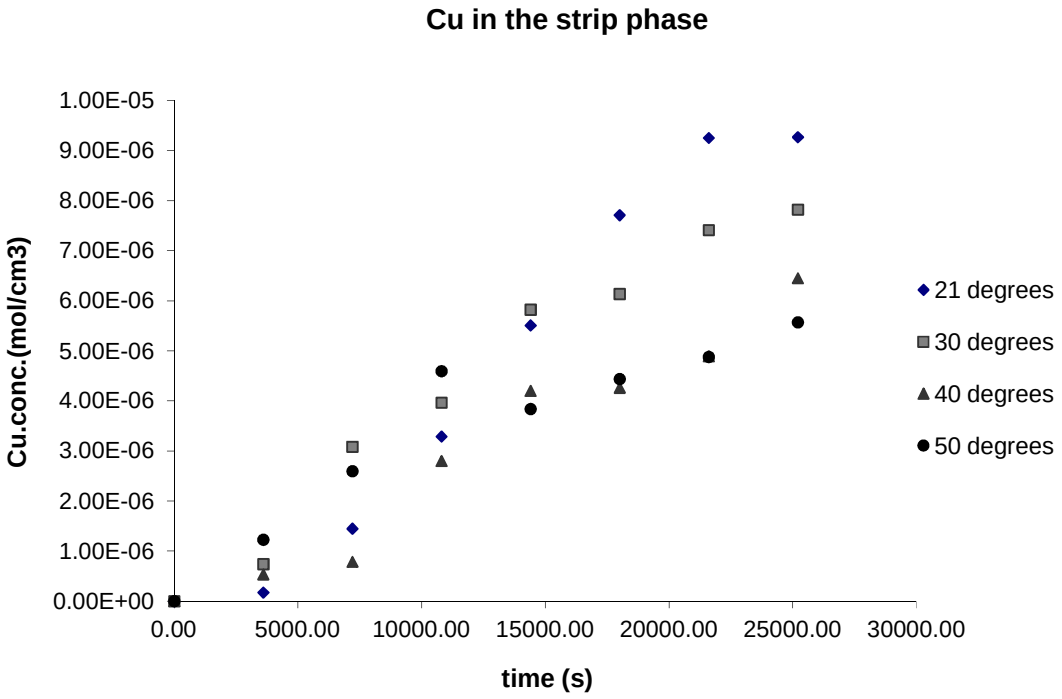

Figure C.20: Copper increase at 90 ml.min^{-1} and varying temperatures

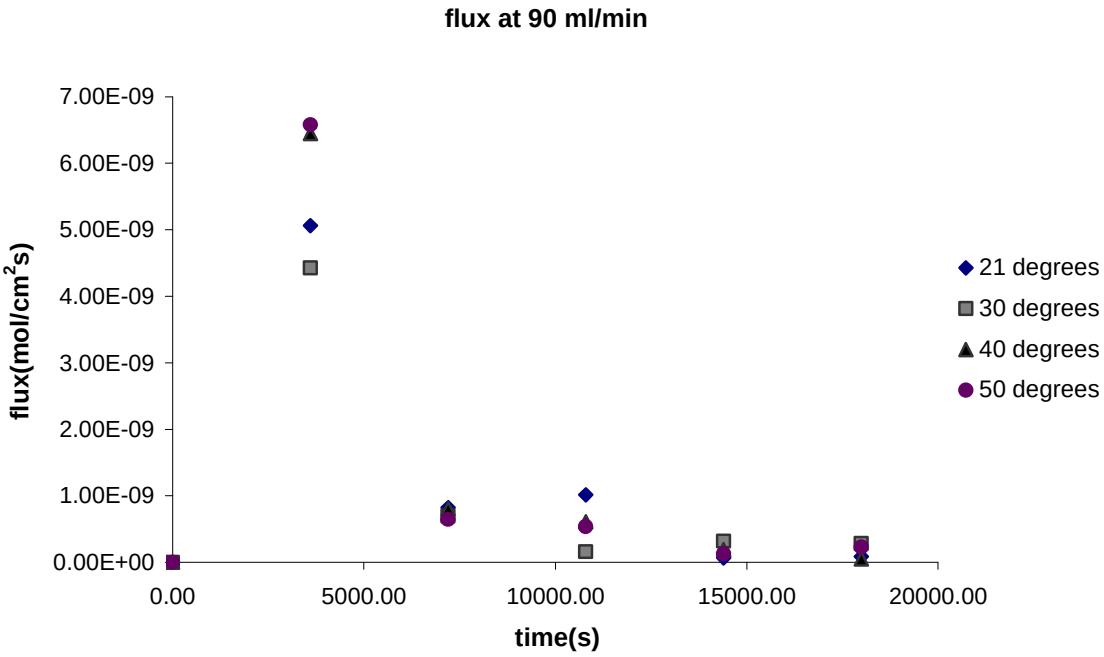

Figure C.21: Mass flux of copper ions at 90 ml.min^{-1} and varying temperatures

Flowrate of 100 $ml.min^{-1}$

Table C. 30: Kinetic results for copper extraction at 21ºC

Time (hr)	time(s)	feed	(mg/L)	strip	(mg/L)	[feed](mol/cm^3)	[cu] (mole)	[strip](mol/cm^3)	ΔC	$C_{bulk,average}$	Moles	Ncu(mol/cm^{2}s)	k_f	Sh
0.00	0.00	9.6	96.00	0	0.00	1.51E-05	3.02E-03	0.00E+00	0.00E+00	1.51E-05	0.00E+00	0.00E+00	0.00E+00	0.00E+00
1.00	3600.00	6.9	69.00	0.71	7.10	1.09E-05	2.17E-03	1.12E-06	4.25E-06	1.30E-05	8.50E-04	3.42E-09	2.63E-04	5.79
2.00	7200.00	6.1	61.00	0.93	9.30	9.60E-06	1.92E-03	1.46E-06	1.26E-06	1.02E-05	2.52E-04	5.06E-10	4.95E-05	1.09
3.00	10800.00	3.5	35.00	1.2	12.00	5.51E-06	1.10E-03	1.89E-06	4.09E-06	7.55E-06	8.18E-04	1.10E-09	1.45E-04	3.19
4.00	14400.00	2.6	26.00	1.3	13.00	4.09E-06	8.18E-04	2.05E-06	1.42E-06	4.80E-06	2.83E-04	2.85E-10	5.93E-05	1.30
5.00	18000.00	1.6	16.00	1.4	14.00	2.52E-06	5.04E-04	2.20E-06	1.57E-06	3.30E-06	3.15E-04	2.53E-10	7.66E-05	1.68

Table C.31: Kinetic results for copper extraction at 30 ºC

Time (hr)	time(s)	feed	(mg/L)	strip	(mg/L)	[feed](mol/cm^3)	[cu] (mole)	[strip](mol/cm^3)	%feed	%strip	ΔC	$C_{bulk,average}$	Moles	Ncu(mol/cm^{2}s)	k_f	Sh
0.00	0.00	10	100.00	0	0.00	1.57E-05	3.15E-03	0.00E+00	100.00	0.00	0.00E+00	1.57E-05	0.00E+00	0.00E+00	0.00E+00	0.00E+00
1.00	3600.00	6.7	67.00	0.52	5.20	1.05E-05	2.11E-03	8.18E-07	67.00	5.20	5.19E-06	1.31E-05	1.04E-03	4.17E-09	3.18E-04	6.99
2.00	7200.00	5.78	57.80	1.64	16.40	9.10E-06	1.82E-03	2.58E-06	57.80	16.40	1.45E-06	9.82E-06	2.90E-04	5.82E-10	5.93E-05	1.30
3.00	10800.00	3.23	32.30	2.5	25.00	5.08E-06	1.02E-03	3.93E-06	32.30	25.00	4.01E-06	7.09E-06	8.03E-04	1.08E-09	1.52E-04	3.34
4.00	14400.00	2.12	21.20	4.5	45.00	3.34E-06	6.67E-04	7.08E-06	21.20	45.00	1.75E-06	4.21E-06	3.49E-04	3.51E-10	8.34E-05	1.83
5.00	18000.00	1.75	17.50	5.11	51.10	2.75E-06	5.51E-04	8.04E-06	17.50	51.10	5.82E-07	3.05E-06	1.16E-04	9.36E-11	3.07E-05	0.68

Table C. 32: Kinetic results for copper extraction at 40 ºC

Time (hr)	time(s)	feed	(mg/L)	strip	(mg/L)	[feed](mol/cm^3)	[cu] (mole)	[strip](mol/cm^3)	ΔC	$C_{bulk,average}$	Moles	Ncu(mol/cm^{2}s)	k_f	Sh
0.00	0.00	10	100.00	0.00	0.00	1.57E-05	3.15E-03	0.00E+00	0.00E+00	1.57E-05	0.00E+00	0.00E+00	0.00E+00	0.00E+00
1.00	3600.00	7.3	73.00	0.91	9.10	1.15E-05	2.30E-03	1.43E-06	4.25E-06	1.36E-05	8.50E-04	3.42E-09	2.51E-04	5.52
2.00	7200.00	6.7	67.00	1.4	14.00	1.05E-05	2.11E-03	2.20E-06	9.44E-07	1.10E-05	1.89E-04	3.79E-10	3.44E-05	0.76
3.00	10800.00	3.1	31.00	2.8	28.00	4.88E-06	9.76E-04	4.41E-06	5.67E-06	7.71E-06	1.13E-03	1.52E-09	1.97E-04	4.33
4.00	14400.00	2	20.00	3.5	35.00	3.15E-06	6.29E-04	5.51E-06	1.73E-06	4.01E-06	3.46E-04	3.48E-10	8.67E-05	1.91
5.00	18000.00	0.36	3.60	4.6	46.00	5.67E-07	1.13E-04	7.24E-06	2.58E-06	1.86E-06	5.16E-04	4.15E-10	2.23E-04	4.92

Table C. 33: Kinetic results for copper extraction at 50 ºC

Time (hr)	time(s)	feed	(mg/L)	strip	(mg/L)	[feed](mol/cm^3)	[cu] (mole)	[strip](mol/cm^3)	ΔC	$C_{bulk,average}$	Moles	Ncu(mol/cm^{2}s)	k_f	Sh
0.00	0.00	9.2	92.00	0.00	0.00	1.45E-05	2.90E-03	0.00E+00	0.00E+00	1.45E-05	0.00E+00	0.00E+00	0.00E+00	0.00E+00
1.00	3600.00	5.6	56.00	1.2	12.00	8.81E-06	1.76E-03	1.89E-06	5.67E-06	1.16E-05	1.13E-03	4.55E-09	0.000391	8.60
2.00	7200.00	4.9	49.00	1.9	19.00	7.71E-06	1.54E-03	2.99E-06	1.10E-06	8.26E-06	2.20E-04	4.43E-10	5.36E-05	1.18
3.00	10800.00	3.5	35.00	2.2	22.00	5.51E-06	1.10E-03	3.46E-06	2.20E-06	6.61E-06	4.41E-04	5.90E-10	8.93E-05	1.96
4.00	14400.00	3.2	32.00	3	30.00	5.04E-06	1.01E-03	4.72E-06	4.72E-07	5.27E-06	9.44E-05	9.49E-11	1.8E-05	0.40
5.00	18000.00	2.11	21.10	3.8	38.00	3.32E-06	6.64E-04	5.98E-06	1.72E-06	4.18E-06	3.43E-04	2.76E-10	6.6E-05	1.45

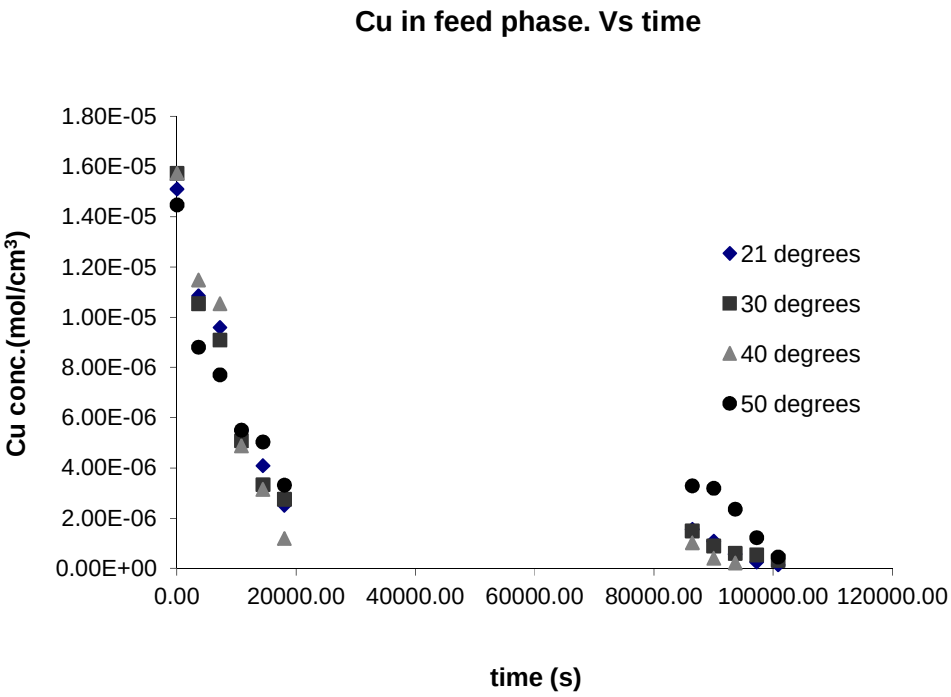

Figure C.22: Copper decrease at 100 ml.min^{-1} and varying temperatures

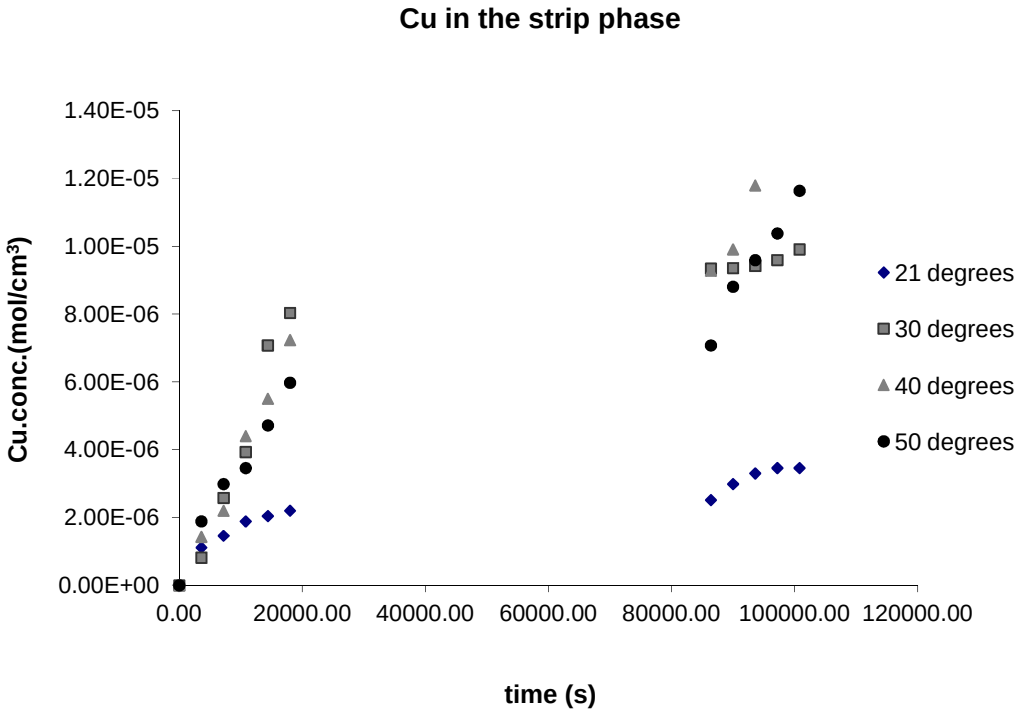

Figure C.23: Copper increase at 100 ml.min^{-1} and varying temperatures

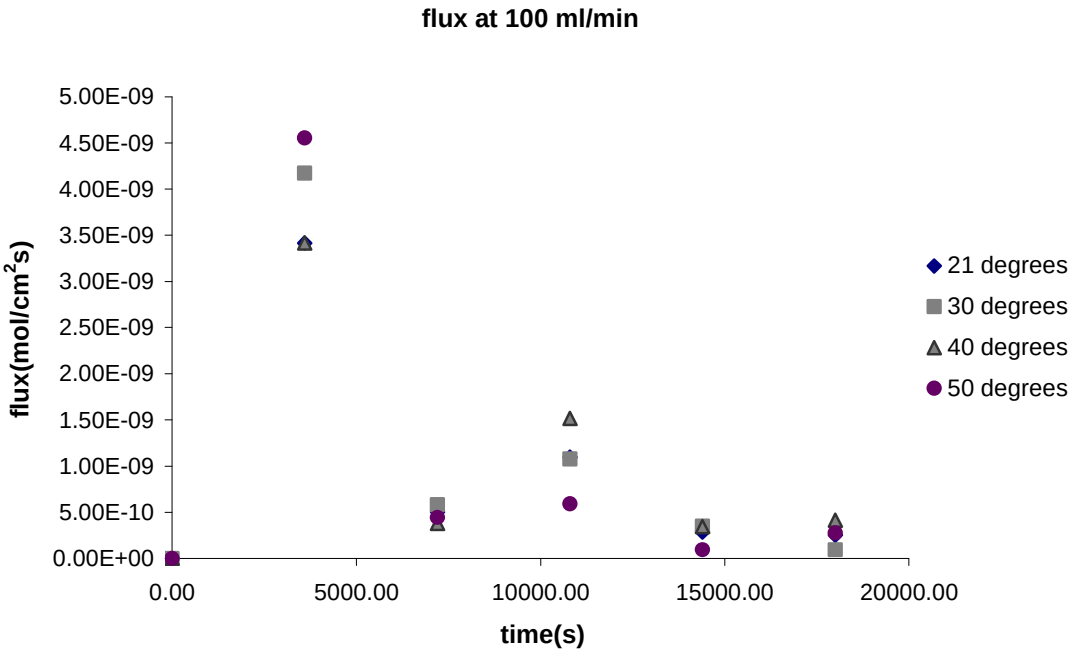

Figure C.24: Mass flux of copper ion at 100 ml.min^{-1} and varying temperatures

Flowrate of 120 $ml.min^{-1}$

Table C. 34: Kinetic results for copper extraction at 21ºC

Time(hr)	time(s)	feed	(mg/L)	strip	(mg/L)	[feed](mol/cm^3)	[cu] (mole)	[strip](mol/cm^3)	ΔC	$C_{bulk,average}$	Moles	Ncu(mol/cm^{2}s)	k_f	Sh
0.00	0.00	9.7	97.00	0	0.00	1.53E-05	3.05E-03	0.00E+00	0.00E+00	1.53E-05	0.00E+00	0.00E+00	0.00E+00	0.00E+00
1.00	3600.00	4.1	41.00	1.1	11.00	6.45E-06	1.29E-03	1.73E-06	8.81E-06	1.09E-05	1.76E-03	7.08E-09	6.52E-04	14.35
2.00	7200.00	2.8	28.00	1.2	12.00	4.41E-06	8.81E-04	1.89E-06	2.05E-06	5.43E-06	4.09E-04	8.22E-10	1.51E-04	3.33
3.00	10800.00	2.2	22.00	1.3	13.00	3.46E-06	6.92E-04	2.05E-06	9.44E-07	3.93E-06	1.89E-04	2.53E-10	6.43E-05	1.41
4.00	14400.00	1.1	11.00	1.6	16.00	1.73E-06	3.46E-04	2.52E-06	1.73E-06	2.60E-06	3.46E-04	3.48E-10	1.34E-04	2.95
5.00	18000.00	0.73	7.30	2.1	21.00	1.15E-06	2.30E-04	3.30E-06	5.82E-07	1.44E-06	1.16E-04	9.36E-11	6.50E-05	1.43

Table C.35: Kinetic results for copper extraction at 30 ºC

Time(hr)	time(s)	feed	(mg/L)	strip	(mg/L)	[feed](mol/cm^3)	[cu] (mole)	[strip](mol/cm^3)	ΔC	$C_{bulk,average}$	Moles	Ncu(mol/cm^{2}s)	k_f	Sh
0.00	0.00	9.7	97.00	0.00	0.00	1.53E-05	3.05E-03	0.00E+00	0.00E+00	1.53E-05	0.00E+00	0.00E+00	0.00E+00	0.00E+00
1.00	3600.00	7.9	79.00	0.91	9.10	1.24E-05	2.49E-03	1.43E-06	2.83E-06	1.38E-05	5.67E-04	2.28E-09	1.64E-04	3.62
2.00	7200.00	7.3	73.00	1.5	15.00	1.15E-05	2.30E-03	2.36E-06	9.44E-07	1.20E-05	1.89E-04	3.79E-10	3.17E-05	0.70
3.00	10800.00	5.2	52.00	2.5	25.00	8.18E-06	1.64E-03	3.93E-06	3.30E-06	9.84E-06	6.61E-04	8.85E-10	9.00E-05	1.98
4.00	14400.00	4.2	42.00	3.08	30.80	6.61E-06	1.32E-03	4.85E-06	1.57E-06	7.40E-06	3.15E-04	3.16E-10	4.28E-05	0.94
5.00	18000.00	3.2	32.00	3.3	33.00	5.04E-06	1.01E-03	5.19E-06	1.57E-06	5.82E-06	3.15E-04	2.53E-10	4.34E-05	0.96

Table C.36: Kinetic results for copper extraction at 40 ºC

Time(hr)	time(s)	feed	(mg/L)	strip	(mg/L)	[feed](mol/cm^3)	[cu] (mole)	[strip](mol/cm^3)	ΔC	$C_{bulk,average}$	Moles	Ncu(mol/cm^{2}s)	k_f	Sh
0.00	0.00	10	100.00	0	0.00	1.57E-05	3.15E-03	0.00E+00	0.00E+00	1.57E-05	0.00E+00	0.00E+00	0.00E+00	0.00E+00
1.00	3600.00	4.4	44.00	0.84	8.40	6.92E-06	1.38E-03	1.32E-06	8.81E-06	1.13E-05	1.76E-03	7.08E-09	6.25E-04	13.75
2.00	7200.00	3.2	32.00	0.98	9.80	5.04E-06	1.01E-03	1.54E-06	1.89E-06	5.98E-06	3.78E-04	7.59E-10	1.27E-04	2.79
3.00	10800.00	1.5	15.00	1.83	18.30	2.36E-06	4.72E-04	2.88E-06	2.68E-06	3.70E-06	5.35E-04	7.17E-10	1.94E-04	4.26
4.00	14400.00	0.9	9.00	2.8	28.00	1.42E-06	2.83E-04	4.41E-06	9.44E-07	1.89E-06	1.89E-04	1.90E-10	1.00E-04	2.21
5.00	18000.00	0.5	5.00	3.3	33.00	7.87E-07	1.57E-04	5.19E-06	6.29E-07	1.10E-06	1.26E-04	1.01E-10	9.19E-05	2.02

Table C.37: Kinetic results for copper extraction at 50 ºC

Time(hr)	time(s)	feed	(mg/L)	strip	(mg/L)	[feed](mol/cm^3)	[cu] (mole)	[strip](mol/cm^3)	ΔC	$C_{bulk,average}$	Moles	Ncu(mol/cm^{2}s)	k_f	Sh
0.00	0.00	10	100.00	0	0.00	1.57E-05	3.15E-03	0.00E+00	0.00E+00	1.57E-05	0.00E+00	0.00E+00	0.00E+00	0.00E+00
1.00	3600.00	3.5	35.00	0.62	6.20	5.51E-06	1.10E-03	9.76E-07	1.02E-05	1.06E-05	2.05E-03	8.22E-09	7.74E-04	17.03
2.00	7200.00	2.2	22.00	0.64	6.40	3.46E-06	6.92E-04	1.01E-06	2.05E-06	4.48E-06	4.09E-04	8.22E-10	1.83E-04	4.03
3.00	10800.00	0.92	9.20	1.61	16.10	1.45E-06	2.90E-04	2.53E-06	2.01E-06	2.45E-06	4.03E-04	5.40E-10	2.20E-04	4.84
4.00	14400.00	0.7	7.00	2.2	22.00	1.10E-06	2.20E-04	3.46E-06	3.46E-07	1.27E-06	6.92E-05	6.96E-11	5.46E-05	1.20
5.00	18000.00	0.63	6.30	2.74	27.40	9.91E-07	1.98E-04	4.31E-06	1.10E-07	1.05E-06	2.20E-05	1.77E-11	1.69E-05	0.37

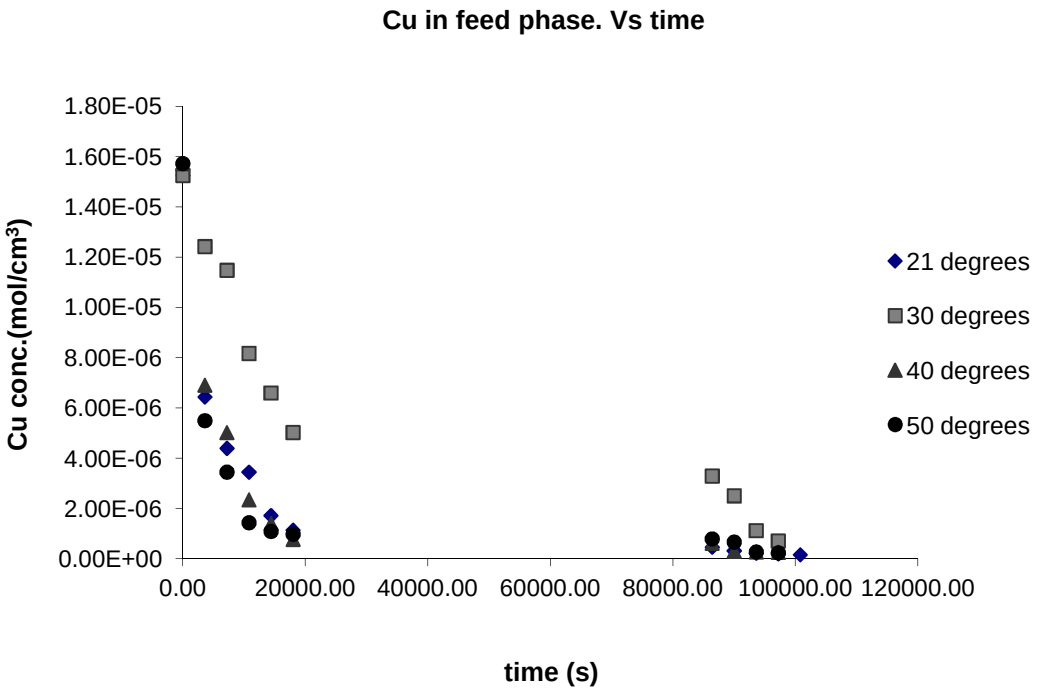

Figure C.25 : Copper decrease at 120 ml.min^{-1} and varying temperatures

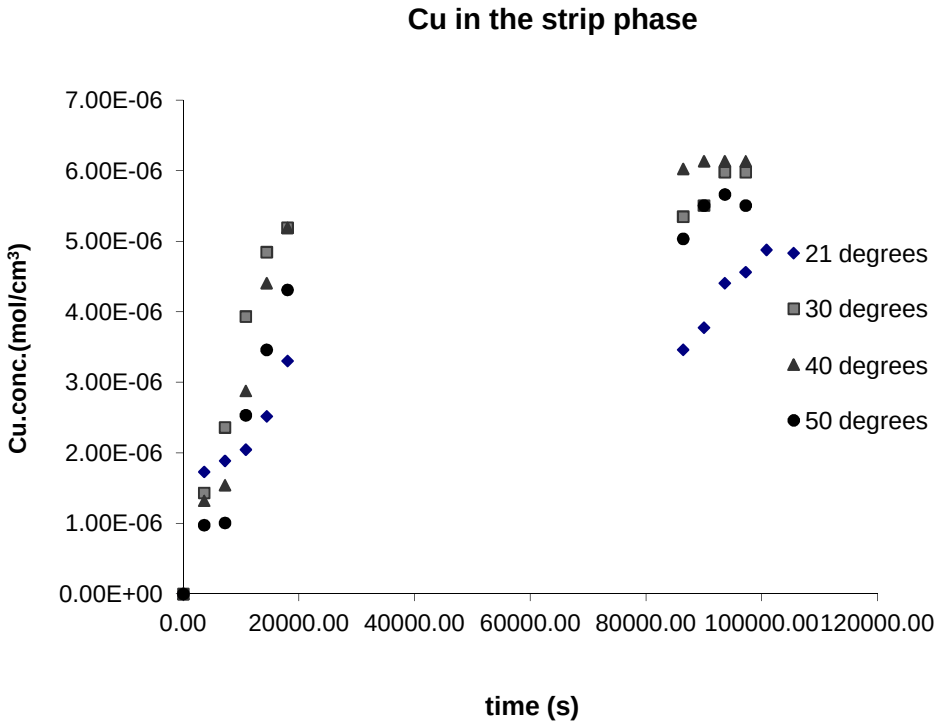

Figure C.26: Copper increase at 120 ml.min^{-1} and varying temperatures

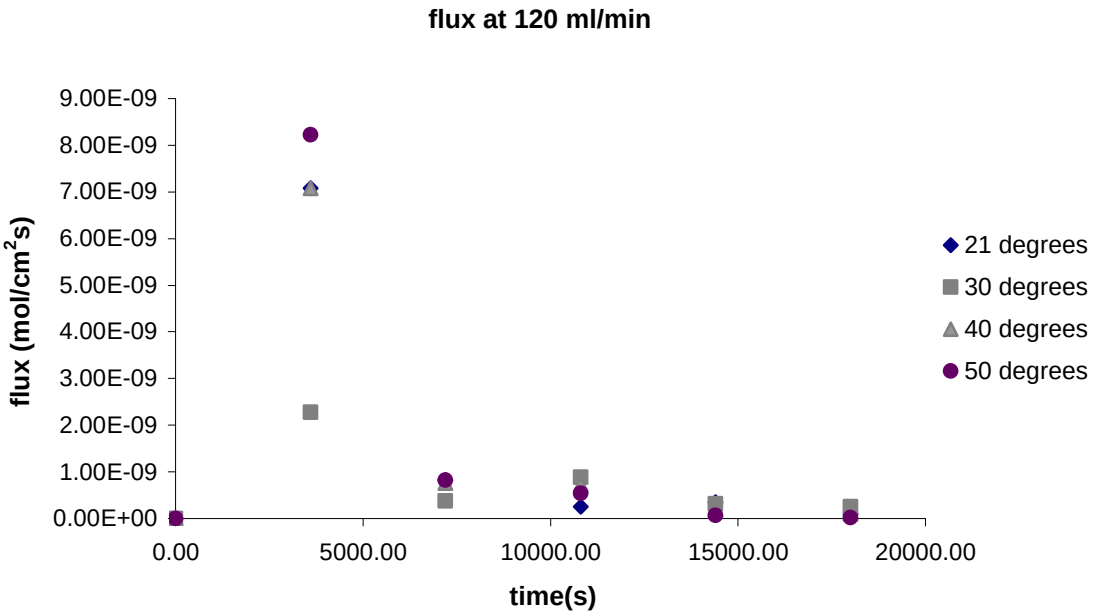

Figure C.27: Copper increase at 120 ml.min^{-1} and varying temperatures

Appendix D: Data used for obtaining dimensional numbers

Interpolation was used for obtaining the values for the viscosity and density for the water properties table D.38.

Table D. 38: Water properties (Incopera)

T	ρ	C_p	μ	k	Pr
$[K]$	$[kg/m^3]$	$[J/kg.K]$	$[10^{-6}\ N.s/m^2]$	$[10^{-3}\ W/m.K]$	[ ]
273.15	1000.0	4217	1750	569	12.99
275	1000.0	4211	1652	574	12.22
280	1000.0	4198	1422	582	10.26
285	1000.0	4189	1225	590	8.81
290	999.0	4184	1080	598	7.56
295	998.0	4181	959	606	6.62
300	997.0	4179	855	613	5.83
305	995.0	4178	769	620	5.2
310	993.0	4178	695	628	4.62
315	991.1	4179	631	634	4.16
320	989.1	4180	577	640	3.77
325	987.2	4182	528	645	3.42
330	984.3	4184	489	650	3.15
335	982.3	4186	453	656	2.88
340	979.4	4188	420	660	2.66
345	976.6	4191	389	668	2.45
350	973.7	4195	365	668	2.29
355	970.9	4199	343	671	2.14
360	967.1	4203	324	674	2.02
365	963.4	4209	306	677	1.91
370	960.6	4214	289	679	1.8
373.15	957.9	4217	279	680	1.76
375	956.9	4220	274	681	1.7
380	953.3	4226	260	683	1.61
385	949.7	4232	248	685	1.53
390	945.2	4239	237	686	1.47

Table D. 39: The Reynold's number

Flowrate-(ml/min)	Q(cm^3/s)	velocity(cm/s)	Re(21deg)	Re (30 deg)	Re(40 deg)	Re (50 deg)
30	0.50	0.007	0.80	0.99	1.20	1.44
40	0.67	0.010	1.07	1.32	1.60	1.92
50	0.83	0.012	1.33	1.64	2.00	2.40
60	1.00	0.014	1.60	1.97	2.40	2.87
70	1.17	0.017	1.87	2.30	2.80	3.35
80	1.33	0.019	2.13	2.63	3.21	3.83
90	1.50	0.022	2.40	2.96	3.61	4.31
100	1.67	0.024	2.67	3.29	4.01	4.79
120	2.00	0.029	3.20	3.95	4.81	5.75

Table D. 40: The Schmidt's number

Flowrate-(ml/min)	Q(cm^3/s)	velocity(cm/s)	Sc(21deg)	Sc (30 deg)	Sc(40 deg)	Sc (50 deg)
30	0.50	0.007	1.99E+02	1.61E+02	1.32E+02	1.11E+02
40	0.67	0.010	1.99E+02	1.61E+02	1.32E+02	1.11E+02
50	0.83	0.012	1.99E+02	1.61E+02	1.32E+02	1.11E+02
60	1.00	0.014	1.99E+02	1.61E+02	1.32E+02	1.11E+02
70	1.17	0.017	1.99E+02	1.61E+02	1.32E+02	1.11E+02
80	1.33	0.019	1.99E+02	1.61E+02	1.32E+02	1.11E+02
90	1.50	0.022	1.99E+02	1.61E+02	1.32E+02	1.11E+02
100	1.67	0.024	1.99E+02	1.61E+02	1.32E+02	1.11E+02
120	2.00	0.029	1.99E+02	1.61E+02	1.32E+02	1.11E+02

Table D. 41: The Sherwood's number

Flowrate-(ml/min)	Q(cm^3/s)	velocity(cm/s)	Sh(21deg)	Sh (30 deg)	Sh(40 deg)	Sh (50 deg)
30	0.50	0.007	9.77E-01	1.55E+00	2.36E+00	3.05E+00
40	0.67	0.010	2.20E+00	2.71E+00	4.37E+00	5.19E+00
50	0.83	0.012	3.46E+00	5.40E+00	6.60E+00	6.16E+00
60	1.00	0.014	1.98E+00	2.55E+00	3.97E+00	4.58E+00
70	1.17	0.017	2.96E+00	3.10E+00	3.73E+00	4.40E+00
80	1.33	0.019	2.69E+00	3.59E+00	1.93E+00	6.66E+00
90	1.50	0.022	3.21E+00	2.49E+00	3.75E+00	3.92E+00
100	1.67	0.024	2.61E+00	2.83E+00	3.49E+00	2.72E+00
120	2.00	0.029	4.70E+00	1.64E+00	5.01E+00	5.49E+00

Table D. 42: The log Reynolds number

Log Re (21 deg)	Log Re (30deg)	Log Re (40 deg)	Log Re (50deg)
-0.10	-0.01	0.08	0.16
0.03	0.12	0.20	0.28
0.13	0.22	0.30	0.38
0.20	0.30	0.38	0.46
0.27	0.36	0.45	0.53
0.33	0.42	0.51	0.58
0.38	0.47	0.56	0.63
0.43	0.52	0.60	0.68
0.51	0.60	0.68	0.76

Table D. 43: The log Sherwood number

Log Sh(21deg)	Log Sh(30deg)	Log Sh(40deg)	Log Sh(50deg)
-0.01	0.19	0.37	0.48
0.34	0.43	0.64	0.72
0.54	0.73	0.82	0.79
0.30	0.41	0.60	0.66
0.47	0.49	0.57	0.64
0.43	0.56	0.28	0.82
0.51	0.40	0.57	0.59
0.42	0.45	0.54	0.43
0.67	0.21	0.70	0.74

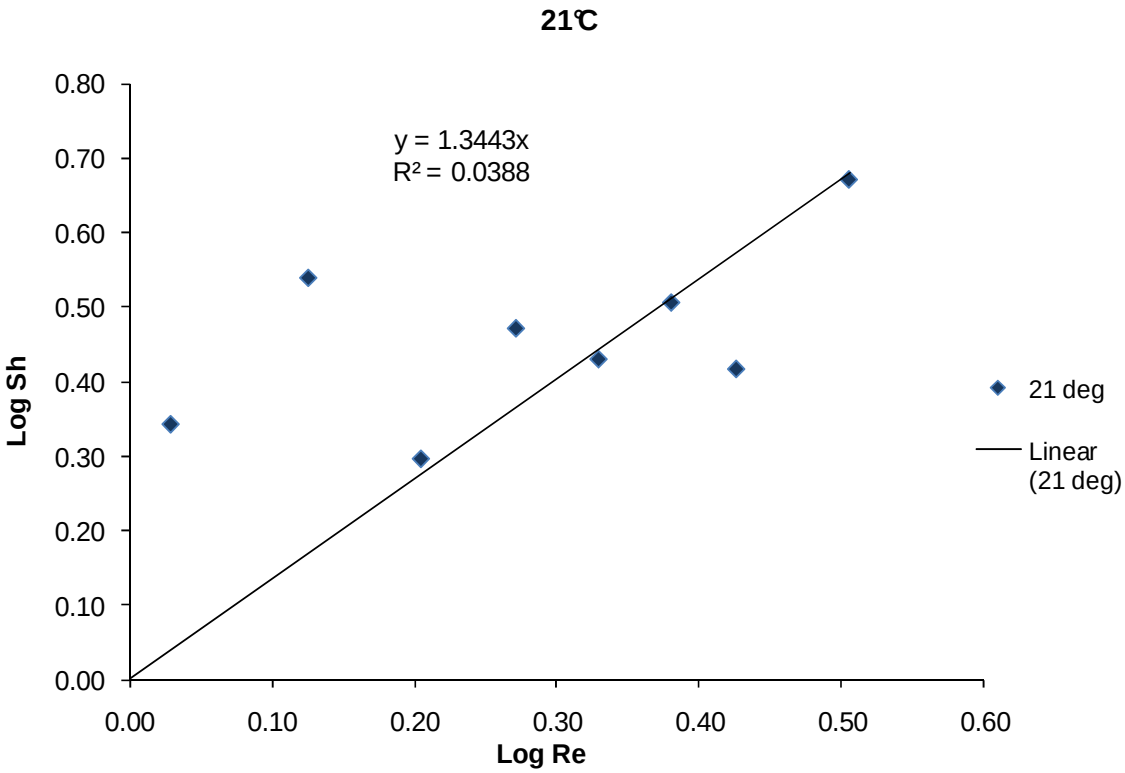

Figure D.28: The log of the dimensionless number at 21 ℃

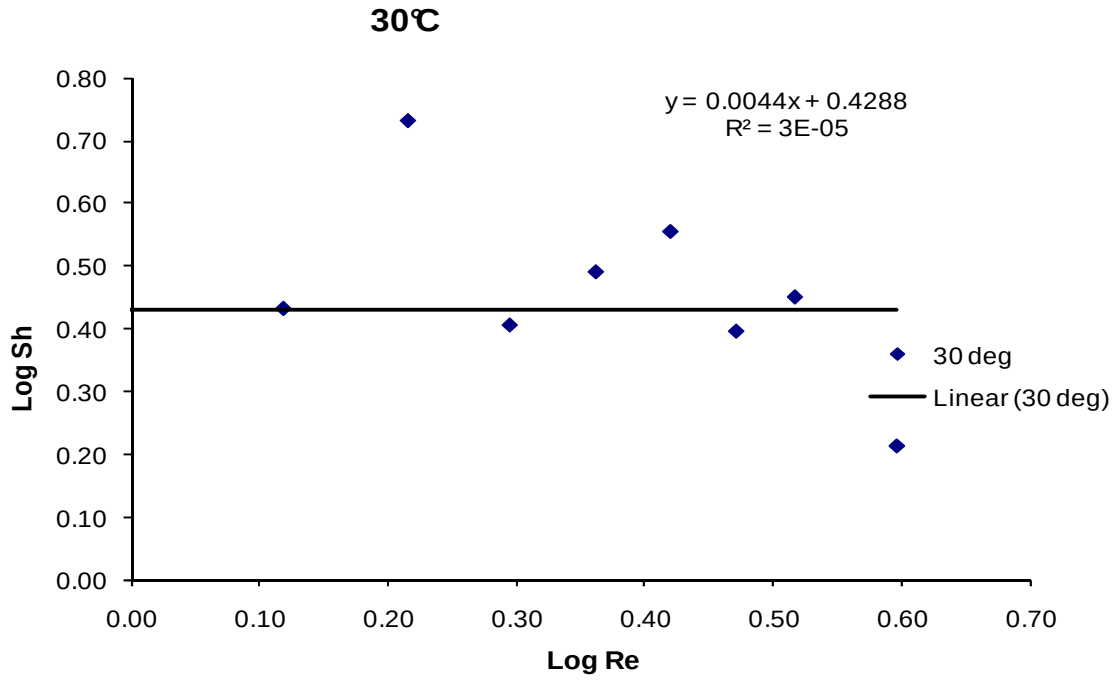

Figure D.29: The log of the dimensionless number at 30 ℃

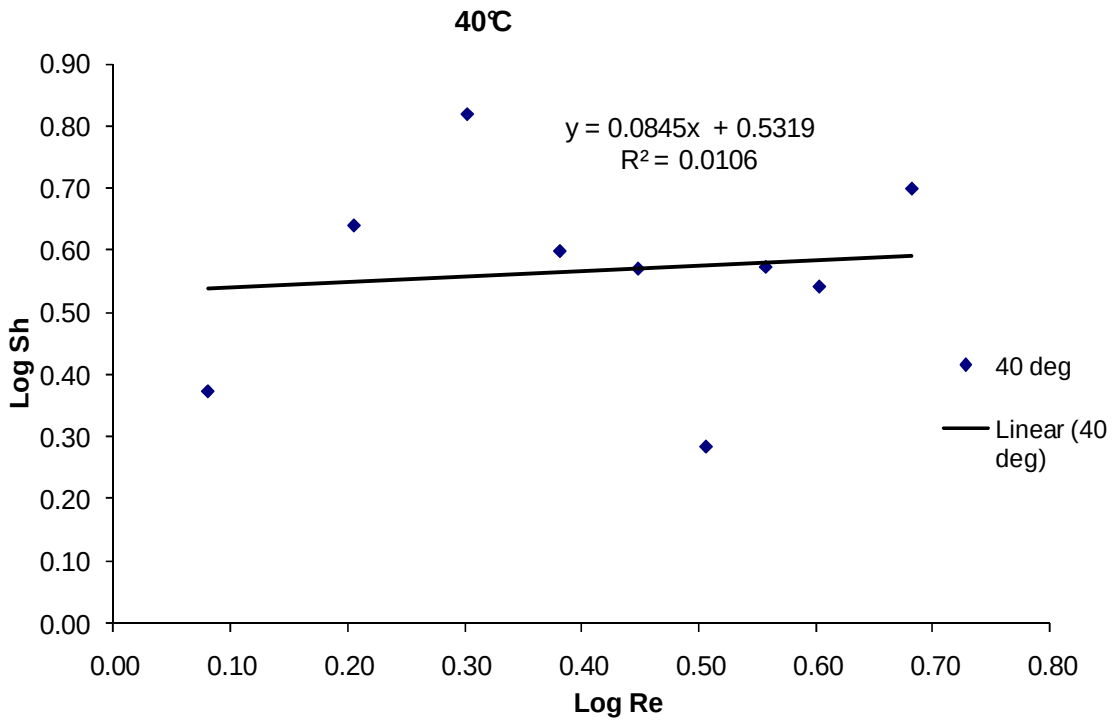

Figure D.30: The log of the dimensionless number at 40 ℃

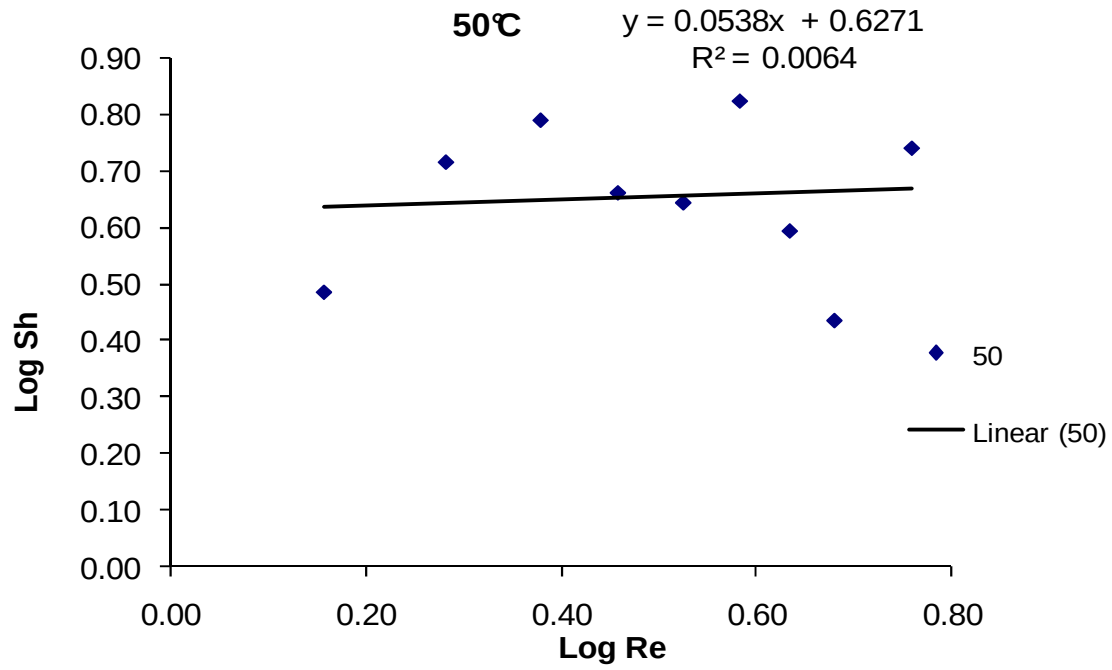

Figure D.31 : The log of the dimensionless number at 50 ℃

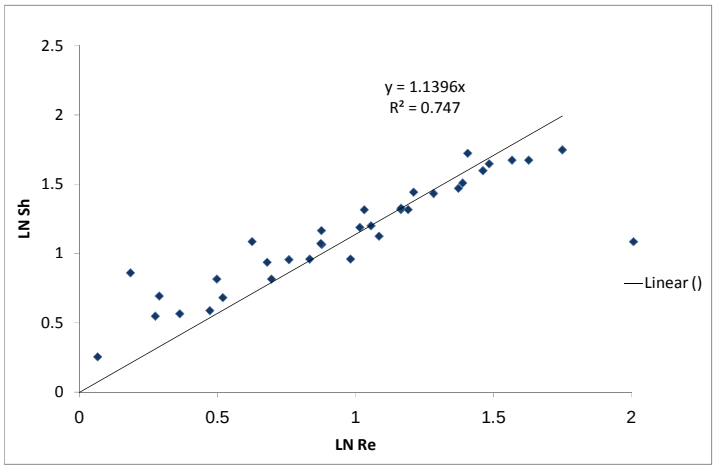

Figure D.32: Ln Sherwood vs Ln Reynolds

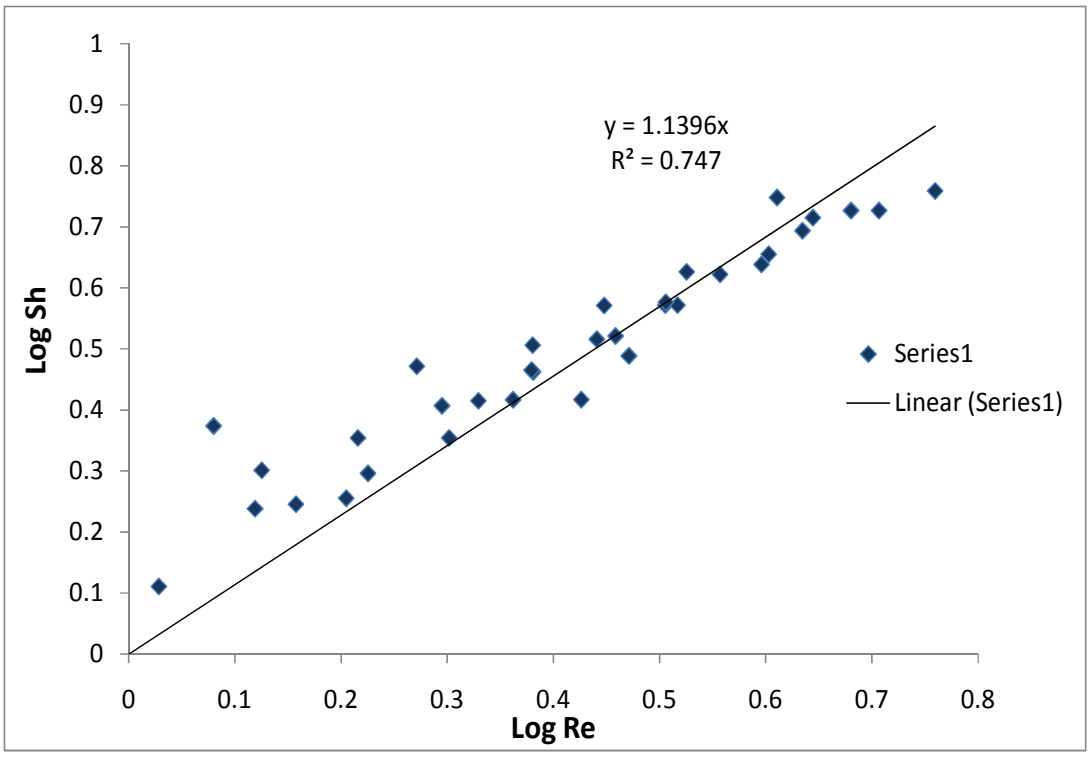

Figure D.33: Log Sherwood vs Log Reynolds

Table D. 44: Data for obtaining the relationship between the dimensionless numbers

C	n	m			
0.163	**0.69**	**0.33**			
Temperature (ºc)	**Sh(calculated)**	**Sh(measured)**	**diff**	**"Re**	**Sc**
	0.00	1.98		0.80	
21	6.44	6.37	0.00	1.07	198.80
	6.93	6.98	0.00	1.33	198.80
	7.36	7.35	0.00	1.60	198.80
	7.74	7.86	0.01	1.87	198.80
	8.09	7.72	0.14	2.13	198.80
	8.41	8.23	0.03	2.40	198.80
	8.71	8.65	0.00	2.67	198.80
	9.25	9.15	0.01	3.20	198.80
	5.43	5.26	0.03	0.99	161.36
30	5.97	5.67	0.09	1.32	161.36
	6.43	6.70	0.08	1.64	161.36
	6.82	6.93	0.01	1.97	161.36
	7.18	7.20	0.00	2.30	161.36
	7.50	7.63	0.02	2.63	161.36
	7.80	7.72	0.01	2.96	161.36
	8.08	8.05	0.00	3.29	161.36
	8.58	8.51	0.00	3.95	161.36
	5.06	5.07	0.00	1.20	132.40
40	5.56	6.00	0.19	1.60	132.40
	5.98	6.05	0.00	2.00	132.40
	6.35	6.28	0.01	2.40	132.40
	6.69	6.60	0.01	2.80	132.40
	6.99	6.80	0.04	3.21	132.40
	7.26	7.35	0.01	3.61	132.40
	7.52	7.30	0.05	4.01	132.40
	7.99	8.16	0.03	4.81	132.40
	4.74	4.65	0.01	1.44	110.73
50	5.21	5.27	0.00	1.92	110.73
	5.61	5.77	0.03	2.40	110.73
	5.96	6.19	0.05	2.87	110.73
	6.27	6.14	0.02	3.35	110.73
	6.55	6.90	0.12	3.83	110.73
	6.81	6.84	0.00	4.31	110.73
	7.05	6.65	0.16	4.79	110.73
	7.49	7.44	0.00	5.75	110.73